ANKARA UNIVERSITY
GRADUATE SCHOOL OF NATURAL AND APPLIED SCIENCES

MASTER THESIS

3D BIOPRINTING OF HYBRID BONE GRAFTS WITH AN INHERENT CONTROLLED DELIVERY SYSTEM

Meriç GÖKER

BIOMEDICAL ENGINEERING DEPARTMENT

ANKARA
2021

ABSTRACT

M.Sc.Thesis

3D Bioprinting of Hybrid Bone Grafts with an Inherent Controlled Delivery System

Meriç GÖKER

Ankara University
Graduate School of Natural and Applied Sciences
Department of Biomedical Engineering

Supervisor: Assoc. Prof. Dr. Pınar YILGÖR HURİ

Bone tissue possesses the ability of repairing itself after a fracture or a damage. However, this regeneration does not occur in all cases, including multi segmental fractures and tumor removal procedures. In such cases, the defects should be filled with a material that is able to support the defect site structurally and mechanically. Tissue engineering is a promising and developing field for generating bone tissue that works by isolating viable cells from target tissue and combining them with mechanically appropriate structures that allow mineralized tissue regeneration *in vitro* and implanting this structure into the defect. A promising method in tissue engineering is encapsulating growth factors in scaffolds enabling localization and controlling their spatiotemporal release profile. 3 dimensional (3D) printing method enables to control porosity, pore size, rigidity and permeability of scaffolds accurately compared to traditional scaffold production methods. Within the scope of this thesis, 3D printed scaffolds with an inherent controlled delivery system is addressed. By stimulating specific regions of the graft with spatially distributed osteogenic and angiogenic factors, namely bone morphogenetic protein (BMP-2) and vascular endothelial growth factor (VEGF), respectively, it was aimed to produce vascularized bone by using adipose derived stem cells (ASCs) as the only source of cells. Osteogenic differentiation of mesenchymal stromal cells and formation of vascular structures by the endothelial cells that are present within the heterogeneous ASC population was addressed via encapsulation of BMP-2 and VEGF and their spatial positioning within the graft while 3D printing. 3D constructs were then cultured within a perfusion bioreactor system to be able to produce viable clinically relevant-size grafts. This approach will provide a methodology for the generation of off the shelf constructs for vascularized bone regeneration.

January 2021, 89 Pages

Key Words: 3D printing; Tissue Engineering; Biomaterials; Bone Tissue; Controlled Release; Cell Culture

ÖZET

Yüksek Lisans Tezi

Kontrollü Salım Sistemi İçeren Hibrid Kemik Greftlerinin 3B Biyobaskılamayla Üretimi

Meriç GÖKER

Ankara Üniversitesi

Fen Bilimleri Enstitüsü

Biyomedikal Mühendisliği Anabilim Dalı

Danışman: Doç. Dr. Pınar YILGÖR HURİ

Kemik dokusu bir kırık veya hasar sonrası kendini tamir edebilme yeteneğine sahip bir dokudur. Ancak rejenerasyon her koşulda tamamen gerçekleşememektedir. Örneğin, çok parçalı kırıklar ve kemik tümörü çıkarılması sonucu oluşan büyük defektler tamir edilmeden kalabilmektedir. Bu gibi durumlarda defektlerin yapısal ve mekanik destek sağlanması amacıyla bir dolgu malzemesi ile doldurulması gerekmektedir. Doku mühendisliği yöntemi günümüzde kemik dokusu oluşturulması esasını dayanan hedeflenen dokudan izole edilen sağlıklı hücrelerin hedefe uygun yapısal ve mekanik özelliklere sahip bir taşıyıcı üzerine ekilmesi ve laboratuvar ortamında mineralize doku elde edilmesinin ardından hedef bölgeye implante edilmesi prensibine dayanır. Doku mühendisliğinde yeni yaklaşım ise büyüme faktörlerinin doku desteği içerisine hapsedilmesi, böylelikle lokalize edilmesi ve aynı zamanda ortamda bulunma süre ve konsantrasyonunun kontrol edilmesidir. 3 boyutlu (3B) baskılama metoduyla klasik doku üretim yöntemlerine göre doku iskelelerinde porozite, porozite boyutu, poroziteler arası bağlanma, malzeme sertliği ve geçirgenlik gibi parametreler tam olarak denetlenebilmektedir. Bu tez kapsamında 3B biyobaskılama ile kontrollü salım stratejisinin bir arada ele alınmasıyla, tek hücre popülasyonu olarak kullanılacak yağ-kaynaklı kök hücrelerin (ASCs) farklı büyüme faktörleri ile greftin belirli bölgelerinde stimüle edilmesiyle vaskülarize kemik dokusu üretimi ele alınmıştır. ASCler heterojen bir hücre popülasyonu olup içeriğindeki mezenkimal stromal hücrelerin osteojenik farklılaşması ile greftin kemik yapısını ve endotel hücrelerin greftin damar yapısını sırasıyla tasarımın belli bölgelerine polimerik nanotaşıyıcılar içine enkapsüle edilmiş BMP-2 ve VEGF stimülasyonu ile özgün tasarımlı olarak oluşturması hedeflenmiştir.

Ocak 2021, 89 sayfa

Anahtar Kelimeler: 3B biyobaskılama; Doku Mühendisliği; Biyomalzemeler; Kemik Dokusu; Kontrollü Salım; Hücre Kültürü

ACKNOWLEDGEMENTS

I wish to start by expressing my deepest acknowledgement to Assoc. Prof. Dr. Pınar YILGÖR HURİ for her scientific counselling, technical insights, and motivation. I sincerely thank her for the time and effort she has put into my thesis.

After my supervisor, I would like to thank my lab mentor, my colleague, Emre ERGENE whom I was lucky enough to work with. He shared his experience and guided me to succeed in my experiments. I am truly grateful that he was always instructive, insightful, and most importantly patient towards me.

In addition, I wish to send my kindest regards and my deepest appreciation to every member of MTE lab. My dearest colleagues: Şeyda GÖKYER, Ebru TALAK, Abdullah EYİDOĞAN, Mervesu GÖKYÜREK and Barış Burak ALTUNAY thank you for putting up with me when I was teasing you.

I also would like to thank Dr. Menekse Ermiş Şen from the METU BIOMAT and Dr. Tuğba ENDOĞAN TANIR from the METU CENTRAL LABORATORY for provision of CLSM and SEM images.

This thesis was conducted within the frame of TUBITAK 119S131 Project. I would like to acknowledge their financial support for making this study happen.

Finally, I wish to thank my family for being there for me and supporting my academic endeavours.

Meriç GÖKER
Ankara, January 2021

TABLE OF CONTENTS

LIST OF FIGURES

LIST OF TABLES

LIST OF ABBREVIATIONS

3D	Three-Dimensional
ALP	Alkaline Phosphatase
AM	Additive Manufacturing
ASC	Adipose-derived Stem Cells
BMP	Bone Morphogenetic Protein
BSA	Bovine Serum Albumin
CAD	Computer-Aided Design
CAM	Computer-Aided Manufacture
CT	Computerized Tomography
DAPI	4′,6-Diamidino-2-Phenylindole
DBM	Demineralized Bone Matrix
DCM	Dichloromethane
DMEM	Dulbecco's Modified Eagle Medium
DMSO	Dimethyl Sulfoxide
ECM	Extracellular Matrix
EGF	Epidermal Growth Factor
ESC	Embryonic Stem Cells
FBS	Fetal Bovine Serum
FDM	Fused Deposition Method
FGF	Fibroblast Growth Factor
GELMA	Gelatin Methacrylate
GF	Growth Factor
HA	Hydroxyapatite
HCL	Hydrochloric Acid

ICM	Inner Cell Mass
MRI	Magnetic Resonance Imaging
P/S	Penicillin/Streptomycin
PBS	Phosphate Buffer Saline
PCL	Poly(ε-caprolactone)
PDGF	Platelet-derived Growth Factor
PEG	Poly(ethylene) Glycol
PEGDA	Poly(ethylene) Glycol Diacrylate
PGA	Poly(glycolic) Acid
PLA	Polylactic Acid
PLGA	Poly(lactic-co-glycolic) Acid
pNPP	Para-nitrophenyl Phosphate
PFA	Paraformaldehyde
PPF	Poly(propylene) Fumarate
PVA	Polyvinyl Alcohol
SEM	Scanning Electron Microscopy
SLA	Stereolithography
SLS	Selective Laser Sintering
SSC	Somatic Stem Cells
STL	Standard Tessellation Language
TCP	Tricalcium Phosphate
TE	Tissue Engineering
TGF-β	Transforming Growth Factor Beta
TPU	Thermoplastic Polyurethane
VEGF	Vascular Endothelial Growth Factor
XRF	X-Ray Fluorescence

1. INTRODUCTION

In this thesis, it was scoped to construct of 3 dimensional (3D) scaffolds with an inherent built-in controlled growth factor delivery system which would contribute to vascularized bone formation using a single stem cell source *in vitro* conditions. Production and characterization of such a system will make future single-step *in situ* bioprinting procedures possible to generate vascularized bone upon application within bone defects.

1.1 Structure of Bone Tissue

Posture of the body, protection of inner organs from the outer environment, mineral deposition such as calcium ions, storage of various growth factors and blood cell production are enabled by the skeletal system to the individual. Other than bone cells and mineralized tissue, bones comprise both nerves and blood vessels that establish a network. Figure 1.1 illustrates this network and the overall structure elaborately.

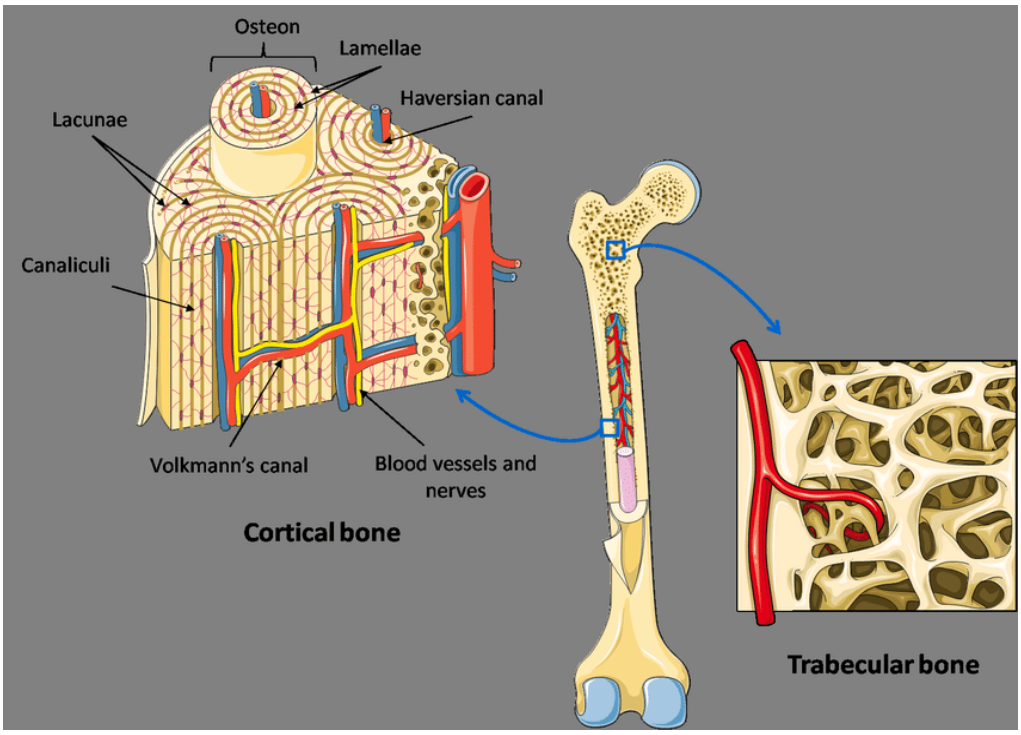

Figure 1.1 Schematic representation of bone structure (Chabanon 2015)

Bone is a mineralized connective tissue that constantly changes, with highly organized and relatively complex structure. In the adult skeleton, 80% of the total bone mass is cortical bone, whereas the 20% is cancellous. The distribution of these structures is different in different regions of the skeleton. For instance, trabecular bone exists at the vertebrae, distal section of long bones and the calcaneus whereas cortical bone is dominated in the femoral neck and the shaft part of the long bones (Ralston 2013). The purpose of cancellous bone tissue is to fill the interior and create enough space for bone marrow and blood vessels. The constituents of cancellous bone tissue are rod and plate-like elements which are responsible for shaping up the overall light architecture.

1.1.2 Natural Bone Regeneration Process

Natural bone tissue possesses the ability to remodel itself throughout life, yet the capacity declines with age. This process of remodeling is made possible by the activity of osteoclasts and osteoblasts working in a manner of antagonism. Bone structure gets resorbed by osteoclasts and subsequently gets produced by osteoblasts. As the process of remodeling occurs, processes take place in an order. Firstly, calcium homeostasis is regulated, and then micro-scale fractures are mended. Consequently, the skeleton sculpts for the renewal ultimately.

Bone tissue does have the capacity of self-reconstruction and healing upon defects to some extent which is addressed as “critical size defect”. If the fracture itself is narrower than this criterion of critical size defect, bone tissue can regenerate itself without any external intervention. There are three major steps in the process of fracture healing which are inflammation, reparation and remodeling, respectively. The inflammation step occurs after as soon as fracture happens and at the same time a fibrin clot occurs at the fracture site. Afterwards, human body produces cytokines and growth factors locally within the hematoma and enables osteoprogenitor cells to migrate to the defect site and force them to differentiate into specific lineages (chondroblasts which are responsible for hyaline cartilage production while osteoblasts are responsible of spongy bone

development, reciprocally). Presence of these cells in the fracture site also regulates cell

proliferation and production of extracellular matrix (ECM). Furthermore, it is proven that bone morphogenetic proteins (BMPs) and growth factors such as transforming growth factor-beta (TGF-β), insulin-like growth factor (IGF), fibroblast growth factor (FGF), platelet-derived growth factor (PDGF) and vascular endothelial growth factor (VEGF) are secreted in a harmony. This tremendous phenomenon sets up regulation of bone regeneration (Olwin and Hauschka 1986). For instance, as Marden et al. (1993) reported, PDGF gets expressed primarily during the early inflammatory stages and stimulates the proliferation of mesenchymal stem cells (MSCs). Cowan et al. (2007) proved that these osteoinductive growth factors can induce osteogenic differentiation in various cells such as fibroblasts and MSCs. Furthermore, it was revealed that BMP-2 is the initiative factor that peaks at the first day of fracture and followed by BMP-7 expression after 15 days. Linkhart et al. (1996) introduced that other TGF-βs were also expressed in higher concentrations especially during active matrix secretion. Eventually, epidermal growth factor (EGF) gets expressed in order to upregulate the production of the matrix metalloproteinases which promotes the final stage of bone repair "remodeling" (van der Zee et al. 1998).

1.2 Conventional Methodology for Bone Repair

It has been recognized that bone can regenerate and self-restore its functions without leaving any scar tissue, yet this is not always satisfactory. In 2003, various researchers reported that in most of the large bone defects involving specifically bone tumor resections or comminuted fractures the regeneration potential of human bone is insufficient (Carano and Filvaroff 2003). It was also reported that the insufficient healing can happen in much smaller defects which leads to nonunion healing in up to 1 to 5 percent of the cases observed. In those cases, as it is a conventional method that a suitable filler material had to be doped to and infuse the space created by the defect in order to reconstruct the structure and make the bone functional again.

In today's clinical conventional methods, various materials are utilized as grafts which serve the function of filling these bone gaps mentioned. Various types of biological and synthetic materials are made as grafts to be used in clinics. These grafts have to meet

some essential requirements such as mimicking the porous structure of bone tissue, carrying osteoconductive factors and osteogenic cells.

1.2.1 Biologic & Synthetic Grafts

In current clinically available therapeutic options, biological grafts are often preferred which are either autogenic, allogenic or xenogeneic origin. There are also different applications which focus on decellularizing the cadaver tissue and using that as a biological graft (Ebraheim et al. 2001).

Autografts are the current golden standard of therapy. They are considered as biocompatible, do not transmit any disease and possess viable osteoblastic cells which enable in new bone formation (Sutherland and Bostrom 2005). Although they seem to be the proper candidates, autografts have some severe drawbacks such as limited availability and donor site morbidity which leads to increased rate of infection risk, increased periods of anesthesia and potential loss of blood during the isolation procedure. These cons make the autografts tangling and less desirable and severely limits their use (Younger and Chapman 1989).

Allografts on the other hand, are tissues that are harvested from one person to transplant into another. Allografting does not possess the disadvantage of limited availability of autografts. Even though transplantation of allografts has been remarkably developed, the risk of inception, rejection, infection and allograft fracture sits as experienced complications. Since allografts require pre-sterilization and testing before implantation, they undergo several processes that affect osteoinductivity and overall osteogenic properties of the grafts negatively. That is why allografts must be utilized only when they are freshly harvested. Mostly they are preserved in -60°C prior to sterilization or they undergo lyophilization which is potentially destructive for osteoprogenitor cells, osteoinductive factors and leads to mechanical stiffness decrease when they are rehydrated.

Bones that are taken from cadavers can be considered as potential allograft source and they undergo the same treatment with allografts taken from healthy patients. That is why allografts are considered as scaffolds with osteoconductive properties.

Demineralized bone matrix (DBM) which is also a heavily investigated source of bone grafts, is obtained when allograft bones are treated with acid extraction. Acid extraction treatment unfortunately ends up bone with mineralized components loss as well as the organic component including the growth factors (GFs). Since the efficacy of a DBM relies on how much of the total BMP present within the bone graft, it is the only allograft with osteoinductive properties, yet its efficiency varies highly. It was shown that differences in allograft processing methods results with significant changes in capability of the DBM to induce spinal fusion (Peterson et al. 2004).

Xenotransplantation is the eldest way of transplanting organs and tissues among species. Initially it has been thought that it can universally solve the organ shortage issue in clinics. However, ethical issues aside, medical problems such as transmission of zoogenic diseases to humans remain intact. In world's history, the first xenogeneic bone transplantation recorded was a canine bone to a human cranial defect done by a Dutch surgeon Job van Meekeren in 1668. After three centuries, bones of bovines are commercialized as graft materials which are more compatible to the human body than canine bones (Maatz and Bauermeister 1957).

As well as allografts require pre-transplantation treatments, xenografts must undergo sterilization and should be processed to make them non-toxic, non- immunogenic in order to assure that they are free of pyrogens which leads them to function as only as osteoconductive matrices (Chau and Mobbs 2009).

Graft material availability stands as a challenging issue worldwide, around 6.2 million patients have fractures occur per year solely in the US and 15% of the fractures need transplantation (Sutherland and Bostrom 2005). Since biological grafts have their own challenges, a seek for the ultimate graft material with sufficient biocompatibility and mechanical rigidness continues. Besides biologic and mechanical attributes, the demanded material has to be reproducible in vast quantities. Thus, along with natural biologic grafts synthetic grafts such as metallics, ceramics and their combinations: composites are investigated.

Mostly these metallic grafts and their derivatives do not possess the ability to fully seal the defect region leading to failure of the structure mechanically. Additionally, they are not compatible to interact with the surrounding tissues properly.

In orthopedic surgery the general materials used as fixation devices are metallic; mostly stainless steels, cobalt-chromium alloys, and titanium alloys. Among all these materials, titanium alloys are the highly favored ones since they show substantial corrosion resistance and they become connected into bone which is a positive contributing factor for long-term behavior. Titanium alloys are also utilized as meshes to transform the shape of the transplanted material In 1993 a research group manufactured a BMP-Ti composite by infiltrating a titanium mesh with a solution of noncollagenous ECM laden with BMP that allowed to a cartilage and bone development simultaneously on the surface of the implant in addition to bone ingrowth. Likewise, different groups reported that they showed a titanium mesh wetted with bone marrow aspirate that contains collagen/calcium phosphate as a promising bone graft (Erbe 2007). In a review by Schug and colleagues, it was reported that titanium meshes to treat mandibular fractures showed successful union of the majority of the cases (Schug et al. 2000).

In addition to metals, ceramics are also used as bone graft substitutes. In 2006, it was reported that approximately 60% of the bone grafts that are commercially eligible are either ceramics alone or combined with a different material (Laurencin et. al., 2006). Due to their physical properties, ceramics lack high temperature processing for scaffolding, and they are brittle which means they need to be mixed to become a superior composite. Tricalcium phosphate (TCP) and synthetic hydroxyapatite (HA) including groups are the highest favorable ceramics in bone tissue engineering since the hydroxyapatite molecule is the primary inorganic component of the native bone. It was shown that, by their nature, calcium phosphates can be osteoconductive as well as osteointegrative and possibly osteoinductive in some studies (Ambrosio et al. 2001).

None of the grafts and the conventional methods mentioned previously are perfect and they have some serious drawbacks in various ways. When you compare advantages and disadvantages of these grafts, you cannot find a single one that meets the criteria of being the ultimate substitute to replace bone defects. That is how tissue engineering has emerged so that a new approach for tissue repair can be accomplished through creating

the bone tissue from scratch using the stem cells, biomolecules and biomaterials in harmony.

1.3 Tissue Engineering as an Alternative for Conventional Bone Grafts

Tissue engineering is a promising approach to replace either damaged or failed organs and tissues with their healthy counterparts. Due to the previously mentioned shortages and complications attributed to autografts, allografts and xenografts such as immune system reactions, disease transmissions among species and inadequacy of the availability of tissues to be transplanted, an alternative approach has emerged. This new field is named as tissue engineering and it targets to manufacture tissues and organs (ultimately) of interest which are functional and ready-to-transplant to patients.

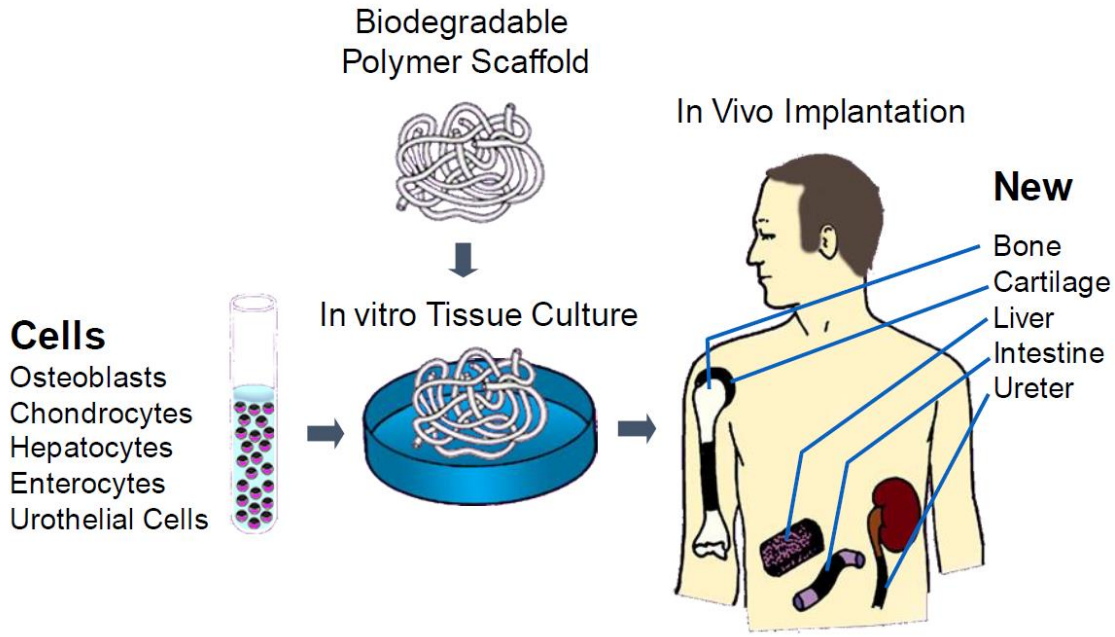

Figure 1.2 Schematic illustration of tissue engineering applications (Langer 2019)

As being one of the pioneers of the tissue engineering field, R. Langer states that "tissue engineering is an interdisciplinary science that involves the use of biological sciences and engineering to develop tissues that restore, maintain, or enhance tissue function" (Langer and Vacanti 1993). With tissue engineering techniques researchers aim to erase

waiting lists of organ transplantation and produce patient-specific tissues and organs *in vitro* (Khademhosseini and Langer 2016).

Figure 1.2 depicts the steps of tissue engineering applications illustratively. Firstly, stem cells are harvested from the patient himself by either surgical operations or biopsies and then his/her cells are multiplied *in vitro*. Those multiplied cells are combined with scaffolds which can be done with various techniques. Once the integration of the cells and scaffold come into being by the help of application-specific bioreactors, "artificially-made tissue" becomes ready to implement to the patient's damaged area.

Bone tissue engineering is the subbranch of tissue engineering which focuses on developing utterly complex bone tissue subtracts including cortical, cancellous and two of them combined tissues.

Bone tissue engineering steps start with isolating stem cells which are most of the time either mesenchymal stem cells and their progenitor cells then continue with expanding these cells *in vitro* and seeding them onto a biodegradable carrier system that possesses sufficient mechanical requirements of the defect site. Needless to say, all the scaffolds used in TE applications have to be biocompatible with the human body. There are a couple of supplementary methods to improve the artificial scaffold plus cells complex one of which is implementing growth factors into scaffolds. Naturally, the human body contains growth factors which play a key role in accelerating bone healing by dictating cell proliferation followed by local osteoprogenitor differentiation. Thus, in order to increase the chance of bone of formation, adding growth factors to the construct should be considered. Second to last step is preferably to have your construct maturated and mineralized by an external factor such as bioreactors. After that, this cell-seeded ultimate construct gets implanted at the defect site. Eventually, ECM gets formed by the cells and the implant is degraded eventually. These processes are indications of what an ideal bone repair environment should be. It should provide intrinsic properties of natural bone tissue which is porous and 3 dimensional. Freyman et al. (2001) reported that such architectures enable osteoprogenitor cell propagation, vascularization of the whole graft and incorporation with the surrounding host bone coincidentally so that remodeling process can be done.

1.3.1 Stem Cells in Tissue Engineering

For tissue engineering, stem cell sources are classified by where they are harvested from. They can either be autogenic meaning derived from the patient himself/herself, allogenic which means derived from the same species or xenogeneic (harvested from a

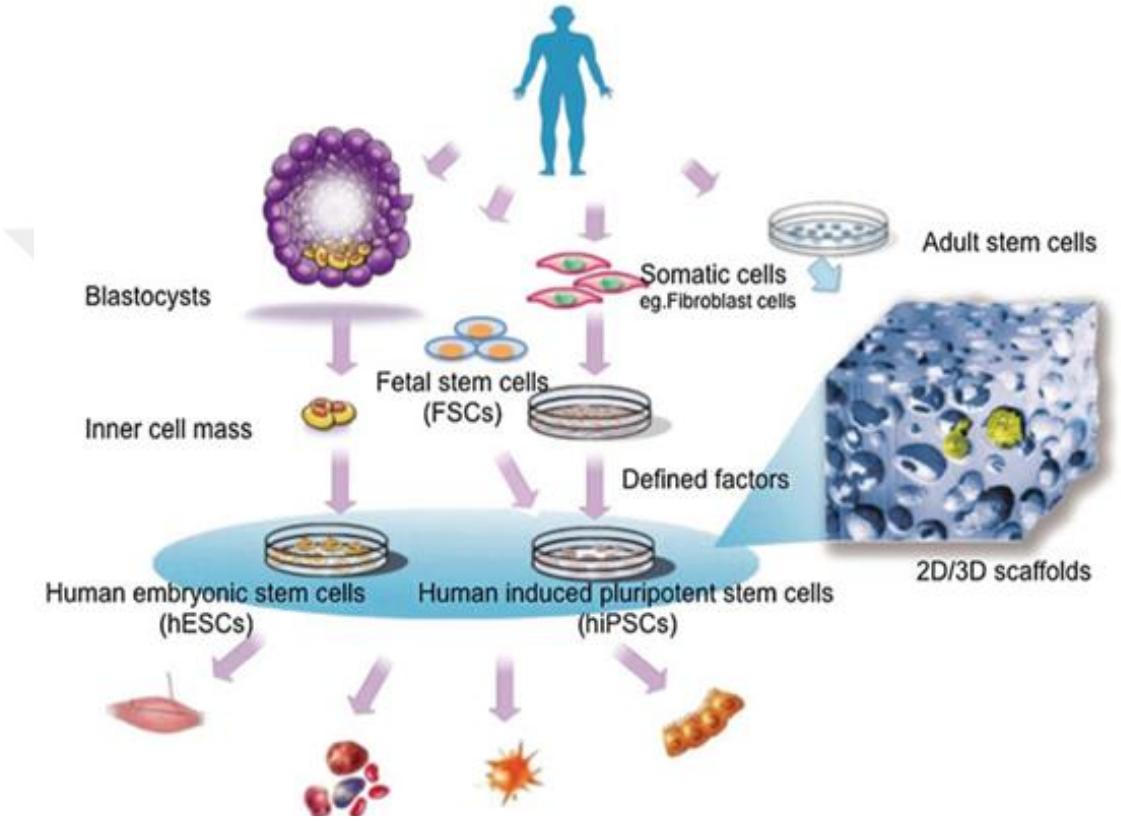

Figure 1.3 Origins and types of stem cells used in TE (Hu et al. 2016)

different species). Cells can also be categorized based on their differentiated stage. Hypothetically, autologous cells acquired from the healthy region of the defected site are the ideal source of cells. However, harvesting of these cells are challenging and they have limited availability, thus steering researchers to other cell sources. Allogeneic cells were reported by Niemeyer et al. (2004) as possibly immune responsive for the host whereas xenogeneic cells are already known for possible severe inflammations and immunologic responses which can eventually lead to tissue rejection. There is also the risk of transmission of diseases among species in usage of xenogeneic cells. (Leyh et al. 2003).

Stem cells that are frequently experimented in bone TE could be either natural or artificial cells such as genetically modified IPSCs. Natural stem cells can be categorized (Figure 1.3) according to their differentiation potential into different cell types under stimulation or based upon their proliferation profile. From the point of differentiation view, stem cells could be totipotent pluripotent or multipotent indicating that their differentiation potency into any type of cell is possible except that are present at placenta and support tissue of uterus.

Considering primary cells such as mature bone cells have no risk of immune reaction and no ethical issue whatsoever, they could be potentially the ideal cell source for bone TE Although, they are very impractical to isolate and multiply properly *in vitro* conditions. Thus, this is making them challenging to utilize in tissue engineering applications.

In today's market there are genetically modified cell lines available for letting researchers to evaluate fundamentals of cell behavior from different aspects *in vitro* and in non-human settings. For bone tissue *in vitro* applications, osteosarcoma cell lines acquired from a bone cancer patient and limitless perpetuating cell lines are examples of these modified cells by genetic engineering.

1.3.1.1 Embryonic Stem Cells (ESCs)

Due to their nature, embryonic stem cells (ESCs) possess high self-renewal, clonogenicity, extensive proliferation and they can differentiate into multi cell lineages both *in vitro* and *in vivo* under well-defined culture conditions, and they are not deteriorated by freeze-thaw cycling. ES cells can differentiate into every embryonic germ layer pathway which are endoderm, mesoderm and ectoderm respectively. Unfortunately, in-vitro made, cancer-driven ES cells are proven to be impractical for clinical applications, but they contributed to scientists for showing the cell proliferation cycle mechanisms of stem cells as a model system *in vitro*. In 1981, first successful ES cells isolation was done in from murine subjects by using culture methods applied to other cell types. The first ES cells were harvested from a pre-implanted blastocyst which is a coagulation of cells covered with trophoblasts on the surface that is

responsible for creating inner cell mass (ICM). Blastocyst's ICM is known to be potent enough to differentiate into every type of tissue in the body, hence allowing the formation of the "embryo" ultimately. It is proven by even though they have brief lifetime *in vivo*, they can be proliferated ad libitum under culture conditions when leukemia inhibitory factor (LIF) is present. Murine ES cells have been impacted on so many fields of biological sciences and established the basis of genome manipulation technology which enabled creation of transgenic animals for investigating gene expression and regulations *in vivo*. Isolation of ES cells also enabled scientists to study mammalian development stages *in vitro* without harvesting actual embryos of subjects and they are still utilized to distinguish the mechanisms of pluripotency and cell lineage specification. After murine ES cell isolation, various experiments have been conducted to isolate ES cells from other species and this led to fabrication of specific cell lines from rodents, rabbits, pigs (Li et al. 2003), most importantly from humans (Orive et al. 2003).

Even though a considerable amount of time has passed since the first successful isolation of ES cells, its technology requires further attention due to its delicacies such as ethics so they can be implemented to clinical applications.

1.3.1.2 Induced Pluripotent Stem Cells (IPSCs)

Due to the technical challenges and ethical issues regarding embryonic cells, scientists directed reprogramming somatic cells to become stem cells again. Initial studies of cloned animals from sheep and frog subjects yielded the generation of induced somatic cells (Wilmut et al. 1997). This ground-breaking progress was done by fusing enucleated oocytes with somatic cells which was the first revelation of the reprogramming process that exists in the oocyte. Later, it was proven that isolated early embryonic stem cells (ESCs) do possess the same mechanism and they are able to reprogram adult cells by cell fusion (Tada et al. 2001). By investigating ES cells activity derived from early embryonic tissue, Takahashi and Yamanaka who are pioneers of induced-pluripotent stem cells (IPSCs) defined factors regarding reprogramming technology (Takahashi et al. 2006). Takahashi et al., induced a group of defined transcription factors Oct ¾, Klf4, c-Myc and Sox2 respectively into fibroblasts of

mouse subjects and they acquired cells that have pluripotency. These reverse-engineered cells have ushered a new age and they were named as IPSCs. Remarkably, these IPS cells retain the same gene profile as ES cells and a similar cell morphology and proliferation profile. Primary studies involved transfer of mouse IPS cells into early embryos so that they can contribute to tissue development *in vitro* and forcing transmittance of the germ line to the next generation (Maherali et al. 2007) (Okita et. al. 2007) (Hanna et al. 2007). After animal studies, it has come to inducing the human somatic cells to IPS cells by Takahashi and his colleagues. Ever since IPSCs have been heavily investigated in different subjects by different groups all around the world, including rats, monkeys, pigs and dogs respectively. (Esteban et al. 2009). The invention of these *in vitro* reprogrammed cells has been a remarkable milestone in stem cell technology and have been drawing attention since they can provide sufficient amounts of patient-specific pluripotent stem cells in every field that concerns cell therapy, toxicology, drug discovery and more.

1.3.1.3 Adult Stem Cells

Adult stem cells can be considered as undifferentiated potent stem cells, which are found in every part of the body after embryonic development and they proliferate progressively to replace and regenerate dying cells/tissues if there is damage present. It is known that maintaining and repairing the tissue (if it is damaged) in a living organism is adult stem cells' primary objective. However, Unlike the origin of the (the ICM of the blastocyst) ESCs, adult stem cells' origins in mature tissue is an area yet to be enlightened (Kalra and Tomar 2014).

Adult stem cells also known as somatic stem cells (SSCs) share two distinctive attributes with other stem cells. First one is possessing the ability of making identical copies of themselves which is termed as self-renewal. Latter one is that they can produce matured cells with specialized functions and characteristic morphologies. There is a middle ground between fully differentiated state of stem cells and their undifferentiated state which is called a precursor or progenitor cell. Stem cells generate this intermediate cell type so that they can reach the fully differentiated state. In adult and fetal tissues, progenitor cells are partly differentiated cells that divide and induce to

differentiated cells. These progenitors are considered as "committed" to a particular differentiation pathway, but this definition of committed is an ongoing dilemma. In a study conducted by Australian scientists (Winslow et al. 2001), progenitor/precursor cells were shown that they can differentiate into different specialized cell types thus falsifying the general perception of progenitor cells being committed to a single pathway (Figure 1.4).

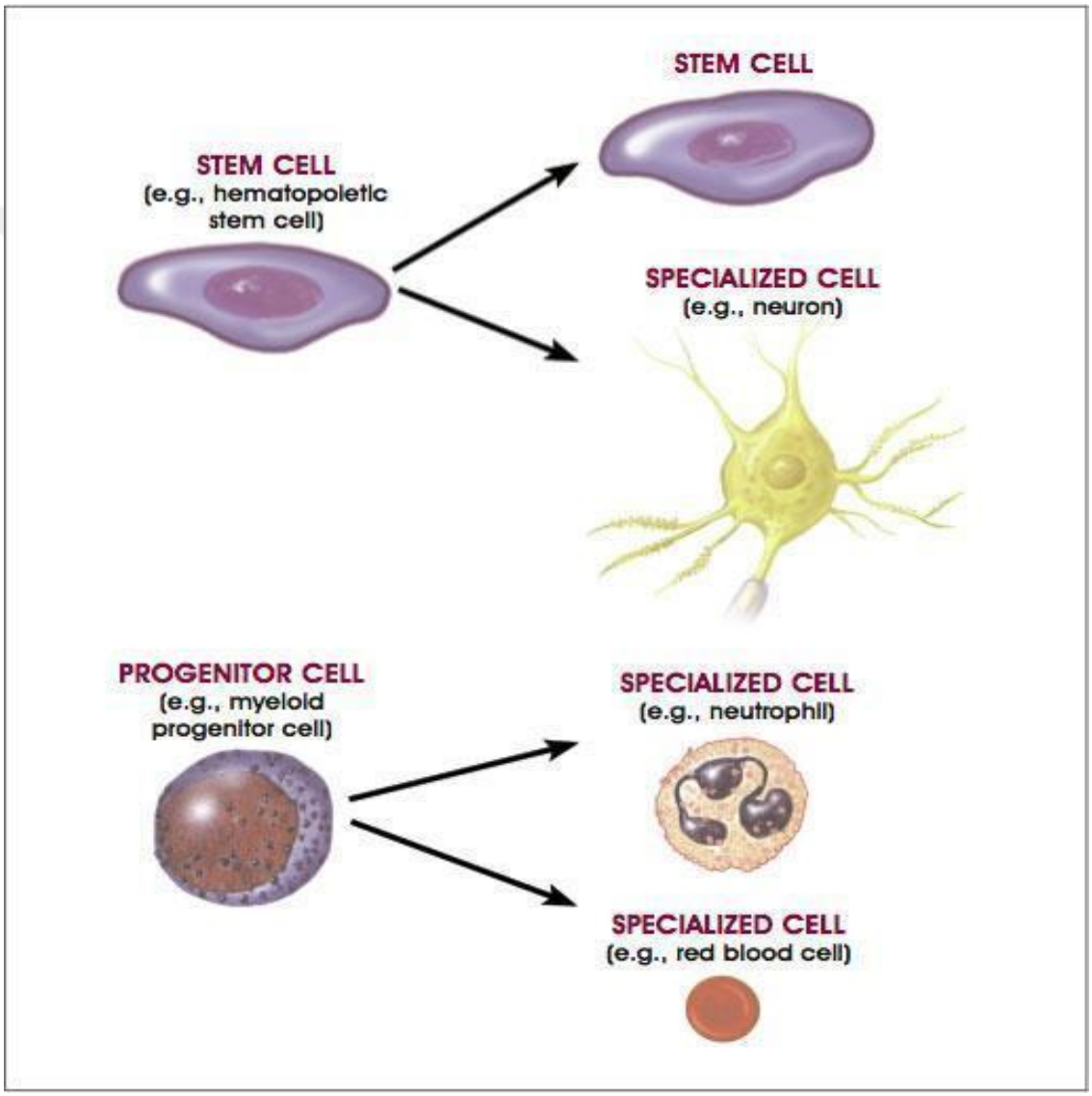

Figure 1.4 Comparison of stem cells and their progenitor/precursor cells (Winslow et al. 2001)

1.3.1.3.1 Adipose-Derived Stem Cells (ASCs)

As it was previously mentioned before in sections 1.3.1.1 and 1.3.1.2. ES cells and IPS cells are highly beneficial for scientists to reveal the underlying mechanisms of stem cells theoretically. However, there are quite a few limitations in practice to use them clinically due to cell regulations, ethical issues. Yet, somatic stem cells are abundantly available with no adverse effect of immune reactions and ethical dilemma if they are autologous. It has been revealed that mesenchymal stem cells which are isolated from bone marrow are potent *in vitro* such as adipogenic, osteogenic, chondrogenic, neurogenic differentiation. Then there is this drawback of bone marrow supply which is extreme pain to patients during the harvesting process and it results with low numbers of yield. That is why scientists were pushed to utilize mesenchymal stem cells (MSCs) as an alternative source. Adipose-derived stem cells (ASCs) have been compared to bone-marrow derived MSCs by such research groups (Yamanaka et al. 2009) and it was demonstrated that they are potent enough to differentiate as much as they are. Since the human adipose tissue is very common within the human body and it is acquirable with ease in massive quantities from liposuction operations without any discomfort given to patients, it provides a great alternative compared to other mesenchymal stem cell sources for tissue engineers.

1.3.2 Scaffolds for Bone Tissue Engineering

Scaffolds, that are used in bone TE, are classified by their raw materials. Commonly either natural or synthetic materials are utilized for bone tissue constructs. However, in the last couple of years there is also a trend of using both in a hybrid structure as this study also being of its examples. The idea of creating hybrid structures holds on the possibility of eliminating the disadvantages of both sides and manages to have the ideal structure with demanded properties. Typically used biomaterials in the scaffold fabrication are elaborated in the Table 1.1.

Table 1.1 Categorization of biomaterials used in scaffold fabrication (Alaribe et al. 2016)

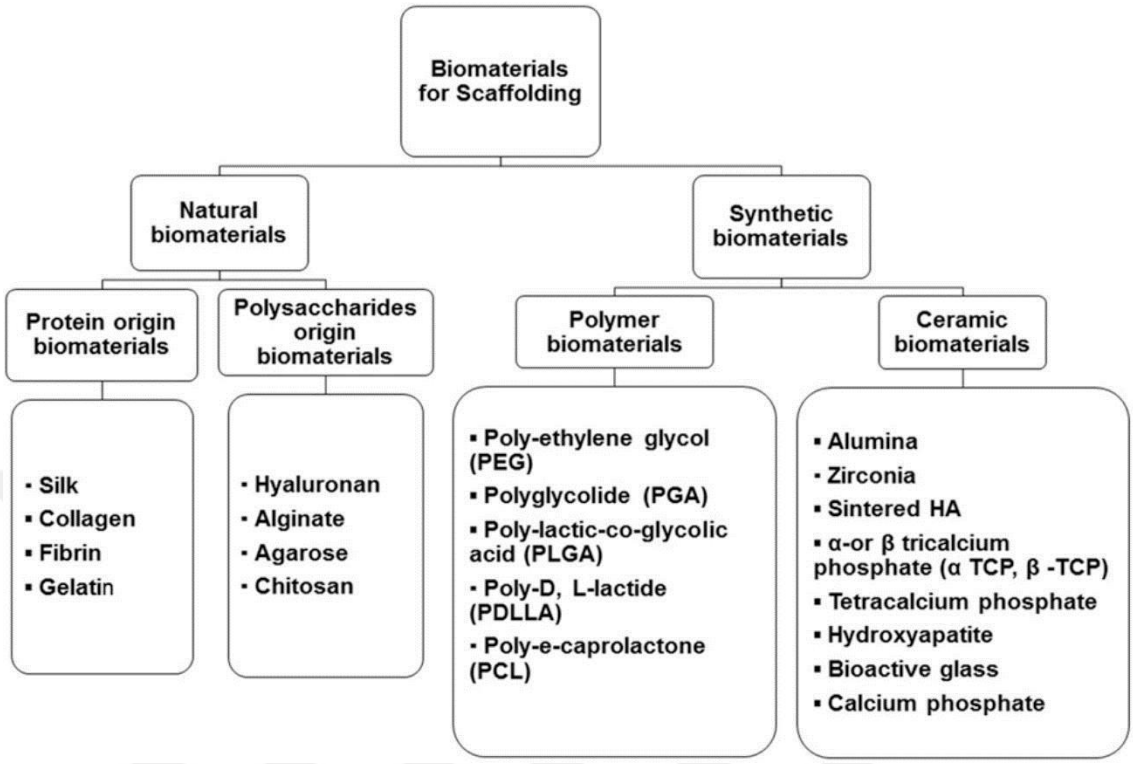

1.3.2.1 Natural Polymers as Scaffold Materials

Currently, there are quite a few natural polymers utilized as candidate materials of scaffolds for bone TE applications. Due to them being the natural components of living structure, naturally derived polymers are focused by researchers since they possess a fair share of similarities to natural tissue in terms of chemical and biological structure. Numerous studies are present in the literature claiming that various proteins have been utilized in studies regarding *in vitro/ in vivo* such as collagen, silk, polysaccharides and chitosan. (Jiang et al. 2009)

1.3.2.2 Synthetic Polymers as Scaffolds

Besides natural polymers, synthetic polymers are heavily investigated as they are already abundant due to industrialization, can be mass produced with relatively low costs and most importantly they are easier to process. Even though in theory, they seem to be more beneficial to be used in TE applications, they have a main disadvantage: accumulation of degraded unnatural products in the body which can be potentially harmful.

Commonly poly(α-hydroxyesters) like, polylactic acid (PLA), polyglycolic acid (PGA), poly(lactic-co-glycolic) acid (PLGA) and their derivatives are studied in bone TE applications (Hacking and Khademhosseini 2009).

Synthetic polymers such as polycaprolactone (PCL), polyethylene glycol (PEG) and propylene fumarate (PPF) have shown to be useful in various applications made by different groups. (Deschamps et al. 2004) (Drury and Mooney 2003)

1.3.2.3 Hybrid Scaffolds

Hybrid scaffolds have risen in the field of bone TE due to the potential they carry. Theoretically, having pros of both synthetic and natural elements is a novel approach to build the optimal structure. If they can be built without any complication, hybrid scaffolds are superior to natural and synthetic based scaffolds since their properties are better both mechanically and structurally. Yet, the hybrid structures tend to be more complex obviously with the involvement of several materials. This makes the scaffold to be more delicate and harder to process and potentially increase the chance of having complications. However, there are significant efforts made in the literature regarding combining different material types in order to create hybrid scaffolds such as hybrid structures made by combining chitosan with alginate for bone TE by (Li et al. 2005), It was reported that silk fibroin with graphene oxide hybrid structures were fabricated by (Lu et al. 2015) for making bone substitutes. Additionally, an article by (Park et. al, 2016) addresses the fabrication of 3D SF/β- TCP hybrid scaffolds for bone tissue reconstruction.

1.3.3 Scaffold Manufacturing Methods

Since the driving factor of cellular activity maintenance and interconversions of the connective tissue cells (osteoblasts, chondrocytes and fibroblasts) depending on their geometry and adhesion, the architecture of a scaffold should be designed according to the geometry of cell adhesion sites so that it can enable their anchorage, propagation and alignment. Due to this cause, architecture of the scaffold has absolute importance along with adaptability to the defect site so that cell behavior can be managed.

One of the properties that have the utmost importance of designing a scaffold structure is porosity. Porosity is the key element of the scaffold structure which facilitates the proliferation of cells by enabling nutrients and oxygen transfer. In addition to substance transfer, they create enough space for bone ingrowth and vascularization of stem cells seeded in the scaffold. For the last two of decades, several techniques have been tried to construct 3 dimensional structures one of which is solvent casting/particulate leaching that is fairly easy to conduct yet results in poor interconnectivity and control over pore size. Other than solvent casting, there are other techniques for scaffold production which have been frequently employed by various groups such as electro/wet spinning techniques, melt molding, gas foaming and membrane lamination (Ashammakhi et al. 2008) (Almirall et al. 2004) (Thomson et al. 1996). However, there is one common drawback for these methods mentioned above that is the inability to construct structures in predetermined properties. Along with their challenge of defined form disability, they also have poor reproducibility rates and irregular pore size on top of insufficient pore interconnectivity. However, there is a new trend of techniques emerging in the tissue engineering field which eliminates all these problems called “Additive Manufacturing Methods”. Additive manufacturing (AM) methods are innovative state-of-art technologies developed within the last two decades. These methods and their virtues are furtherly explained in the section below. This new era of additive manufacturing has the potential for overcoming previously mentioned fabrication methods’ all issues

.

1.3.3.1 Spinning Techniques

Scaffolds that have fibrous homology have been studied for the last three decades since their desired levels of porosity for cell propagation making them potential candidates for bone TE grafts. Spinning techniques are considered as a manufacturing method for fabricating such polymeric fibers. Main constituents of these methods wet, dry and melt spinning respectively. Extrusion of a viscous molten polymer through a spinneret at a constant and fairly high pressure is the mechanism that lies beyond melt spinning. With this technique continuous filaments of polymeric fibers are aimed.

Dry spinning facilitates a polymeric solution as its extruded material rather than a molten polymer. The polymeric solution gets to be ejected through a spinneret rather than a molten solid polymer.

On the other hand, wet spinning facilitates a coagulation bath in order to obtain fibrous filaments. Various synthetic polymers such as thermoplastic polyurethane (TPU), PCL, PLA and PLGA that are rigid enough are fabricated by wet spinning technique in bone TE applications. Additionally, natural polymers like cellular acetate and chitosan have been tried to prepare fibrous scaffolds. (Ergene et al. 2019)

Another spinning method is electrospinning which is a relatively new method (compared to other spinning techniques) and it draws more attention since it enables to form evenly sized fibers at nano and micro-scale. Electrospinning applications can be conducted on both synthetic and natural polymers. Very thin filaments can be extruded, and 3D multilamellar structures can be achieved.

There are also hybrid techniques where a combination of two different spinning techniques happen in order to mimic the micro and the macro structure of the ECM (Lee et al. 2018). Figure 1.5 schematically demonstrates each aforementioned method in detail.

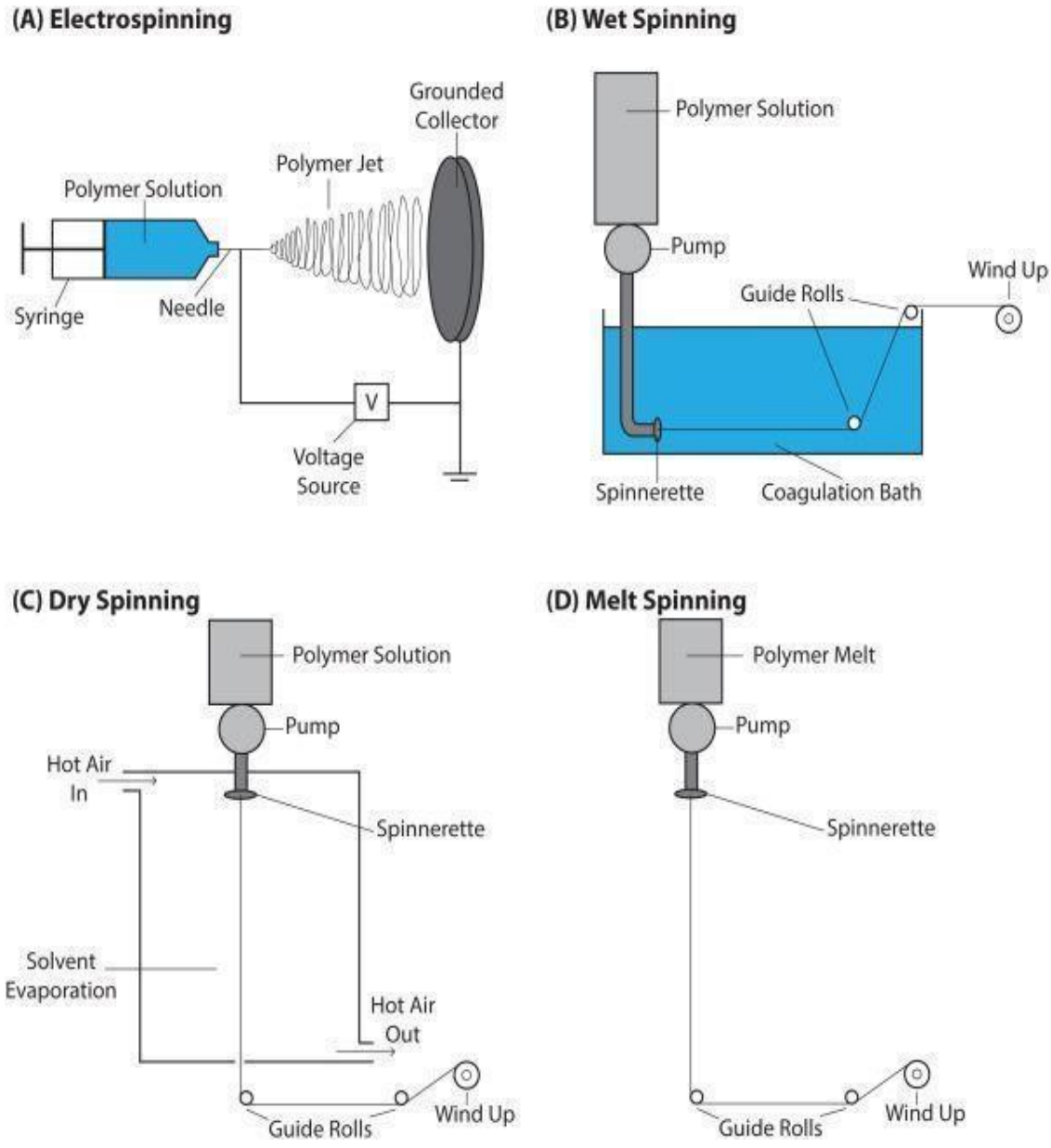

Figure 1.5 Different spinning techniques for fiber production; (A) electrospinning, (B) wet spinning, (C) dry spinning, (D) melt spinning (Tuin et al. 2014)

1.3.3.2 Additive Manufacturing

American Society for Testing and Materials, an association that designates standards for materials available in the market, defined "additive manufacturing" term as 'the process of joining materials to make objects from three- dimensional (3D) model data, usually layer upon layer' (ASTM 2012), and AM has been used for tissue engineering scaffold fabrication. These manufacturing methods involve techniques such as stereolithography (SLA), fused deposition modelling (FDM) and selective laser sintering (SLS) etc. (full list of all methods in TE is given at table 1.2).

As it is briefly explained in section 1.3.2, primary benefits of these techniques are enabling tissue engineers to obtain their scaffolds in a desired geometry with high resolution and fully interconnected porous architecture. This benefit allows them to customize their scaffolds in shape, size and pore distribution. Integration of 3D modelling methods such as "Magnetic Resonance Imaging" (MRI) and "Computerized Tomography" (CT) with these manufacturing methods created the field "computer-aided manufacturing" abbreviated as "CAM". Initially 3D model data is acquired through these modelling methods and this data is incorporated with computer-aided design (CAD), thus making a suitable design for additive manufacturing techniques. Alternatively, a 3D model can be sketched without any scanned/acquired data from imaging methods and can be directly implemented to computer-aided manufacturing (CAM). Moreover, there are examples of designs based on mathematical equations (Gabbrielli et al. 2008) or topological information optimization (Freitas Júnior et al. 2010) gathered from an object's surface geometry by X-ray fluorescence (XRF) scanning. There is a universal extension for CAD conversions to CAM designs which is called standard tessellation language (STL) that can be read by every additive manufacturing device. This STL file contains information regarding the design's 3D structure and surface geometry. Depending on the method of the device, .stl file is then sliced into layers which is acknowledged digitally by the printer's computer and commands the machine's motions accordingly. Consequently, the design gets manufactured layer by layer either from top-to-bottom or bottom-to-top with varying resolutions.

Table 1.2 General classification of additive manufacturing methods (Madrid et al. 2019)

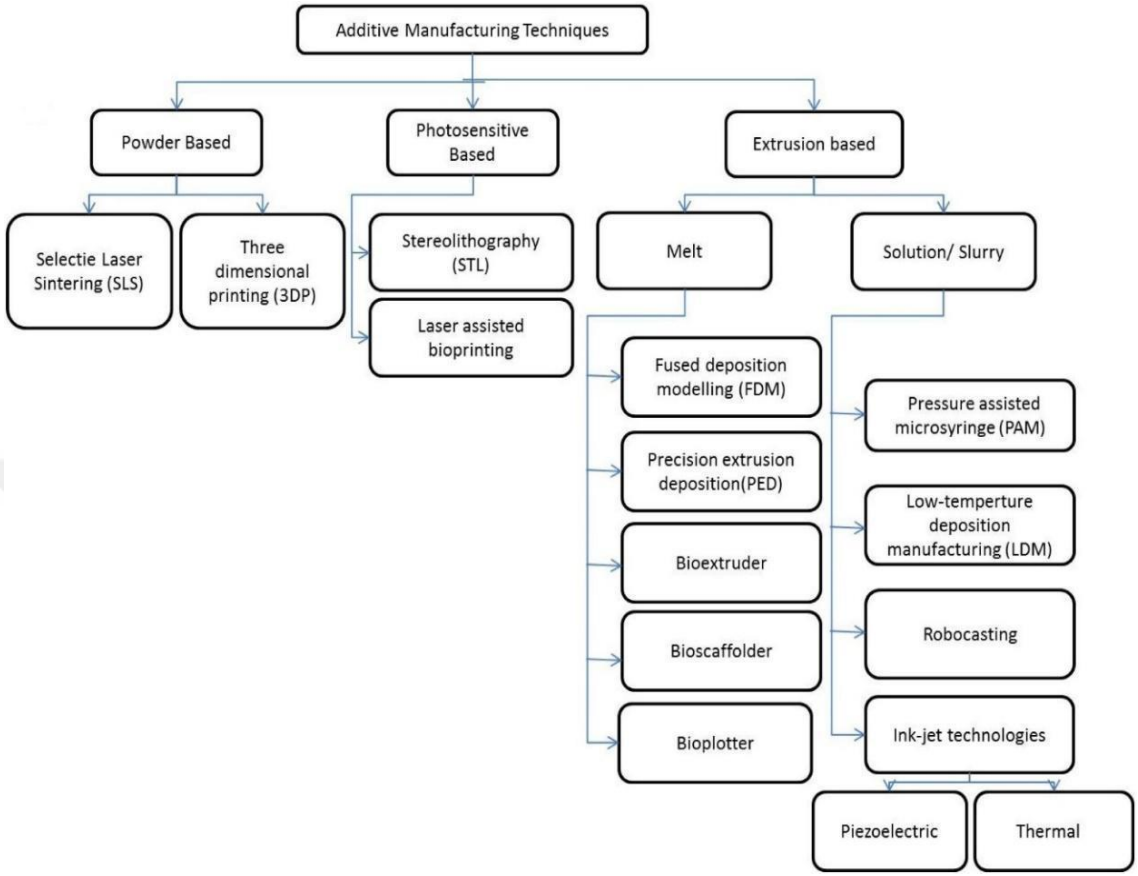

Figure 1.6 represents each stage of a TE application carried out by using additive manufacturing. Initially, (a) anatomic 3D data is received from the patient by an imaging method, then (b) the defect is processed to CAD. According to the 3D CAD of the defect, (c) biomimetic scaffold is designed and converted into a STL file, leading to the manufacture of the scaffold with desired geometry. Fabrication of scaffold is done by (d) extruding ink material through a nozzle and the (e) final construction was obtained. Depending on the application, processes carried on with cell culturing (f) statically or (g) dynamically using bioreactors. In the end, primed scaffold undergoes (h) implantation in the patient generating (i) tissue regeneration on the defect site.

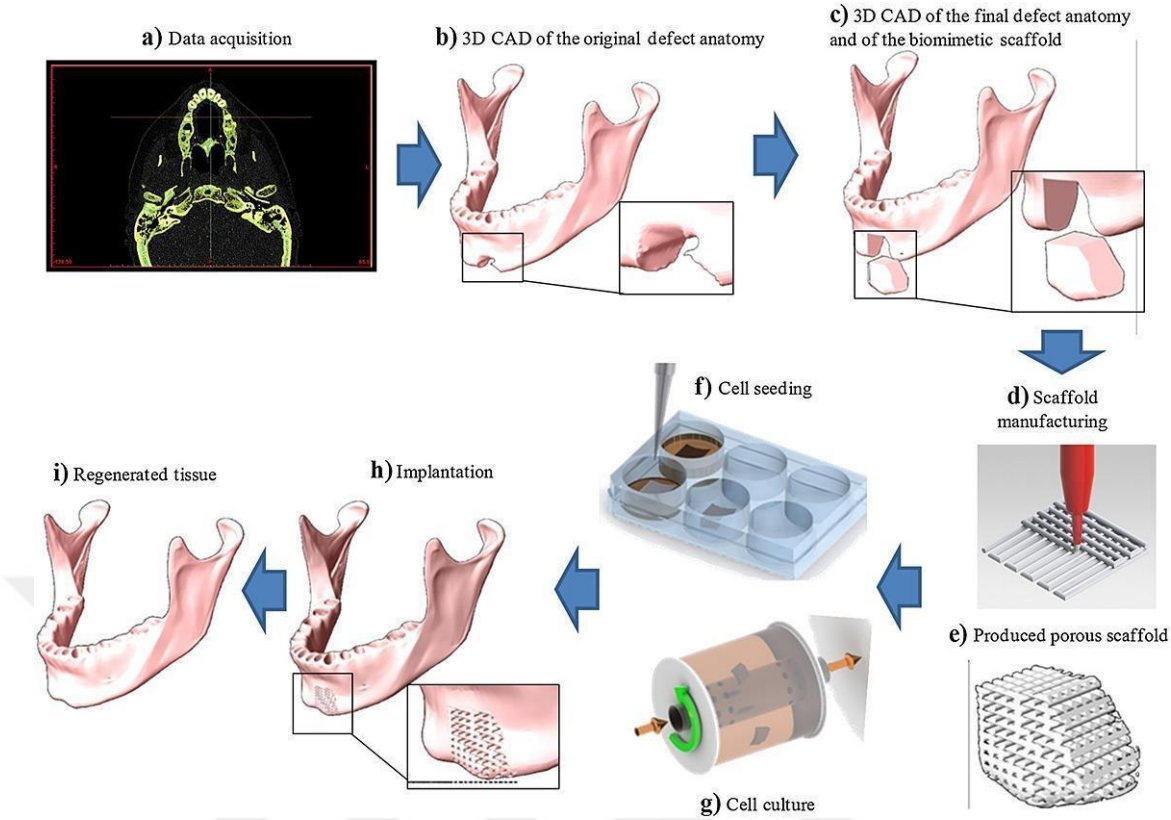

Figure 1.6 Schematic representation of steps performed in scaffold-based tissue engineering applications (Mota et al. 2012)

By each passing day, there is an emergence of custom-made novel additive manufacturing methods by well-known industries and academics for developing tissue engineering scaffold fabrication. Despite that, for the last decade, most common and well-established methods are generally SLA, SLS and FDM techniques.

1.3.3.2.1 Extrusion Based Additive Manufacturing

1.3.3.2.1.1 3D Bioprinting & Bioinks

3D bioprinting, as it is the investigated subject of this thesis, is a method based upon depositing bioinks through a nozzle with either encapsulating cells or loading cells within the bioink. This technique allows printing the bioink in the required shape in order to form subtle structures that can be compared to tissues. 3D bioprinters usually consist of either a moving nozzle with fixed platform or a fixed nozzle with moving platform in three dimensions (x, y, z axis). The nozzle's movement is controlled by the coordinates acquired from the CAD file. Over the past years, 3D bioprinting applications have been massively increasing since its merits such as cost-effectiveness, simplicity, relatively precise deposition and cell distribution controllability. In order to enhance the printability parameter of 3D bioprinters, bioinks should be furtherly investigated and optimized for a larger extent of applications.

Table 1.3 Comparison table of bioinks currently used in TE applications (adapted from Panwar et al. 2016)

Materials	Advantages	Disadvantages	Crosslinking methods
Alginate	Relatively low cost, high gelation rate, biocompatible, good printability	Relatively low cell adhesion, can degrade during culturing	Ionic
Agarose	Simple, mediocre mechanical properties, good stability	Poor cell adhesion, not biodegradable	Thermal
Methylcellulose	Decent printability and biocompatibility	Can degrade during cell culture, not ideal for long-term culturing	Thermal
Chitosan	Biocompatible, can be processed to be antibacterial	Poor mechanical property, slow gelation rate	Ionic or covalent
Hyaluronic acid	Substantial cell proliferation, high gelation w/ modifications	Fast degradation, low stability	Ionic or covalent

Table 1.3 Comparison table of bioinks currently used in TE applications (adapted from Panwar et al. 2016) (Continued)

Gelatin	Relatively cheap, High cell adhesion and viability, biocompatible	Low printability, poor mechanical strength	Thermal
Gelatin Methacrylate (GELMA)	Versatile, good biocompatibility, tunable properties, photocurable	Relatively low printability	Photocurable, UV light
Polyethylene Glycol Diacrylate (PEGDA)	Photocurable, relatively biocompatible	Requires chemical modification, not degradable	Photocurable, UV light

Bioinks possess a substantial amount of significance considering they are the main constituent of the 3D bioprinting concept. Recently, there are various studies in the literature regarding bioink development and printability (Ozbolat et al. 2016). Majority of the studies concern synthetic and natural polymers such as hydrogels. Some of the materials used as bioinks and their properties are elaborately noted at table 1.3. Endless potential of creating new bioinks for better biocompatibility, precise resolution, and biomimicry lies ahead to overcome the limitations.

1.3.4 Growth Factors and Their Use in TE

Growth factors have been utilized extensively since the beginning of the tissue engineering field. It has been known that they are crucial biomolecules for cell proliferation and inducing differentiation on stem cells. That is why, their incorporation into TE applications is a common practice among tissue engineers. Growth factors are members of large polypeptide molecules which are naturally released in healthy cell lines of the living body. It was proven that GF's respond with variably different mechanisms under different levels of concentration and exposure time on cells. Already proven effects of growth factors are manifested as follows (Chen et al. 2010):

- Enabling direct migration of cells (chemotactic)
- Triggering cell division process (mitogenic)

- Inducing cell differentiation (morphogenic)
- Initiating apoptosis of cell (apoptotic)
- Regulating metabolic activity (metabolic)
- Downregulating acute inflammatory process (anti-inflammatory)
- Stimulating blood vessel formation (angiogenic) and their combinations of all above.

1.3.4.1 Bone Morphogenetic Proteins (BMPs)

Bone morphogenic proteins are a subfamily of the TGF-β growth factor family. As it is mentioned in the previous section's growth factors are multifunctional molecules and BMP's are no exception. Since the beginning of first identification of BMP activity, they have been drawing attention from scientists who have expertise in different fields such as neuroscience, genetics, orthopedics, regenerative medicine. (Di Chen et al. 2004) Currently, it has been identified that BMP subfamily consists of more than 20 types and subtypes. Figure 1.7 reflects a detailed categorization of TGF-β superfamily and BMP subfamily.

BMPs are such valuable assets in tissue engineering due to their multifunctionality. Initially, it has been thought that the secretion of these signaling molecules are triggering bone and cartilage formation. To date, it is known that they are also pivotal molecules that can orchestrate tissue architecture.

In bone TE applications, BMP-2 is a frequently used member of BMP subfamily due to their proven effect of inducing osteogenic differentiation in various cell types. (Reddi and Reddi 2009) That is why, BMP introduction to an artificially engineered tissue substitute is essential due to their profound capacity of turning stem cells into specific cell-lineages like osteoblasts.

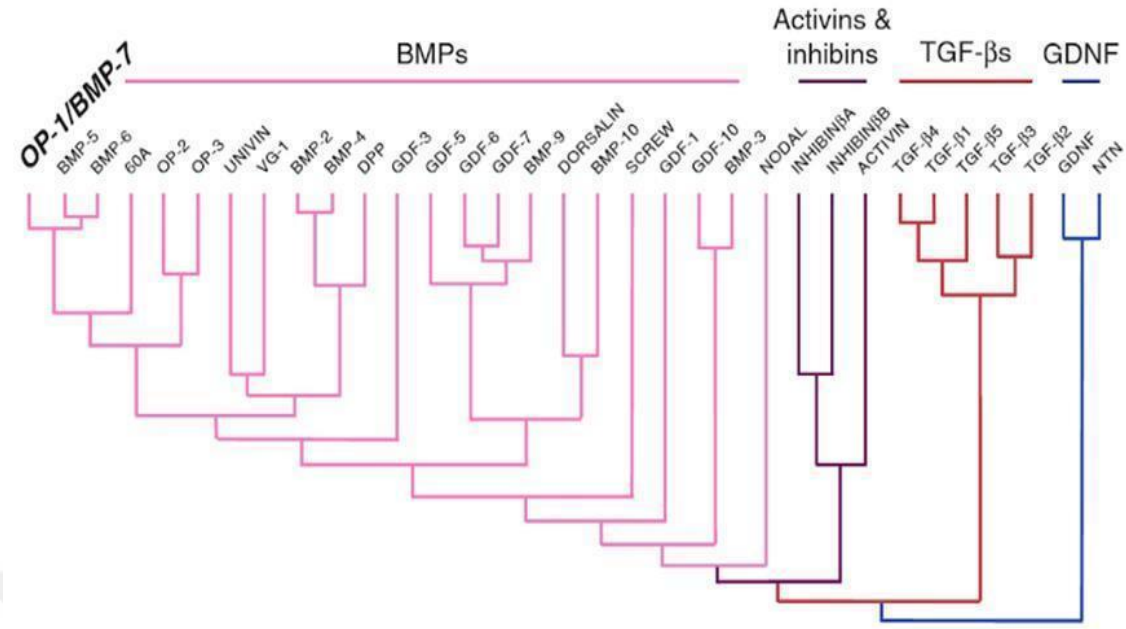

Figure1.7 TGF-β superfamily chart (Anonymous n.d.)

In such pathologic occasions such as cancer, it has been shown that BMP signaling often results with misregulation (Zabkiewicz et al. 2017). By the virtue of their multimodality, these molecules and their expression are investigated in order to understand the molecular mechanism of diseases.

1.3.4.2 Vascular Endothelial Growth Factors (VEGFs)

Presence of vascular formation is a prerequisite for vertebrates and their embryogenesis. It comprises two main routes which are vasculogenesis and angiogenesis respectively. Vasculogenesis is the initial differentiation of endothelial cell progenitors and their development into the primary capillaries. This process is followed by angiogenesis which is formation of new capillaries and their spreading into surrounding tissues pre-existing vessels.

By bioinformatics technology, it has been determined that VEGFs are members of the platelet-derived growth factor (PDGF) family which is a subfamily of cystine-knot like protein superfamily. These cystine-knot like proteins are hormones that are responsible for transmitting signals extracellularly (Ursula et al. 2001). Cystine-knot structures are formed by combination of eight cysteine residues by disulfide bonds (Figure 1.8).

VEGFs, being a glycoprotein hormone, mostly resemble mucin-like proteins and are related to the TGF-β family distantly.

Yeast is a unicellular eukaryote organism which does not possess any cystine-knot type protein, this proves that evolutionarily cysteine structure has come out to perform extracellular-signaling among cells in organisms that have tissue organization.

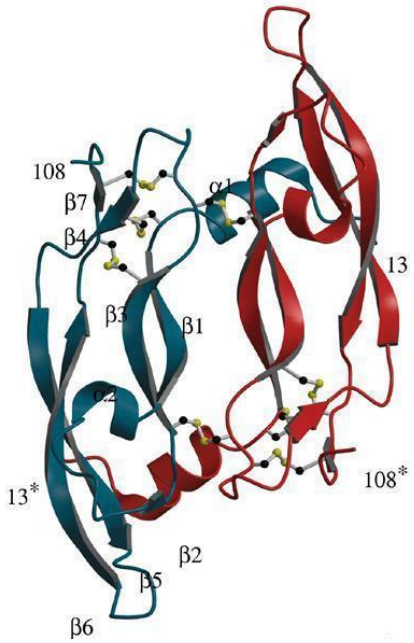

Figure 1.8 Illustration of molecular structure of VEGF (Muller et al. 1996)

Since improved vascularization of a newly-formed tissue is crucial for overcoming a tissue-loss, VEGFs are key molecules that have been used in TE applications. Without the formation of blood vessels, sustaining the viability of an artificial substitute is not probable due to inadequate exchange of nutrients and oxygen cells within the tissue. That is why, VEGFs are delivered to tissue-scaffolds using different methods (Soker et al. 2000).

A comprehensive investigation of the role of VEGF in the human body can pave the way of discovering novel therapies for diseases that are related to blood vessel damage. Therapeutics for ischemic diseases such as coronary artery disease, myocardial ischemia and stroke have been studied by using VEGFs (Maharaj and D'Amore 2007).

1.3.5 Bioreactors

Final step of engineering a tissue is to put the bioprinted/cell-seeded scaffold material into a culturing environment. This culturing environment can either be static or dynamic. Conventional method of static culturing of cells/tissues is a simple method yet has certain limitations. In 2D culture, the transfer rate of nutrients/oxygen and accumulation of waste products are issues that should be dealt with. Consequently, the search for new culturing methods emerged (Selden and Fuller 2018).

Table 1.4 Comparison of different culturing methods with the use of bioreactors (Mabvuure et al, 2012)

Types of Culture	**Description**	**Mass Transfer Mechanism**	**Shear Stress**	**Advantages & Disadvantages**
2D - Static Culture	*In vitro* culturing with no flow of medium	Diffusion	None	Simple, requires no specific equipment
Stirrer Flasks 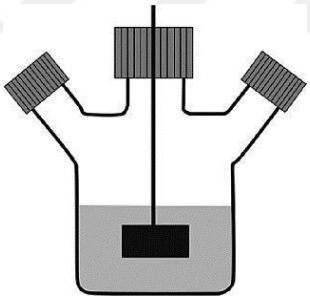	Constant stirring of culture medium with magnetic field	Convection	High	Increased mass transfer compared to static culture yet applies high shear stress to cells.
Rotating Wall Systems 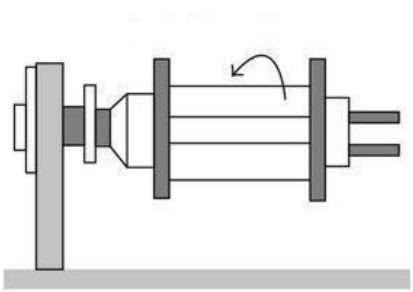	A cylindrical system that rotates cell/medium suspension	Convection	Very Low	No turbulence effect of stirrer flasks, allows large body culturing

Table 1.5 Comparison of different culturing methods with the use of bioreactors (Mabvuure et al, 2012) (Continued)

Perfusion Bioreactors 	Direct flow of medium through the cell-laden scaffolds	Convection	Mode rate	Better controlled culturing environment compared to static culturing, applies moderate levels of shear to cells

With the help of developing technology and manufacturing methods, application-specific machines known as bioreactors have become more common among TE applications. Bioreactors are complex custom-made machinery that allows tissue culturing to take place in a 3D environment with different methods. Table 1.4 represents common 3D culturing bioreactors and explains general description, mass transfer mechanism, and pros/cons of each bioreactor technique (Salehi-Nik et al. 2013).

In every bioreactor system following parameters must be adjusted in order to perform a successful 3D cultivation (Marijanovic et al. 2016):

- Temperature
- pH
- Oxygen diffusion
- Nutrient transport
- Waste removal

The dimensions of engineered-tissues are mostly small since fabricating a larger-scale scaffold is one of the greatest TE challenges. Culture-dish driven cells do not possess their own feeding mechanism and are obliged to be taken care of. Utilization of bioreactors is beneficial for simplifying the culturing process by regulating the flow of

fresh media and waste products constantly. Specific bioreactors can also contribute to increased oxygen diffusion to scaffolds. By the aid of bioreactors, it is feasible to culture macro scaled tissues that can be clinically applicable compared to statically cultured tissues.

Another purpose of bioreactors is to stimulate the scaffolds and induce specific differentiation. Some differentiation pathways of stem cells necessitate external stimulus. For instance, skeletal muscle histogenesis of muscle progenitor cells can be mechanically induced by applying tension with a suitable frequency (Maul et al. 2011).

The future of ex-vivo tissue engineering relies on developing more enabling, complex, beneficial bioreactor systems. Implementing bioreactors to such tissue culturing applications will eventually replace 2D- static culturing since it is superior in every aspect except the price. This is mainly dependent on the speed of bioreactor machinery manufacturers and their cost-cutting measures.

1.4 Controlled Drug-Delivery Systems

Drug delivery systems are specifically designed approaches that focus on provision of optimum levels of therapeutics. These systems should be able to respond to such physiological changes when delivered *in vivo*, hence being capable to "sense" the environment and change its release profile accordingly (Kost and Langer 1992).

These systems are adapted within the frame of TE since sustained delivery of required biomolecules to induce differentiation and tissue formation is demanded. Naturally, the human body regulates the number of biomolecules (aforementioned in section 1.3.3) released and their duration within the circulation in a strict manner. In order to mimic this regulation of release profile, smart vehicles are needed to control delivery of such growth factors from scaffolds.

In conventional therapies, growth factors are administered by applying excessive doses with either single or multiple injections into the defect site. Nevertheless, this approach eventually ends up with a significant amount of injected agent loss through leakage to

surrounding regions of the defect site. This serious issue emerges a need for more localized delivery of bioagents in a controlled manner.

To eliminate leakage/loss during injections, researchers have been developing growth factor encapsulation methods. Encapsulating such bioagents enable constant levels of concentration for long periods on the defect site so as to achieve ideal therapeutic effect. Moreover, adding such delivery systems to conventional bone TE approaches is also beneficial for governing new bone tissue formation if such parameters as release kinetics and drug entrapment are optimized. Natural ECM possesses GFs within itself and modulates the secretion levels of GFs, that is why to imitate this natural phenomenon, controlled delivery systems should be integrated with TE applications so that the fabricated constructs can act multifunctional. Multifunctionality of these tissue substitutes should involve osteoinduction, osteoconduction and osteointegration (Albrektsson and Johansson 2001). Osteoinduction is a part of the natural bone regeneration process after a fracture occurs within the body. This phenomenon has utmost importance since the majority of bone healing is dependent upon its occurrence. During this process, immature cells differentiate into pre-osteoblasts trying to replenish lost cells due to fracture. Furtherly, osteoconduction is the following step which comprises bone growth on the surface of a bone implant and finally osteointegration comes up which is, as its name implies, a parameter of how efficient and solid an implant integrated with the surface it is implemented on.

To deliver desired bioactive materials which have eligible above mentioned properties, simple yet efficient carrier systems are needed. Since the carried molecules are mostly proteins that can be easily denatured by external factors such as high temperature or toxic solvents, these systems are mostly based on polymeric carriers which are free of these hazardous external factors.

There are heaps of different polymeric carriers designed within the literature, yet most commonly used ones are microspheres, nanospheres and injectable gels (Tayalia and Mooney, 2009). Polymeric vehicles are also utilized in TE as plasmid DNA carriers to enable growth factor production with the host cells that receive the factor and express the given DNA at the defect site (Storrie and Mooney 2006). Besides, D.J. Mooney, a pioneer in polymeric drug delivery systems, and his colleagues also have different

studies involving polymeric vehicles that carry cells for desired growth factor secretion (Chen and Mooney 2003).

For the last two decades, various strategies were adapted in order to release BMPs in bone TE applications. Synthetic polymers such as PLA, PCL (Miyamoto et al. 1992) (Huang et al. 2010) and natural-based polymers like alginate, collagen and chitosan (DeLustro et al. 1990) (Hu et al. 2007) (Pandey and Khuller 2004), or block copolymers (Miyamoto et al. 1993) of these polymers are widely used for developing GF carrier systems. Hydroxyapatite based carriers are also promising materials for BMP carrier systems; it has been reported that absorbability and controlled release rates of BMP-2 has positive effects on bone formation (Xie et al. 2010). Another group shared their results which involve PLGA coated β-TCP scaffold permitting high mechanical stiffness and desired biocompatibility with the aid of controlled VEGF release (Khojasteh et al. 2016).

1.4.1 Nanotechnology Influence on Delivery Systems

Nanotechnology, the technology that refers to the atomic scale that has lengths of one billionth of a meter, unveiled thousands of possibilities to researchers after its discovery. This ground-breaking technology set a milestone on fields like aerospace engineering, materials science, microchip technology, agriculture as well as medicine. By the aid of nanotechnology, technically unreachable sites in the body such as tight junctions of hair follicles (Lademann et al. 2009), intraocular membrane (Baba et al. 2011) and blood-brain barrier (Hwang and Kim 2014) of the brain were penetrated, hence enabling the accumulation of agents in demanded regions. Due to their incredibly diminished sizes, nanocarriers are advanced vehicles for increasing drug uptake by the cells because of their high mobility through condensed ECM of tissues compared to larger scale microparticles.

Despite the fact that, there is a matter of debate going on with nanomaterial and nanoparticle definition (Boholm and Arvidsson 2016), generally particles that at least one dimension of its size between 1nm to 100nm are considered as nanoparticles. Intended delivery of the molecules are entrapped within the nanoparticles with either adsorption, encapsulation, or direct dissolution of the material within the nanoparticle

containing batch. These nanoparticles can either have hollow (nanocapsules) or bulky (nanospheres) structure where its porous surface permits material release to the surrounding exterior. Nanotechnology has enabled researchers to modify their elder methods of microcapsule fabrication methods such as water-in-oil emulsion. Other than nanoparticles, dendrimeric micelles are also a hot topic in the field of therapeutics due to their potential as being drug delivery agents. (Zhang et al. 2003)

Polymeric nanoparticles such as PCL-based nanocapsules are approved products by the Food and Drug Administration (FDA), US in terms of biocompatibility and another profit of them is to be able to degrade over time which qualifies them ideal candidates for drug-delivery systems. There are several successful researches concerning controlled release of bioactive agents (Yilgor et al. 2009) (Carletto et al. 2016) (Mahmoudi et al. 2020). The key parameters that should be noticed are molecular weight of the polymer, degradation rate over time, crystal structure and its hydrophilicity. It has been shown that by altering these attributes it is possible to perform the expected release rate of encapsulated molecules (Fox et al. 2009).

1.4.2 Multiple Growth Factor Delivery

In today's drug delivery systems used in TE, the upcoming trend is to deliver multiple bioactive molecules from one tissue construct considering various molecules are expressed during natural bone healing (Suárez-González et al. 2014). For instance, in a research article concerning neural TE, it has been reported that co-delivery of neurotrophic factors resulted with early regeneration of nerve conduits in mice subjects (Madduri et al. 2012). Additionally, during the bone regeneration process it was found that alkaline phosphatase (ALP) activity was increased upon delivery of BMP-2 and BMP-7 sequentially in comparison to single growth factor delivery (Basmanav et al., 2008). In a cartilage TE related work, it was demonstrated that spatiotemporal delivery of IGF delivery prior to BMP delivery from a bilayered alginate composite, can have synergistic effect in osteochondral defects (Lu et al. 2014). A novel injectable delivery system made from hydrogel was developed for delivering dual growth factors of bFGF and BMP-7 respectively, facilitating osteoblastic cellular differentiation in a scaffold (Dyondi et al. 2013).

In this thesis, multiple delivery of GFs was studied in order to administer simultaneous occurrence of osteoblastic differentiation of low passage ASCs and angiogenesis of new blood vessels coming out from newly formed tissue. The endothelial capacity within low passage MSCs results with greater angiogenesis potential compared to overly passaged cell lines.

1.5 Scope and Novelty of the Study

In this thesis, 3D printing and controlled release technology were used in coordination where ASCs were utilized as a single cell source to produce vascularized bone using spatiotemporal cues. ASCs are a heterogeneous source of cells possessing mesenchymal stromal cells that can produce bone through osteogenic induction with BMP-2, and endothelial cells that can produce vessels within the graft through stimulation with VEGF. BMP-2 and VEGF were encapsulated within polymeric nanocarriers that were placed in predetermined positions within the graft during 3D bioprinting. Haversian and Volkmann canals of cortical bone are formations along the bone which enables nutrient and oxygen exchange for tissues that they go through (Figure 1.1). In this research proposed graft was designed with a specific architecture where enough vacancy is present for vessel formation in order to mimic the structure of these canals of native bone (Figure 1.9).

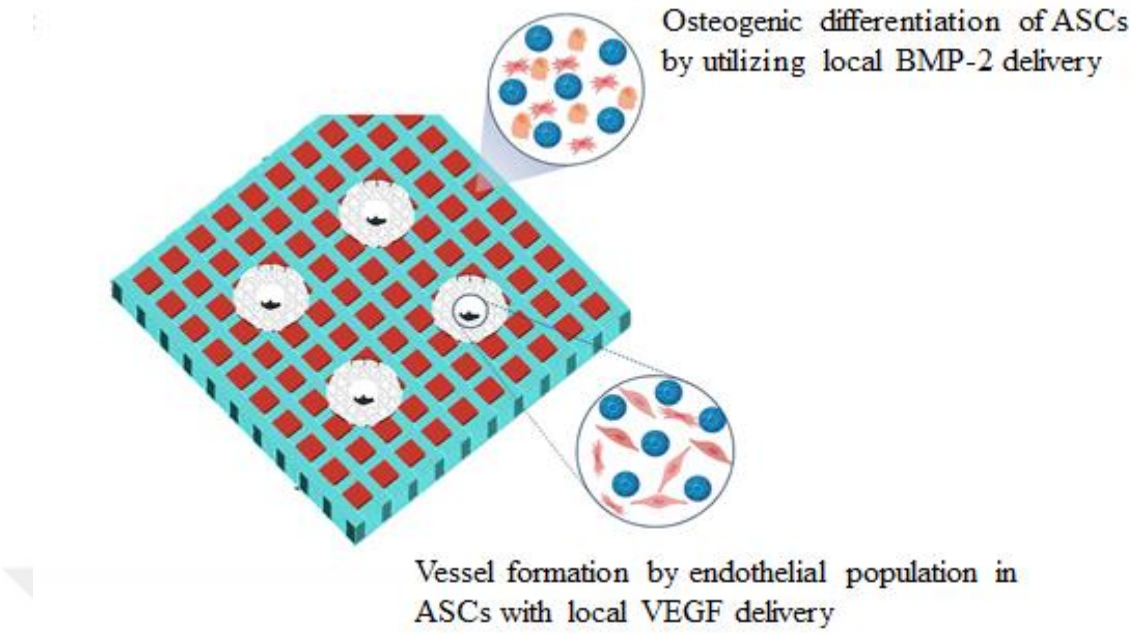

Figure 1.9 CAD design of the architecture from the top view; red areas represent osteogenic tissue formation within alginate fibers from BMP-2 release where white canals portray alginate fibers that generate angiogenesis by the aid of localized delivery of VEGF

Customizable 3D models were uploaded to the 3D bioprinter (Envisiontec GmbH, Germany) which has two simultaneous print heads. One of the heads was used to 3D print poly(ε-caprolactone) (PCL), a hard and biocompatible thermoplastic polymer, to provide the anatomical shape. The other print head was used to print alginate within which autologous ASCs and PCL nanoparticles loaded with BMP-2 and autologous ASCs and PCL nanoparticles loaded with VEGF were loaded before printing. BMP-2 and VEGF that were released from the PCL nanoparticles were expected to induce the osteogenic differentiation of ASCs and vessel formation, respectively. By means of unique architectural design of the scaffold, native bone structure is practically imitated, thus creating a desired graft candidate that can be an off-the-shelf product. On top of the design, benefits of having a single cell source and less material combination which are PCL and alginate makes the graft potentially feasible as well as reproducible. It was surveyed that currently there is no research in the scientific literature including simultaneous bone formation and vascularization from one scaffold using solely adipose-derived stem cells as a cell source. In future, it will be aimed to implement this ready-to-use, uncomplicated graft design into clinical applications.

2. MATERIALS & METHODS

2.1 Materials

Several materials used within the context of this study are demonstrated involving their purpose and the companies provided them in table 2.1.

Table 2.1 Materials used, manufacturers and their intended use

Material	Brand/Company	Intended Use
Capsule Production		
Poly(caprolactone) (PCL) oligomeric form (M_w=37000 g/mol)	Perstorp AB	Particle Preparation
Polyvinyl alcohol (PVA)	Sigma Aldrich	Particle Preparation
Dichloromethane (DCM)	Sigma-Aldrich	Particle Preparation
Bovine Serum Albumin (BSA)	Sigma-Aldrich	Model protein
Recombinant Human/Mouse/Rat Bone Morphogenetic Protein-2 (BMP-2)	BioLegend	Growth factor
Recombinant Human Vascular Endothelial Growth Factor-165 (VEGF)	GenScript	Growth factor
Trizma® base	Merck	Buffer
Hydrochloric acid (HCL)	Sigma-Aldrich	Buffer
Dulbecco's Phosphate Buffer Saline (PBS)	Sigma-Aldrich	Buffer

Table 2.2 Materials used, manufacturers and their intended use (continued)

Scaffold Production		
Poly(caprolactone) (PCL) oligomeric form (M_w=37000 g/mol)	Perstorp AB	Polymer
Alginic Acid Sodium Salt Powder	Sigma Aldrich	Polymer
Dichloromethane (DCM)	Sigma-Aldrich	Solvent
Calcium chloride dihydrate ($CaCl_2$)	Sigma-Aldrich	Cross-linker
In Vitro Study		
Cell type		
Adipose-derived stem cells (ASCs)	Isolated from human abdominal fat tissue	*In vitro* studies
Cell Culture Medium		
Fibroblast growth factor (bFGF)	Sigma-Aldrich	ASC expansion medium
High-glucose DMEM	Biological Ind.	ASC expansion medium
Fetal Bovine Serum (FBS)	Biological Ind.	ASC expansion & differentiation medium
Penicillin-Streptomycin (10X) Solution	Biological Ind.	ASC expansion & differentiation medium

Table 2.3 Materials used, manufacturers and their intended use (continued)

L-Ascorbic acid	Serva	ASC differentiation medium
Sodium-β-glycerophosphate	Serva	ASC differentiation medium
Low-glucose DMEM	Biological Ind.	ASC differentiation medium
Dexamethasone	Merck	ASC differentiation medium
Trypsin	Biological Ind.	Cell passaging
Dimethyl Sulfoxide (DMSO)	Sigma-Aldrich	Cell freezing
Assays		
Pierce™ Coomassie (Bradford) Protein Assay Kit	Thermo Fisher	Release kinetics analysis
Live/Dead™ Viability/Cytotoxicity Kit	Thermo Fisher	Cell viability analysis
Alamar Blue	Thermo Fisher	Cell viability analysis
Alexa Fluor 488 Phalloidin, DAPI	Thermo Fisher	Morphologic study
Alexa Fluor 594 Goat Anti-Rabbit IgG H&L	Abcam	Immunofluorescent staining
Mouse Monoclonal Anti-CD31 antibody	Abcam	Vascularization analysis
Rabbit Polyclonal Anti-Osteopontin antibody	Abcam	Immunofluorescent staining

Table 2.4 Materials used, manufacturers and their intended use (continued)

Alkaline Phosphatase Assay Kit (Colorimetric)	Abcam	Osteogenic differentiation analysis
Alizarin Red Staining Solution	Sigma-Aldrich	Calcium deposition analysis
Bovine Serum Albumin (BSA)	Sigma-Aldrich	Immunofluorescent staining
Triton X100	Merck	Cell permeabilization
Tween20	Merck	Cell permeabilization
Paraformaldehyde	Merck	Cell fixation

2.2 Methods

2.2.1 BMP-2 and VEGF Encapsulation within PCL Capsules

2.2.1.1 Preparation of PCL Capsules

For PCL capsule production, the manufacturing process of previous studies (Yilgor et al. 2010) was followed. Double-emulsion technique was utilized for preparing capsules. Shortly, different amounts PCL were dissolved in methylene chloride and doped with BMP-2/VEGF or BSA as a model protein and the mixture was sonicated for 60 seconds in 50Hz frequency (Bandelin electronic GmbH & Co. KG, Germany). Then this emulsion was added into polyvinyl alcohol (PVA) solution and the sonication was repeated with the same conditions. This double emulsion was homogenized in PVA solution and the solvents were evaporated. Finally, evaporated capsules were washed with Tris-HCL (10mM, pH: 7,4) and freeze dried for overnight.

2.2.1.2 Scanning Electron Microscopy (SEM) Imaging

Produced particles mentioned above were assessed by using QUANTA 400F Field Emission Scanning Electron Microscopy (SEM) (FEI Company, US) at METU Central Laboratory. Samples were washed with distilled water three times for eliminating any excess salt residual came from Tris-HCL washing. Overnight air dry in a vacuum chamber was done for sample preparation. Conductive double coated carbon tape was applied at the back of the samples for gluing them on top of stubs. Afterwards, gold sputtering on samples was done prior to SEM imaging in order to cover the surface of the sample with a conductive coating.

Surfaces of the scaffolds were also examined under SEM imaging for evaluating cell behaviour. Cell seeded scaffold samples were fixed 3.7% PFA prior to dehydration step with 100% ethanol. Lastly, scaffolds were glued to the SEM stubs before making their surface conducive.

2.2.1.3 Encapsulation Efficiency

Encapsulation efficiencies of different groups were assessed by applying the following procedure. Briefly, 5mg of capsules from varying concentrations (10%, 15%, 20% w/v) were put into glass bottles and then solved in 2mL Dichloromethane (DCM). 2 mL of distilled H_2O was added on top and then exposed to vigorous vortex for 60 seconds. Consequently, phase separation was observed, and water phases of the samples were collected. Watery phase of the samples was then subjected to Bradford protocol that is broadly explained in the next section.

2.2.1.4 Release Kinetics Assessment

In order to evaluate the release profile of the produced capsules several release kinetics assessments were done. Initially, Bovine-Serum Albumin (BSA) was selected as the model protein due to its similar molecular size compared to BMP-2 and VEGF. Bradford assay (Thermo Fisher, Germany) was used for in-situ BSA release assessment where Coomassie blue dye reflected the amount of BSA protein present in the capsules. The Beer-Lambert equation (2.1) below was used to calculate the concentration of the

BSA in specimens where A stands for absorbance level at 595 nm wavelength, L stands for optical length (which is constant in every measurement) and Ɛ being the molar absorption coefficient.

Equation 2.1 $A = \varepsilon L C$

2.2.1.4.1 BSA Release Study from Free & Embedded PCL Capsules

Release kinetics of PCL Capsules were assessed with the model protein BSA. BSA-encapsulated capsules were distributed into Eppendorf tubes (5mg per tube) with 1mL of phosphate buffer saline (PBS) (pH 7.4) and incubated in 37°C degrees for 21 days. For consecutive time periods (day 1, day 3, day 7, day 14, and day 21) samples were centrifuged and the supernatants were collected. Incubation process was continued by adding fresh-PBS into tubes. The amount of BSA in supernatants was assessed by micro-Bradford assay. 150µL of supernatant samples of each day were put into 96 well plates and were added with 150µL of Bradford solution (Coomassie Plus, Bradford Assay; Pierce, US). Then, the samples were incubated in 37°C degrees for 10 minutes prior to 30 seconds of mixing process at the reciprocal shaker. The absorbance level was measured in the plate reader at 595nm wavelength. The amount of BSA concentration and absorbance level were correlated with a calibration graph (Appendix 1).

After assessing release kinetics of free PCL capsules, they were embedded into an alginate solution and printed as scaffolds for the next step of the study. The release kinetics assessment was repeated for scaffolds incorporating BSA-encapsulated ncapsules (n=3). Thus, the effect of alginate as the carrier system for controlled release was evaluated.

2.3 Designing the Architecture of the Scaffolds

It was aimed to produce a homogeneous, anatomically shaped vascularized bone graft from a single autologous cell source with the use of PCL and alginate, 3D printing and the controlled release strategy altogether. As shown schematically in Figure 2.1, PCL and alginate fibers were designed to be printed simultaneously using the dual heads of 3D bioplotter device (Envisiontec GmbH, Germany).

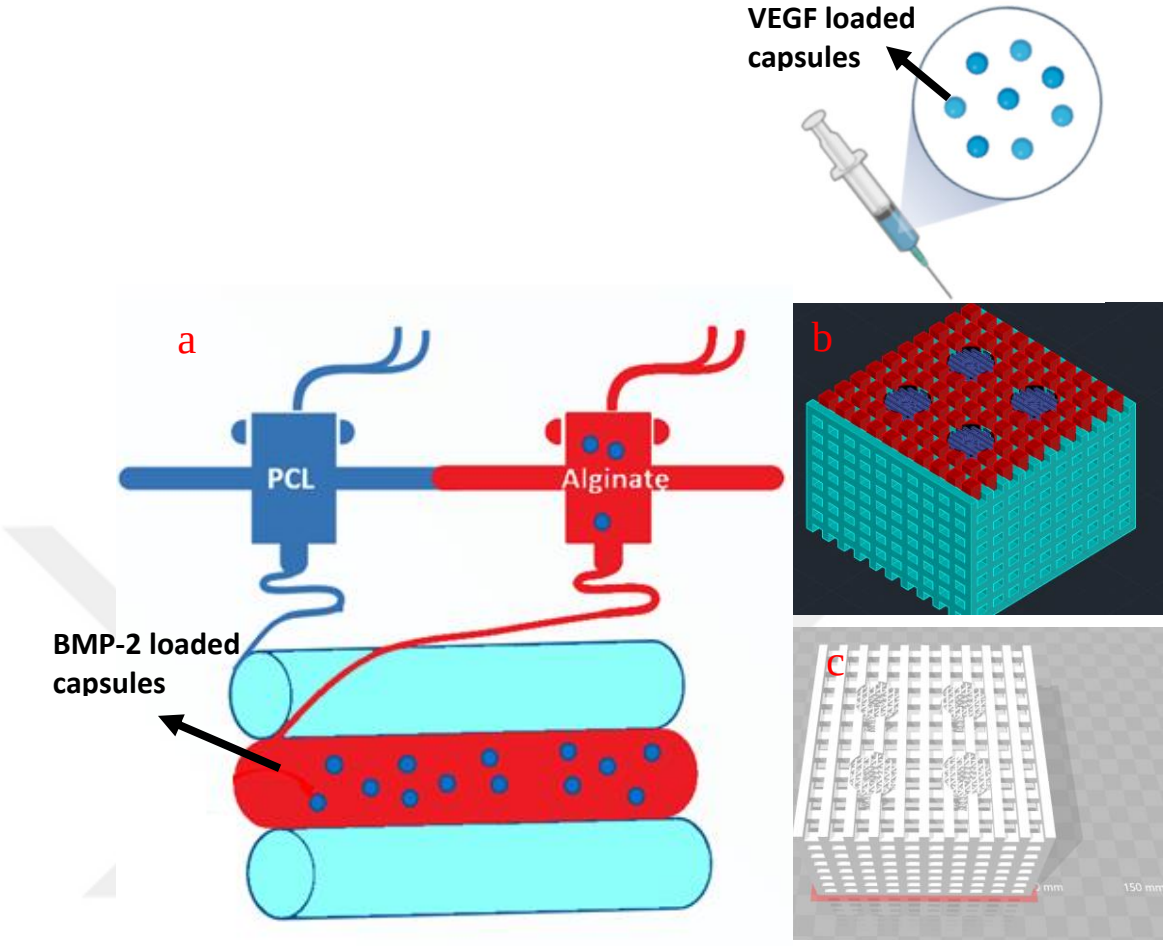

Figure 2.1 Schematic illustration of the (a) co-printing process, visual image of the anatomically shaped 3D graft's unit cell from (b) side and (c) top perspective respectively. Using both heads of the bioprinter, PCL (blue) and alginate (red) fibers shown in (a) were printed side by side. In the dark blue region depicted in (b), VEGF carrying PCL capsules incorporated in alginate was injected circularly around the canal

The purpose of entrapping alginate fibers in between PCL fibers is to increase overall stiffness of the graft as well as providing better structural geometry since hydrogels are struggling with defined printability characteristics. By virtue of BMP-2 encapsulated PCL capsules embedded alginate, it was planned to decorate the graft osteogenic and osteoinductive sequentially. In addition, vascularization in the graft was projected due to exposure of sustained release of VEGF from PCL particles to autologous ASC cells that are seeded. With the help of this novel design, functional anatomically shaped grafts can be produced after optimization studies conducted in cubic structures. In other

words, the strategy of this architecture is to develop a patient-specific vascularized bone graft ready for implantation using autologous cells and biodegradable biomaterials in the laboratory.

The hallmark of this design is to limit the usage of different materials, making the graft practically adaptable and less complex. For instance, the synthetic polymer PCL was aimed to be used in both filament formation and particle production processes. Similarly, alginate has been designed as a bio-ink material to carry growth factors and (ASC cells in future) loaded release systems. In this way, it was aimed to obtain a structure with the least components and the simplest structure, which is less science fictional and applicable and has the potential to be transferred to the clinic.

2.4 3D Printing of Cubical Hybrid 3D Constructs

PCL powder was added into high-temperature metal head of the 3D Bioplotter and was heated up to 130° degrees by using Envisiontec 3D-Bioplotter software (Figure 2.2).

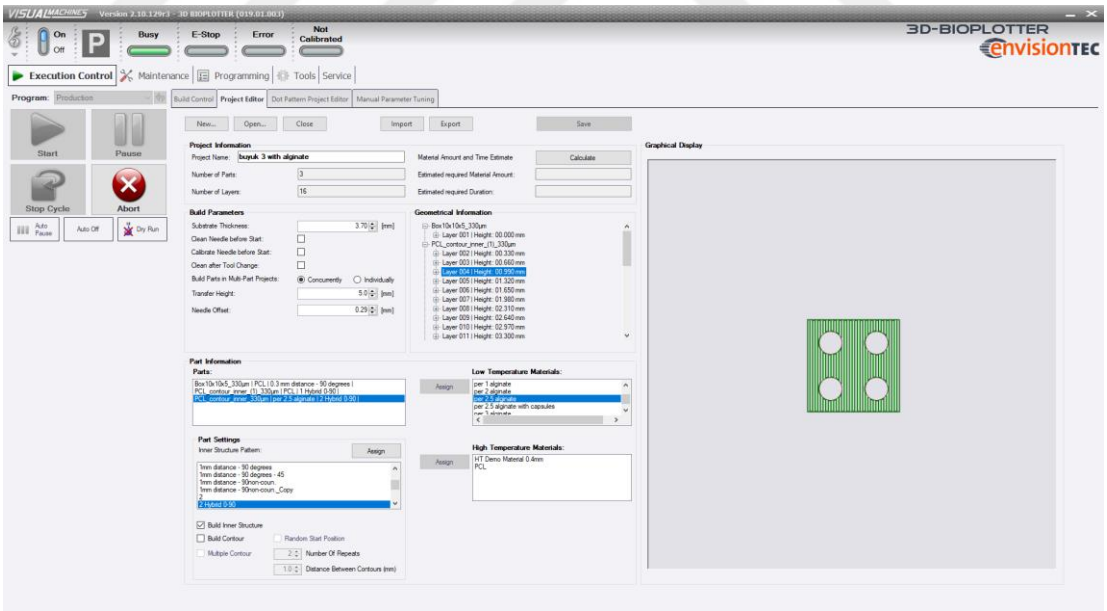

Figure 2.2 Design tab of Envisiontec Visual Machines software

Molten PCL subsequently was extruded through a syringe (0.4mm needle tip) with sufficient pressure and printed on top of a 37°C degrees film surface in the form of filaments (Figure 2.3-c). The other head of the bioprinter was loaded with hydrogel

(alginate) and were co-printed as filaments with PCL. A needle tip that has 0.26mm inner diameter was used for the alginate containing cartridge. Cross-linking of hydrogel was done by 0.5M $CaCl_2$ spraying. In preliminary studies, different weight per volume ratios of alginate (1%, 2%, 3%, 4%) were optimized for ideal viscosity and enough space for capsules to spread within the solution.

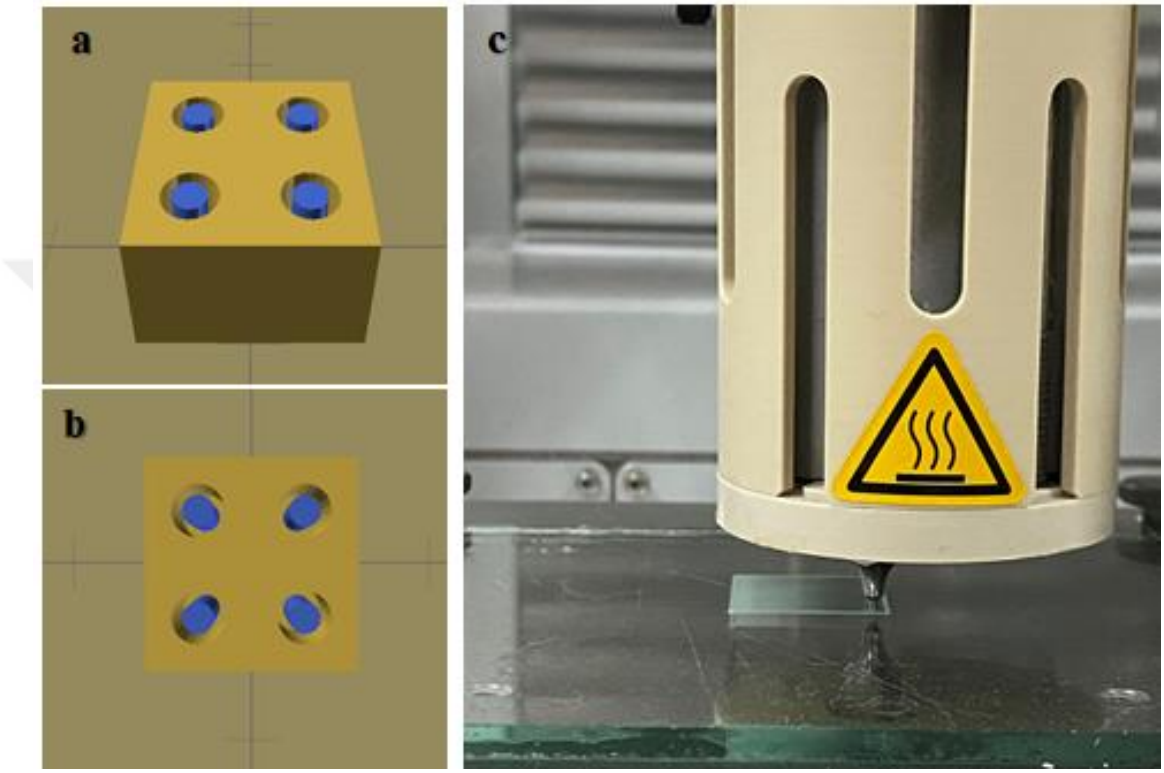

Figure 2.3 3D representation of the CAD design from (a) side view, (b) top view and (c) real time photography of printing process

Cubicle scaffolds with square grid geometry(20x20x5mm) were printed beforehand of anatomically shaped grafts in order to optimize and characterize the manufacturing process. The design of the structure is depicted with CAD image and real-time printing process was captured at Figure 2.3(c). The vacancies (circular canals) within the structure are designed for vascularization of the tissue (Figure 2.3 (a), (b)). Optimization was made for parameters such as reproducibility, repeatability, and rigidity as well as fiber distance and fiber formation. Besides, linear speed of the machine, loading density, print pressure and temperature were also optimized for the ideal print of inner structure.

2.5 Uniaxial Compression Testing

10 x 10 x 1.5mm prints with varying interior architecture were subjected to uniaxial compression test by using Universal Testing Machine (Shimadzu Autograph AGS-X Series, Japan). a 50kN load cell was selected for the testing purpose and linear compression speed was selected as 200μm/min. The amount of stroke applied was adjusted according to the thickness of the specimen. Each scaffold architecture was tested in triplicate specimens and the real time images are demonstrated in figure 2.4. Raw data of force per displacement were processed by using the MS Excel software and the mechanical stiffness results for multiple scaffold structures were given at table 3.2.

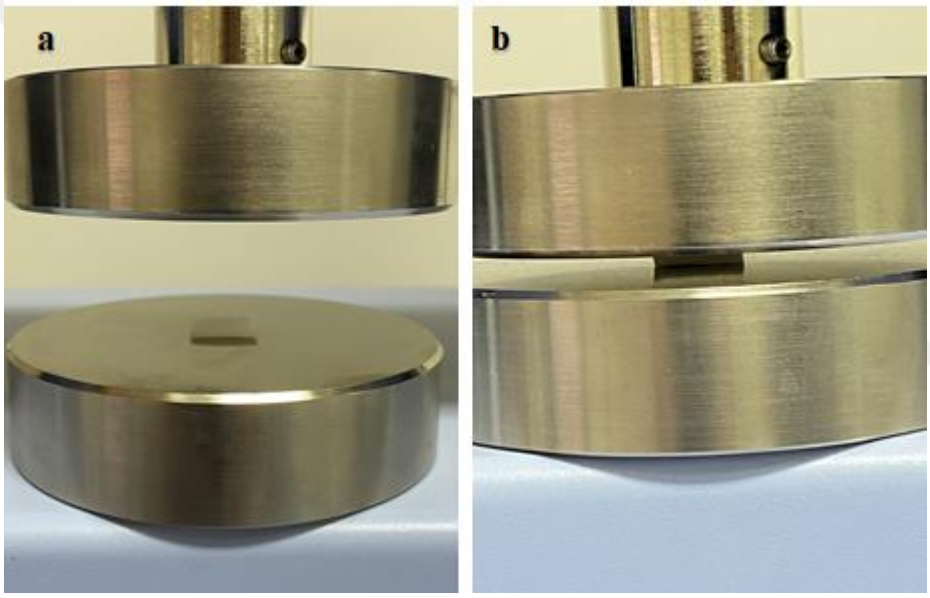

Figure 2.4 (a) Before and (b) after photographs of the specimen taken during the compression test

2.6 In Vitro Studies

2.6.1 Cell Seeding on 3D Printed Scaffolds

In this thesis, cell isolation and characterization steps were skipped and already isolated ASC's from a previous study (Huri et al. 2018) were utilized in all cell culture studies. Vials of passage zero isolated human ASCs were thawed with standard cell expansion medium under right conditions, and then seeded on T-75 tissue culture flasks for

expansion. Cells were cultured with stem cell expansion medium (high-glucose Dulbecco's Modified Eagle Medium (DMEM), 10% fetal bovine serum (FBS), %1 Penicillin/streptomycin (P/S), 1ng/mL FGF-2 at 37°C and 5% CO_2 conditions until desired number of cells were achieved. When there is enough confluency present at T-75 flasks, cells were detached from the surface using Trypsin and reseeded into T-175 flasks for expanding the cells to a greater extent. Cells were counted with trypan blue (Biochrom, UK) exclusion method (Louis and Siegel 2011) prior to the seeding process. Cells that were harvested from the T-175 flasks were centrifuged for 5 minutes at 3500 rpm. Obtained passage three cell pellets was again resuspended in enough fresh media that can be distributed for every sample. 40 µl of cell/medium mixture was poured on top of the (10 x 10 x1.5mm) samples homogeneously by roving the micropipette tip on the surface. In order to prevent cell precipitation, media that contain cells were resuspended at certain intervals during the seeding process. It was calculated to culture 250.000 cells per sample which is found out to be the optimum amount for the surface area of fabricated scaffolds from preliminary studies. Excess cell pellets were frozen with 90% FBS, 10% dimethyl sulfoxide (DMSO) solution. Seeded scaffolds were cultured with the induction medium (low-glucose DMEM, 10% FBS, %1 P/S, 0.05 g/mL Sodium β-glycerophosphate, 1.45 ng/mL L-ascorbic acid, 100nM dexamethasone at 37°C and 5% CO2 conditions for 21 days.

2.6.2 Determination of Viable Cell Number

The number of living (metabolically active) cells in the grafts produced was determined by the Alamar Blue test (US Biological). In this method, medium on the samples were removed from the wells prior to sterile PBS washing. Then, Alamar Blue solution which was prepared with 10% v/v in colorless DMEM was added to the wells. Incubation was made for 1 hour in 37°C and 5% CO_2 conditions in the incubator and protected from light. At the end of 1 hour, 200 µL of test samples were taken from each well and transferred to 96-well microplates. Absorbance values at 570 and 595 nm wavelengths were determined by a microplate reader. Then the Alamar Blue test solution in the wells containing the samples were washed away with PBS and the culture was continued by adding normal cell culture medium. All operations that were carried out under sterile conditions as demonstrated illustratively in Figure 2.5. Each

reading was made from at least three wells. The feature of the Alamar Blue test is that metabolic activity can be determined without affecting cell viability and metabolism. Thus, the same samples that are used to determine the cell number during the culture (1, 3, 7, 14, 21 days). The reduction amount determined on the absorbance values of Alamar Blue dye was converted to the number of living cells with the help of a calibration curve (Yilgor et al. 2010).

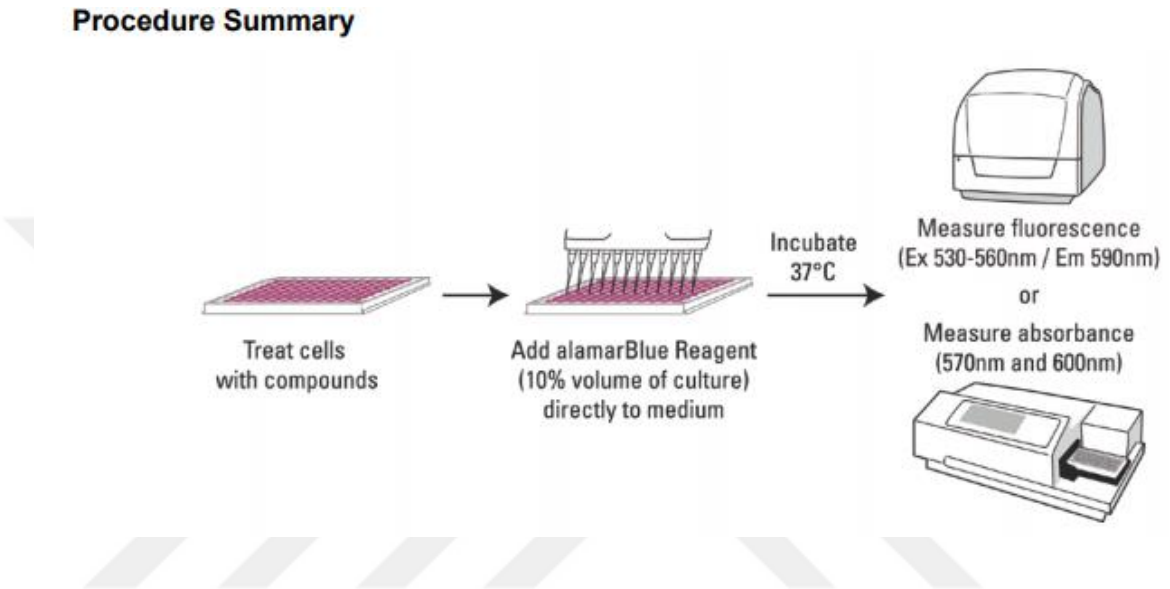

Figure 2.5 Schematics of cell viability assessment procedure

2.6.3 Osteogenic Differentiation Analysis

By the end of different timepoints (7^{th}, 14^{th} and 21^{st} days) of *in vitro* culture, osteogenic differentiation of ASCs in the grafts were evaluated by Alizarin red staining and osteoblast specific alkaline phosphatase enzyme determination used to monitor calcium accumulation. In addition, osteogenesis was determined by performing osteopontin immunofluorescence staining on the sections taken from the grafts.

Alizarin red staining: The samples were fixed by incubation at room temperature for 20-30 minutes on an orbital shaker using 3.7% paraformaldehyde (PFA). After fixation, the samples were washed with distilled water and then incubated with Alizarin Red solution at a concentration of 40 mM at room temperature for 30 minutes. Excess dye was removed by washing with distilled water until the washing environment became clear. The samples were let air dry overnight prior to be examined with light microscopy

(Hutton et al., 2013). The resulting red color intensity and the greater number of dark spots indicated mineral accumulation and hence higher osteogenic differentiation.

Alkaline phosphatase activity determination: Frozen scaffolds were thawed prior to being washed with PBS and then they were lysed in solution containing 1% Tris-TritonX-100. Then, 3 times freeze-thaw cycles were done, and samples were sonicated for 10 minutes (30 sec pulse, 30 sec break). After removing cell debris and other components by centrifugation, 40 µL of supernatant was diluted (1:2 ratio) with ALP Assay buffer (Abcam, US) then incubated in a 96-well culture dish with 50 µL p-nitrophenyl phosphate (pNPP) substrate at 37˚C for 60 minutes. The reaction was stopped with 40 µL ALP Stop Solution (Abcam, US) and the absorbance value was read at 405 nm. The alkaline phosphatase enzyme activity in the samples were determined with the help of the standard curve prepared with pNPP at known concentration (Appendix 2). The higher levels of ALP activity indicated higher osteogenic differentiation.

Immunofluorescent staining: Samples were fixed using 3.7% PFA for 1 hour on the days 7, 14 and 21 of the culture. Then they were washed with PBS for 3 x 30 minutes. After fixation, samples were kept at room temperature for a while, then they were moved to at -20˚C freezer. Immunofluorescence staining was applied using osteopontin (Anti-Osteopontin antibody, Abcam ab8448, mouse) and CD31 (rabbit anti-CD31, Abcam) primary antibody. Briefly, incubation was done in PBS containing 0.1% Tween20 and 1% BSA for 2 hours at 4˚C in order to prevent non-specific binding to sections and permeabilize cell membranes. After blocking and permeabilization, samples were kept at 4˚C overnight with primary antibody staining. Mouse anti-osteopontin antibody was administered and diluted in PBS containing 1% BSA. The samples were viewed with a confocal laser scanning microscope (Carl Zeiss LSM series, Germany) in the BIOMAT Institute of Middle East Technical University.

2.6.4 Perfusion Culture

It was found that anatomically shaped 3D grafts with larger scale cannot allow cell survival under static *in vitro* conditions due to insufficient diffusion (a common situation in the clinic) (Huri et al., 2014). It was also reported that hypoxia and necrotic areas occur in the center of the graft due to insufficient oxygen diffusion.

In order to overcome this problem, preliminary studies with a perfusion bioreactor (3D CulturePro™, TAI Instruments) were done. Samples that possess the same dimensions (10x10x1.5mm) were cultured with perfusion bioreactor for 7 days with the to ensure effective cell nutrition. The speed of the peristaltic pump was selected as 60rpm. For each chamber, 100 mL of osteogenic induction medium was injected through the tubing valves and let the pump circulate the medium continuously for 7 days. Every step of perfusion culturing beginning from the chamber assembly to initiation of cell culture medium circulation was demonstrated in Figure 2.6.

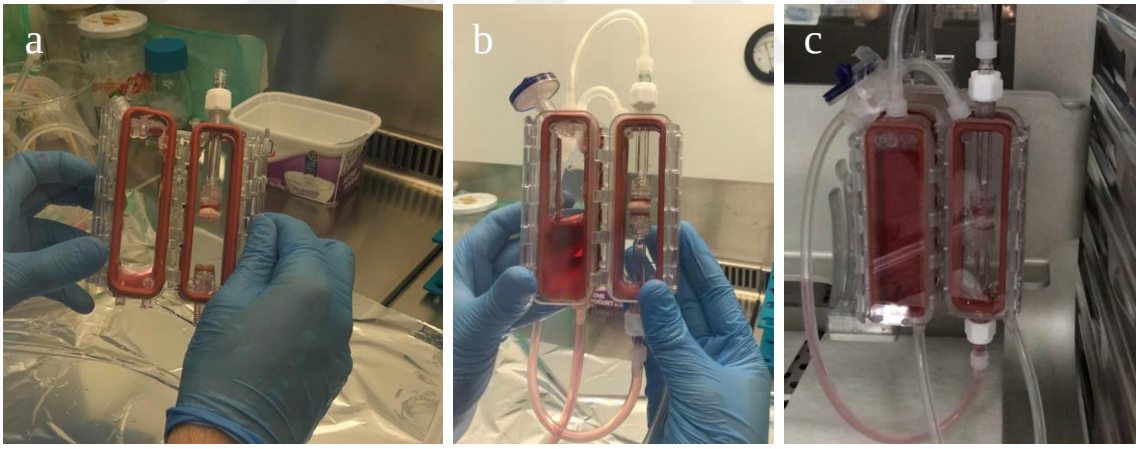

Figure 2.6 Photographs of (a) perfusion bioreactor chamber assembly, (b) initiation of medium circulation with peristaltic pump, (c) active perfusion culture during incubation

3. RESULTS & DISCUSSION

3.1. Preparation of PCL Capsules

Production of PCL capsules were made by using 10, 15 and 20% (w/v) polymer solutions. SEM images of capsules that were produced are shown in Figure 3.1

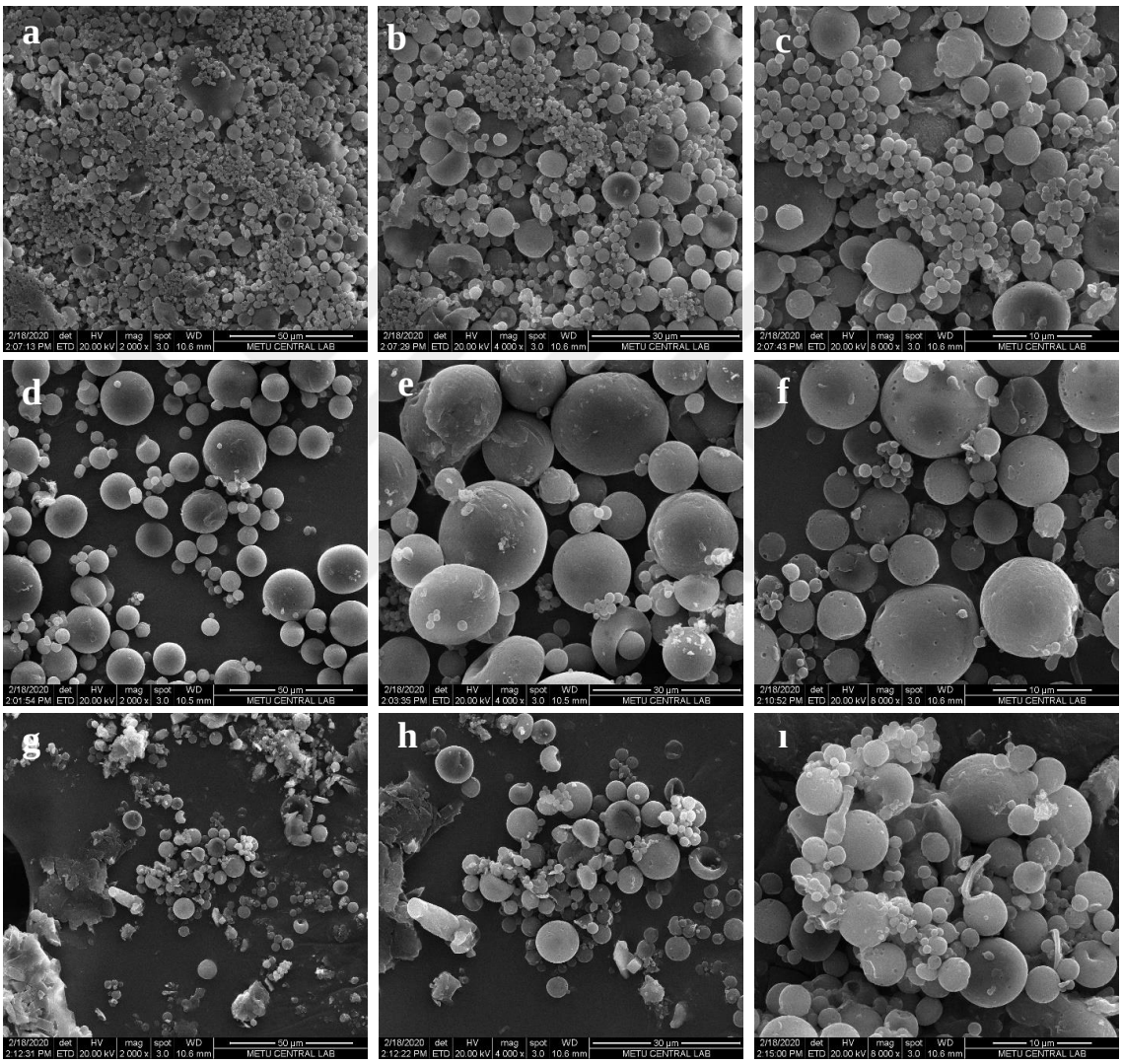

Figure 3.1 PCL capsules loaded with BSA as a model protein. Upper row: 10% PCL (w/v), middle row: 15% PCL (w/v), lower row: 20% PCL (w/v). (a), (d), (g) 2000x magnification, (b), (e), (h), 4000x magnification, (c), (f), (i) 8000x magnification

Higher amounts and relatively uniform capsular structures were acquired by using 10% concentration polymer solution among all three batches. In the preliminary studies, it

was found that 5% PCL concentration was not sufficient to form capsules; thus, SEM characterization of that batch could not be conducted. The insufficient formation and particle loss during fabrication concurs with the results of Yilgor et al. (2009). Consequently, 5% PCL concentration batch was excluded from subsequent studies. Particle size distribution for increasing concentrations of PCL are distinctively explained in the section below.

3.1.2 Particle Size Distribution Analysis

In order to investigate the frequency distribution of capsules, SEM images of different batches under 8000x magnification were evaluated using image processing and analysis software ImageJ. Capsule formation with varying sizes was detected, and the diameters of each sphere were calculated by using ImageJ's straight-line tool (Figure 3.2).

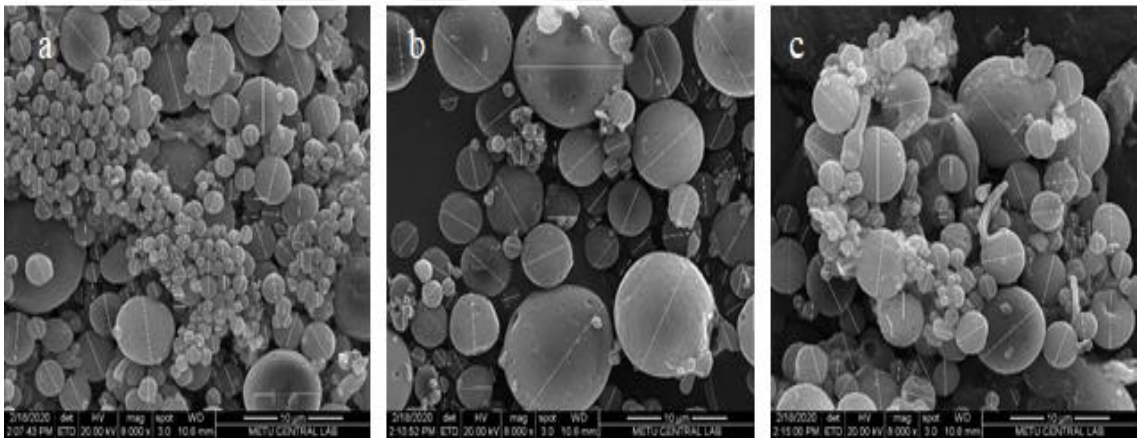

Figure 3.2 Particle diameter measurements of (a) 10%, (b) 15%, (c) 20% PCL capsules under 8000x magnification respectively

By utilizing GraphPad's built-in histogram analysis option, all the measurement data was put into a table and the frequency distribution of capsule over the particle size diameter graph was sketched (Figure 3.3). The bin width of particle size was selected as 200 nanometers for ideal projection of the whole spectrum. For all groups, particle size is varying in the range from 50 nanometers up to 2 micrometers.

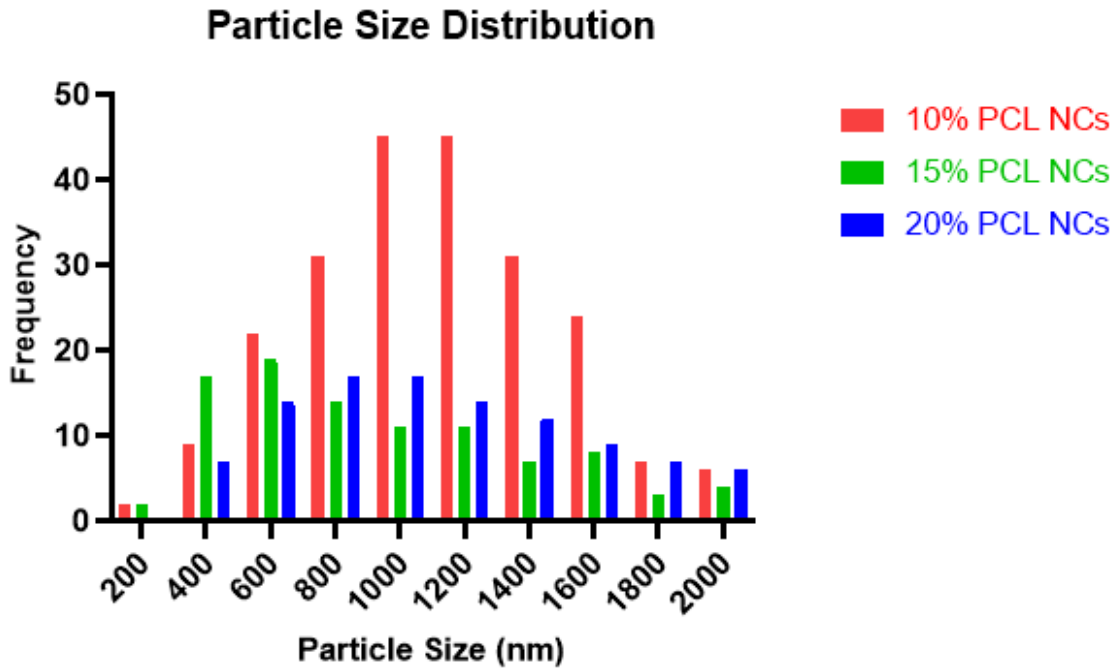

Figure 3.3 Particle size distribution bar graph of capsules with varying concentrations

For 10% w/v PCL capsules, the highest frequency of particle diameter is among 800 to 1400 nanometers whereas smaller and larger particles present in relatively less amounts whereas smaller diameters below 200 nanometers were not observed for 15% and 20% w/v PCL capsules. Majority of the capsule formation in 15% and 20% PCL concentrations were seen around 1000 nanometers and above.

Figure 3.4 demonstrates mean values of every dataset with a graph bar respectively. Average diameter of 10% w/v batch is found to be 1200 nanometer where the average goes up to 1900 nanometer for 15% and 20% w/v batches. The effects of increased diameter were evaluated in the section below by assessing release kinetics.

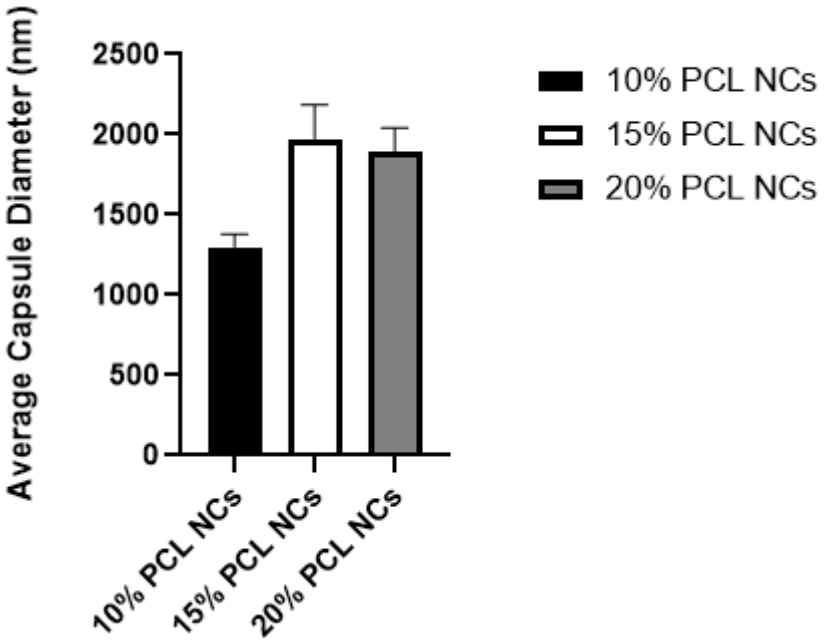

Figure 3.4 Comparison graph of average capsule diameter for all three groups

Since Iqbal et al. (2015) reports that average particle size is dependent on the duration of the ultrasonication process, the period of sonication can be optimized for obtaining better particle distribution. In further studies, new modification methods for the particle production process can be investigated in favor of decreasing the average particle size.

3.2.1 BSA Encapsulation Efficiency & Release Kinetics Assessment

Encapsulation efficiencies of BSA within PCL capsules for different groups (10%, 15%, 20% w/v) were analyzed using the protocol explained in the section 2.2.1.2. As it was previously explained in the capsule preparation section (3.1), due to insufficient formation of the capsules, assessment of release kinetics could not be conducted on that 5% PCL group. The results of the rest of groups are indicated in Table 3.1. The calculation of encapsulation rate in terms of percentage was done by using the formula given below:

EE % = Amount of protein found by Bradford protocol / Amount of protein put in the production batch * 100

Table 3.1 Comparison of PCL concentration with encapsulation efficiency

Loaded Drug	Polymer Concentration (%, w/v)	EE % ± SD
BSA	10	32.32 ± 2.50
BSA	15	45.06 ± 1.09
BSA	20	70.18 ± 0.73

As it is shown in table 3.1, encapsulation efficiency increases with polymeric concentration. As Byun et al. (2011) suggested that increased polymer concentration results with higher efficiency since average particle size is higher. Since bigger particles lead to needle tip obstruction during 3D printing, it was determined to stay with 10% polymeric concentration rather than increasing the encapsulation efficiency.

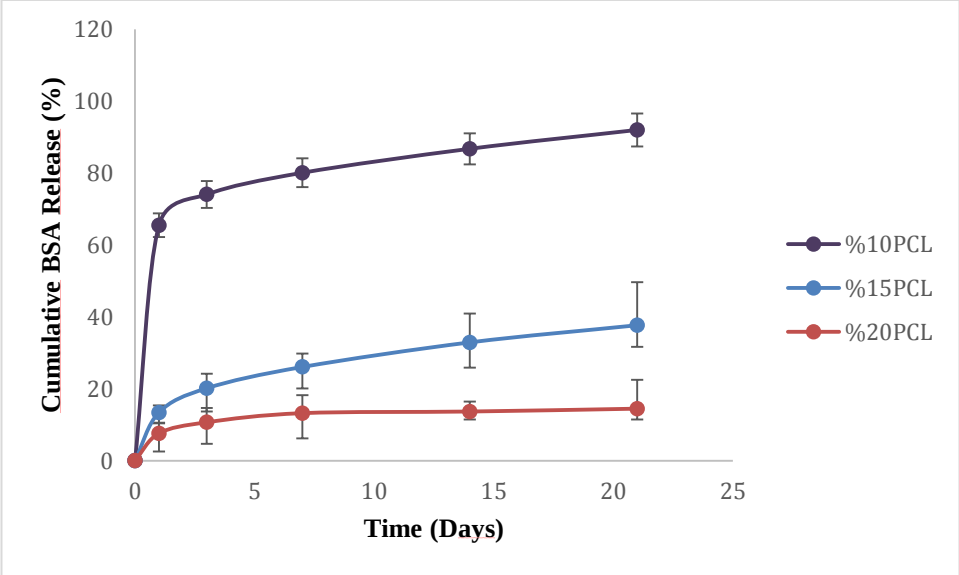

Figure 3.5 BSA amount released from 10%, 15%, 20% PCL capsules respectively at various time points (day 1,3,7,14,21)

In order to analyze release kinetics of different polymeric solutions (10%, 15%, 20%) three batches of BSA encapsulated free particles were subjected to micro-scale Bradford assay. Their cumulative release at the end of 21 days was shown at figure 3.5. It was

noticed that an increase of polymer concentration from 10% to 20% led to BSA release to decrease over time. Considering the thickened walls of capsules, increased polymer concentration has led to slower release rate of the content.

After the preliminary studies done on BSA encapsulated free capsules, three different batches (10%, 15%, 20% respectively) were incorporated within 2% w/v alginate solution prior to scaffold printing. The amount of BSA release from embedded capsules was analyzed for 21 days (Figure 3.6).

Embedding capsules into hydrogel enabled BSA to have a sustained release profile over time. This result indicates that the main goal of long-term release of demanded material can be achievable. As it is exemplified in the review written by Rambhia and Peter (2015), incorporating particles into hydrogel carriers can be the development for enhancing the drug release profile.

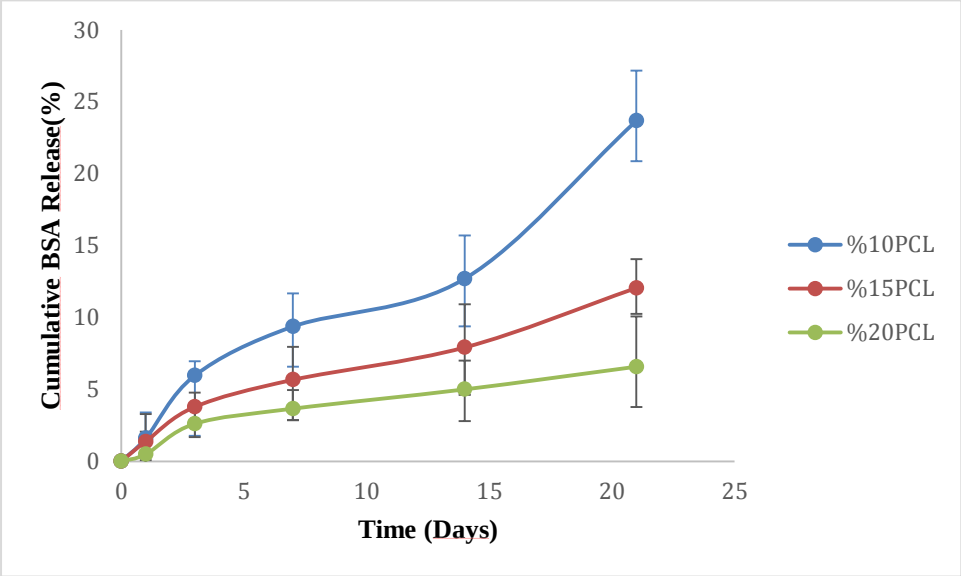

Figure 3.6 BSA amount released from 10%, 15%, 20% PCL capsule laden PCL-Alginate hybrid scaffold at day 1,3,7,14,21 timepoints

In the light of capsule diameter, EE and release profile results, the most suitable polymer concentration was selected in order to be used in controlled release of growth factors. Even though the EE% is higher in 15% and 20% w/v groups, total cumulative BSA release at the end of 21 days is found to be greater in 10% PCL concentration, thus 10% PCL concentration was performed in VEGF and BMP-2 growth-factor

encapsulation. Demanded delivery of BMP-2 (40ng/ml) concentration was determined according to studies in literature by (Yilgor et al. 2009) (Yilgor et al. 2010). Similarly, VEGF (10ng/ml) concentration was defined based on the work done by Temple et al. (2014).

3.3 Optimization of Scaffold Fabrication

Initially the linear speed of the machine and the pressure were optimized in the preliminary studies. It was seen that ideal pressure for PCL fiber printing depends on the linear speed of the printer head. In order to achieve better resolution, various combinations were tried, and it was deduced that most precise printing is possible when linear speed is in between 2mm/s – 3mm/s where pressure is also set to in between 2 – 3 bars. In the light of preliminary speed optimization results, the rest of the printings were done by adjusting speed to 3mm/s and 3bar for the PCL loaded head of the machine. In addition to printing pressure and linear speed of the head, print temperature of the heads was also optimized. Ideal viscosity was observed at 130°C degrees for molten PCL where 37°C degrees was suitable for printing of alginate fibers. Both the studies available in the literature and the unpublished preliminary studies has shown that the thermal effect that occurs during the extrusion of PCL in the capsule-loaded hydrogel materials positioned side by side with PCL suppressed in melt state does not adversely affect cell viability (Izadifar et al. 2016). All the scaffolds were printed at room temperature and the printing platform was heated externally. Pre-flow and post flow rates were set to 0.05 and 0.07 respectively for the sake of better finishing when the head switches from one fiber printing to another. During preliminary studies, it was seen that loading density of the cartridge should not be less than 1 mL since any volume below that amount can cause depletion of the material in-process. That is why, the majority of the experiments were performed with at least 2 mL loading density in both heads for co-printing.

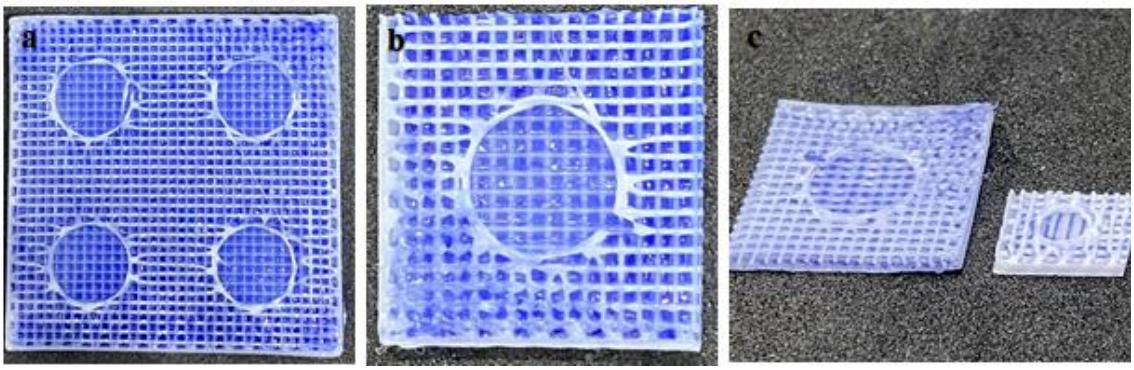

Figure 3.7 3D printed hybrid scaffolds: (a) 20 x 20mm square grid with 4-channel architecture, (b) 10 x 10mm miniaturized square grid with single channel architecture (c) overview of both 4-channel and single channel architecture side by side

Optimization of alginate concentration for printing was conducted in two sections: capsule free alginate and capsule embedded alginate. Preliminary studies indicated that capsule free 1% w/v alginate can be printed with 0.1 bar pressure where 4% w/v must be printed with slightly higher pressure levels, e.g. 0.5 bar. It was observed that linear speed of the head is somewhat less significant for alginate compared to PCL. Decent resolution was acquired ably within the range 2-to-4mm/s printing speed.

Different alginate concentrations varying from 1% to 4% w/v were tested for print resolution and ideal embedment of capsules within the solution. Preliminary studies revealed that something in between 2-3% w/v should be hypothetically better for printability since printing with 1% concentration was slightly fluidic where 3% concentration was hardly viscous. Therefore, 2% w/v was selected, and the rest of the experiments were carried out in this concentration level. Figure 3.7 demonstrates examples of prints in both dimensions 20 x 20mm and 10 x 10mm.

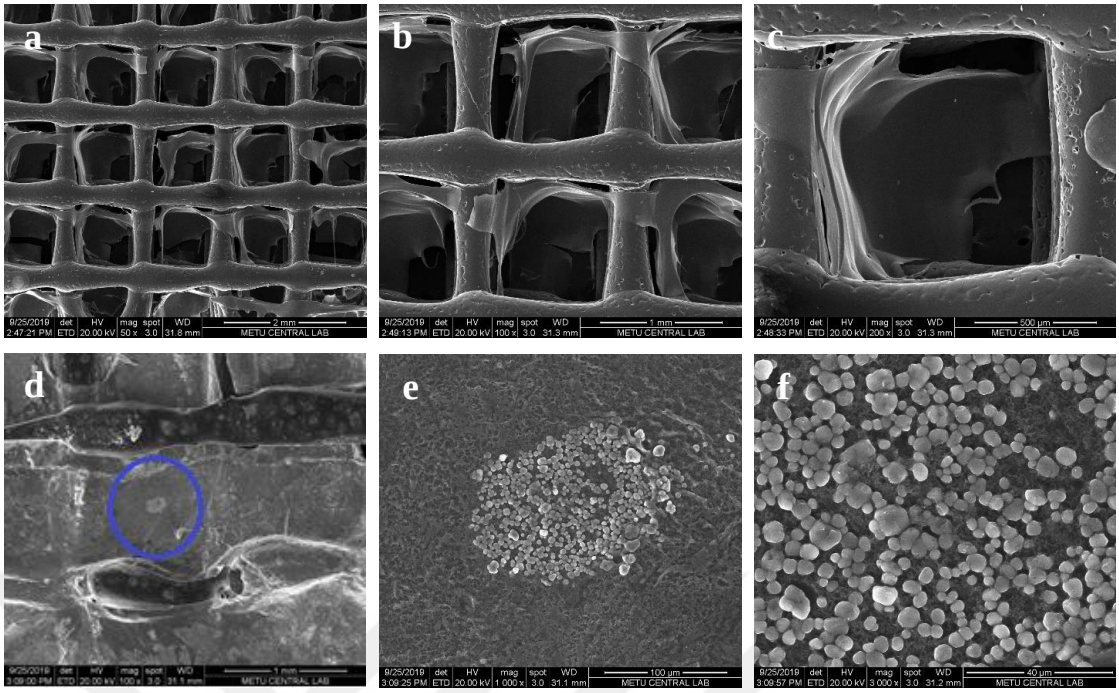

Figure 3.8 SEM images of capsule-embedded PCL/Alginate hybrid scaffold with (a) 50x, (b)100x, (c) 200x, (d) 100x, (e) 1000x, (f) 3000x magnifications respectively

Due to the challenges of static culturing samples with the size of 20x20x5mm, the architecture was downsized for *in vitro* experiments. Thus, cell culture experiments were conducted by using samples with 10 x 10x 1.5mm proportions. Examples of 3D printed molten PCL/Alginate (%2 w/v) hybrid scaffolds with varying dimensions are depicted in the figure 3.6. Alginate solution was mixed with trypan blue dye for better visual clarification.

Mixing capsules into an alginate solution did require a secondary optimization process. Due to increase in viscosity of alginate solution, higher pressure levels had to be reached in favor of better printability. Different needle tips for capsule incorporated scaffold printing were studied in favor of better print optimization with capsules. Capsule-laden scaffold prints were evaluated following the same protocol explained in section 2.2.1.2 with the same microscope used for characterizing PCL capsules (Figure 3.8). Capsules that are embedded into alginate were successfully observed under 3000x magnification.

Table 3.2 Property comparison table of printed scaffolds with alternating designs

Image of the Sample	Scaffold Architecture	Distance Between Strands (mm)	Young Modulus (MPa) ± SD
 (SG -1)	Square Grid	0.3mm	44.33 ± 3.12MPa
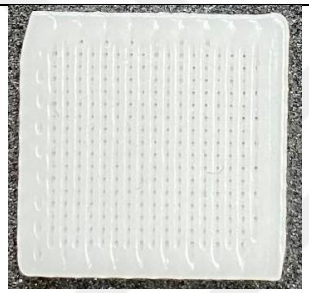 (SG-2)	Square Grid	0.75mm	27.35 ± 9.74MPa
 (SG-3)	Square Grid	1mm	24.91 ± 11.55MPa
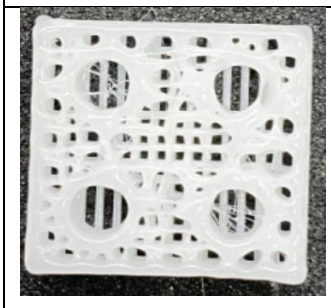 (SGC-1)	Square Grid w/ Channels	1mm	23.23 ± 10.07MPa

Table 3.3 Property comparison table of printed scaffolds with alternating designs (continued)

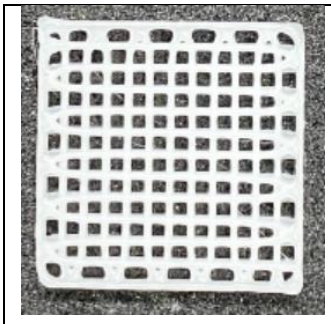 (SG-4)	Square Grid	1.25mm	22.72 ± 3.50MPa
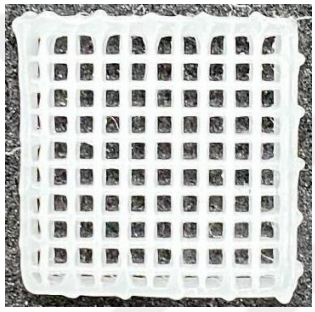 (SG-5)	Square Grid	1.50mm	10.19 ± 4.29MPa
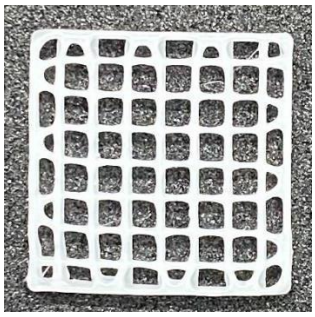 (SG-6)	Square Grid	2mm	9.50 ± 2.28MPa

On top of printing precision and viscosity adjustment, mechanical properties of the printed scaffolds were also investigated. The effect of fiber distance, the change in scaffold geometry were assessed using uniaxial compression test. Compressive values were found by applying linear regression to the obtained stress-strain curves. Table. 3.2 represents the images of the samples and figure 3.9 compares their compressive strength.

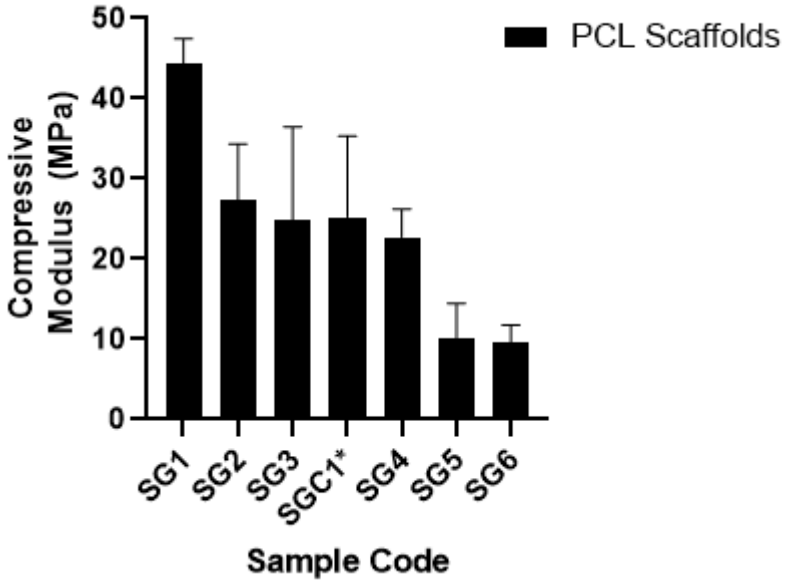

Figure 3.9 Mechanical stiffness comparison graph of PCL scaffolds with varying geometry, sample codes are given in table 3.2

As it is explained in the study by Yilgor et al. (2010) scaffold architecture has utmost importance in terms of cell response. It was reported in that article, fiber distance should be optimized for cell attachment and proliferation. That is why scaffold geometry was investigated for better optimization in this study. It was found that SG-1 has the highest compressive modulus, however due to its diminished porosity, it was not suitable for in vitro studies. That is why, SG3's scaffold geometry with 1mm fiber distance was chosen for this study. It was seen that SGC-1's compressive modulus compared to SG3 is not significantly different even though the porosity is relatively changed.

Shor et. al (2009) reported that, average compressive modulus for PCL scaffolds manufactured by precision extrusion deposition method is 59 MPa where Hutmacher et al. (2001) reported that their FDM made PCL scaffolds with 0/60/120° raster angle has 41.9 MPa. It was believed that the difference between our compressive modulus results and theirs is due to high molecular weight of the PCL they use.

Numerous studies conducted by Bertoldi et al. (2011), Cengiz et al. (2016), Nair et al. (2020) utilizes microCT imaging technique for assessing the porosity and their interconnectivity among the scaffold for characterization. In order to assess the inner

porosity of the printed scaffolds shown in table 3.2, microCT characterization can be implemented in future.

3.4 Results of Static Cell Culture

3.4.1 Cell Viability

Cell viability of the ASCs that are seeded onto hybrids scaffolds were assessed with Alamar Blue Assay. Cell proliferation of cells between control and treated groups were compared in figure 3.9. Cell seeded control scaffolds were cultured with the standard expansion medium and the treated groups were cultured with osteogenic medium in order to see the cell proliferation profile of induction applied scaffolds. Also, incorporation of growth factor carrying agents into the system was investigated in terms of cell viability. It is clearly visible at figure 3.10, cells were successfully attached to the scaffolds in all groups and multiplied overly at the end of the 21-day culture period. Live/dead staining and MTT assays done by Kim et al. (2014) agrees with the idea of PCL/alginate hybrid scaffolds being non-toxic. As it is shown in the figure 3.9, addition of PCL carriers into the system did not adversely affect the cell viability. However, induction of osteogenic differentiation into cells resulted with significantly less proliferation compared to the control group. This result indicates that cells that are in the pathway of differentiation tend to be more compact and less proliferative.

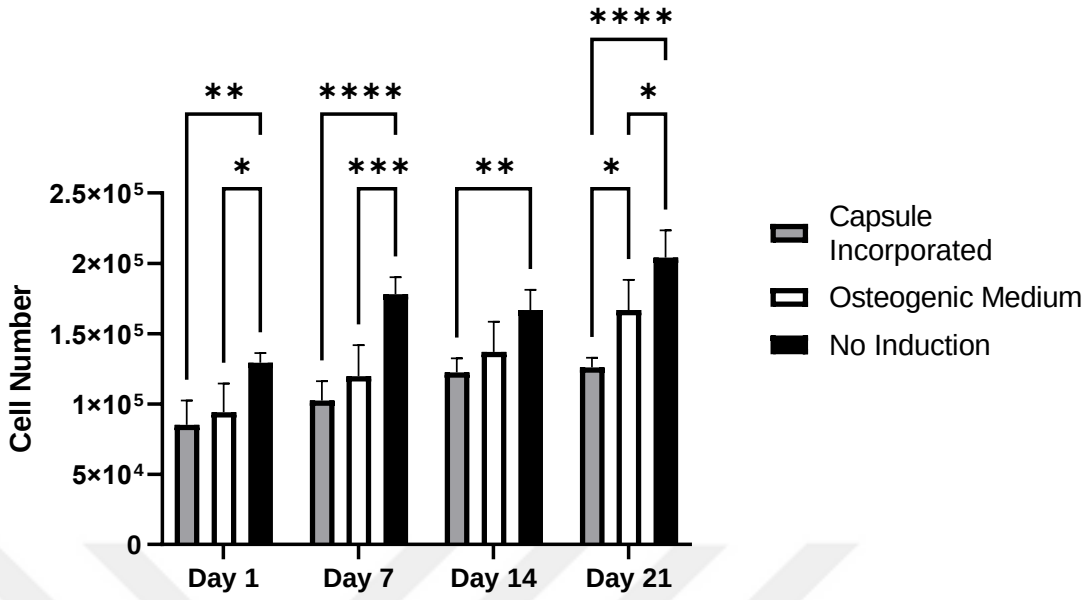

Figure 3.10 Cell viability results of seeded ASC's on scaffolds. Results are given in the amount of living cells calculated by using Alamar Blue assay. Data is expressed as mean ± standard deviation of 3 different experiments. Significant differences are marked with asterisks (* P-value < 0.05, ** P-value < 0.01, *** P-value < 0.001, **** P-value < 0.0001)

3.4.2 Cell Attachment and Morphology

Apart from the Alamar Blue results, the attachment of cells and their orientation upon the scaffold geometry were also evaluated under fluorescent microscope using LIVE/DEAD™ Viability/Cytotoxicity kit. Scaffolds were cultured for 7 days and at the end of each time point scaffolds were put under the microscope as soon as staining was done. It was observed that cells successfully attached on both fibers of the hybrid scaffolds and after 7 days it is clearly discernible that cells had covered the whole surface. Figure 3.10 represents live and dead cells after seeding with 4x and 10x magnification respectively.

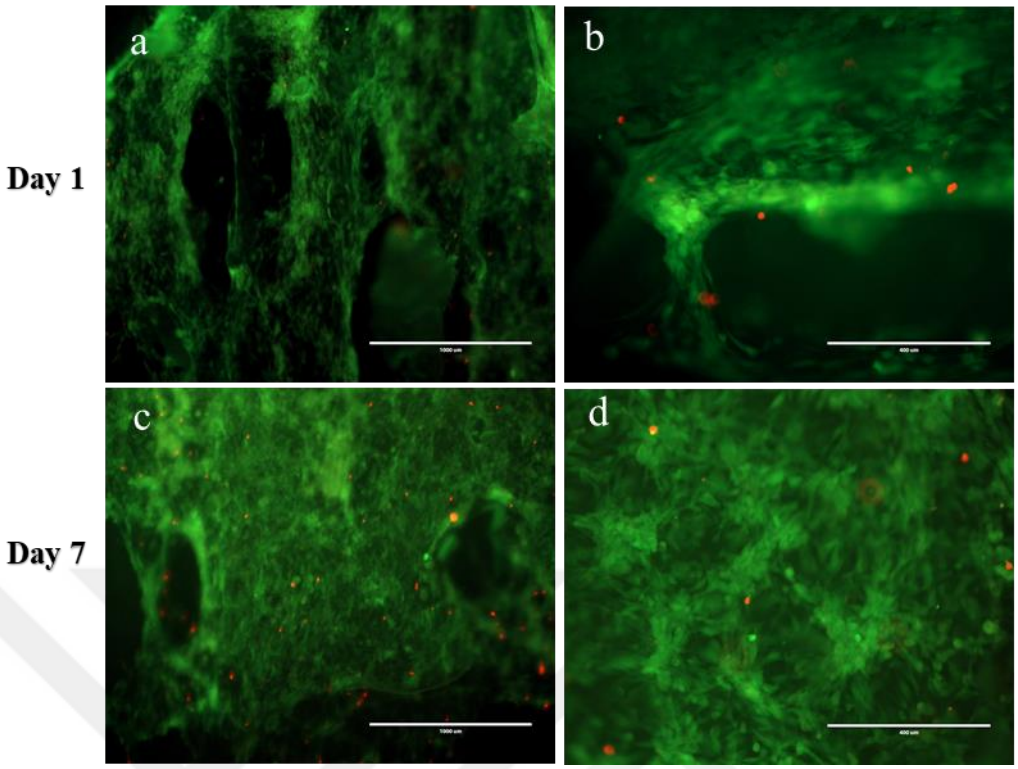

Figure 3.11 Fluorescence images of live/dead staining of ASCs that are seeded on scaffolds, live cells were stained with calcein-AM (green) and ethidium homodimer-1 was used to stain dead cells (red) that lost cell membrane integrity. Figure (a) and (c) depict the fibers of the scaffolds under 4x magnification where (b) and (d) under magnification. (for (a) and (c) Scale bar = 1000µm, for (b) and (d) Scale bar = 400µm

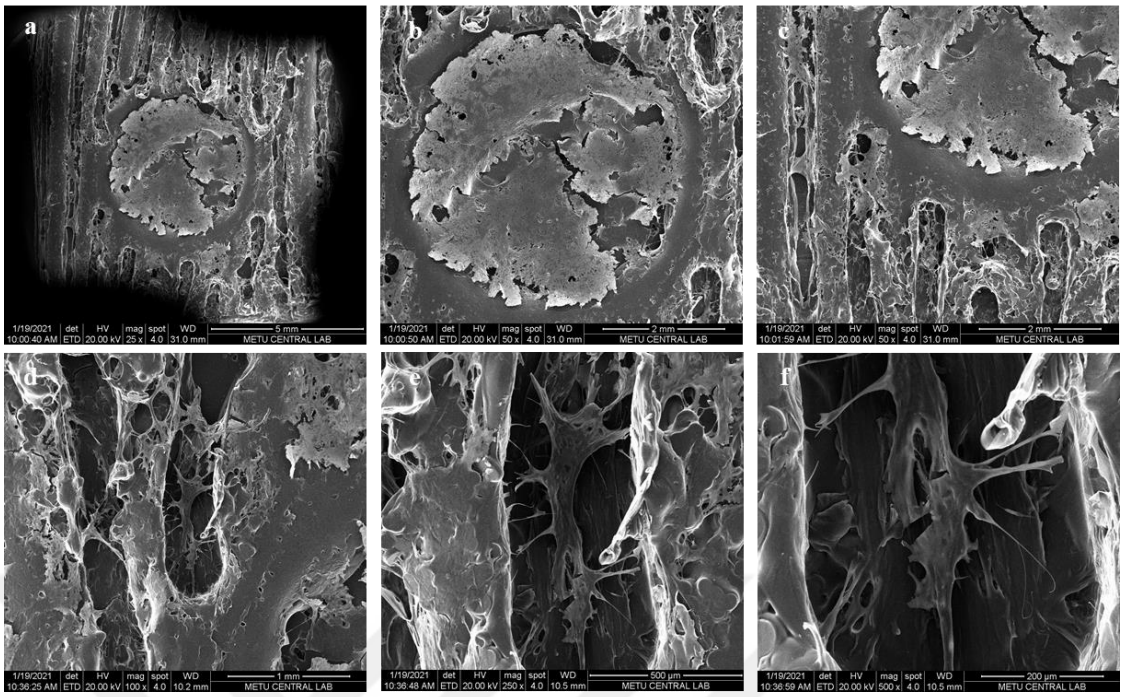

Figure 3.12 SEM Micrographs of ASC seeded samples from day 21. Images were taken under (a) 25x magnification, (b) and (c) 50x magnification, (d) 100x magnification (e) 250x magnification, (f) 500x magnification for observing the localized cell attachment and morphology in between fibers PCL and alginate fibers. For (a) scale bar = 5mm, for (b) and (c) scale bar = 2mm, for (d) scale bar = 1mm, for (e) scale bar = 500μm and for (f) scale bar = 200μm.

For comparing the effect of BMP-2 incorporation to the system in terms of cell attachment, scaffolds were prepared for SEM analysis by implementing the same procedure explained in the section 2.2.1.2. The attachment of the cells on both PCL and alginate fibers were seen under 250x magnification in figure 3.12 (b), (d), (f) and (h). It is clearly visible from the images (a), (c), (e) and (g) cells were spread on the whole surface.

3.4.3 Results of Osteogenic Induction

3.4.3.1 Alizarin Red Staining

Samples from different timepoints were evaluated under the optic microscope after 30 minutes of alizarin red staining. Images were taken from the same area of interest in all samples. Figure 3.13 reflects the amount of red color intensity for both control and treated groups. The column on the left of the figure belongs to the no induction group which was cultured with standard medium. The middle column belongs to the BMP-2 free scaffold group that was cultured with the osteogenic induction medium where the column on the right belongs to the BMP-2 capsule incorporated scaffold group that was also cultured with osteogenic induction medium.

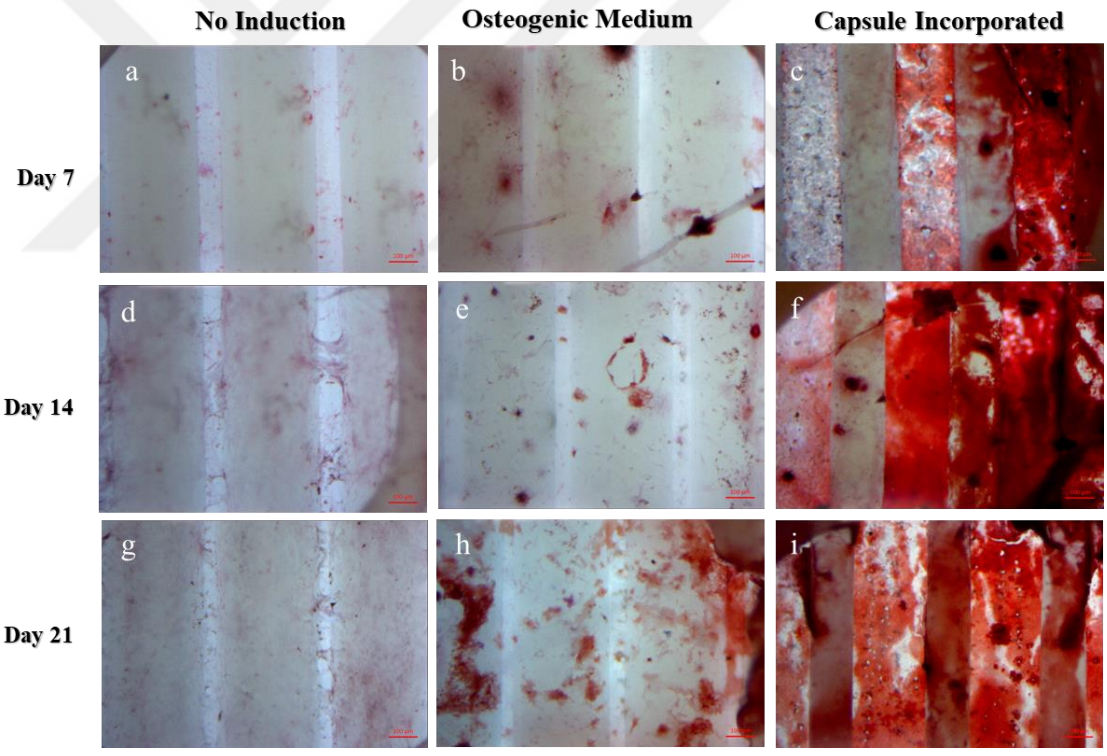

Figure 3.13 Light microscopy images taken from the representing Alizarin red staining results of (a), (d), (g) no induction, (b), (e), (h) osteogenic medium and (c), (f), (i) capsule incorporated groups for day 7,14 and 21 respectively. Scale bar = 100 µm

The visual red color difference between groups reflects how much calcium was deposited within the scaffolds for the period of 21 days. Mineralized extracellular

matrix gets stained by Alizarin red staining reagent, the intensity of red color per image in figure 3.12 was correlated using ImageJ. A white area was selected for background subtraction, and measurements for average light intensity were done from 5 different regions of interest with the same area. The multi comparison of red color intensity among the groups and the time points were given in the figure 3.13. It was found that there is a significant difference in red color intensity between images from day 7 and day 14 for the BMP-2 treated group as well as day 7 and day 21 for the osteogenic medium group.

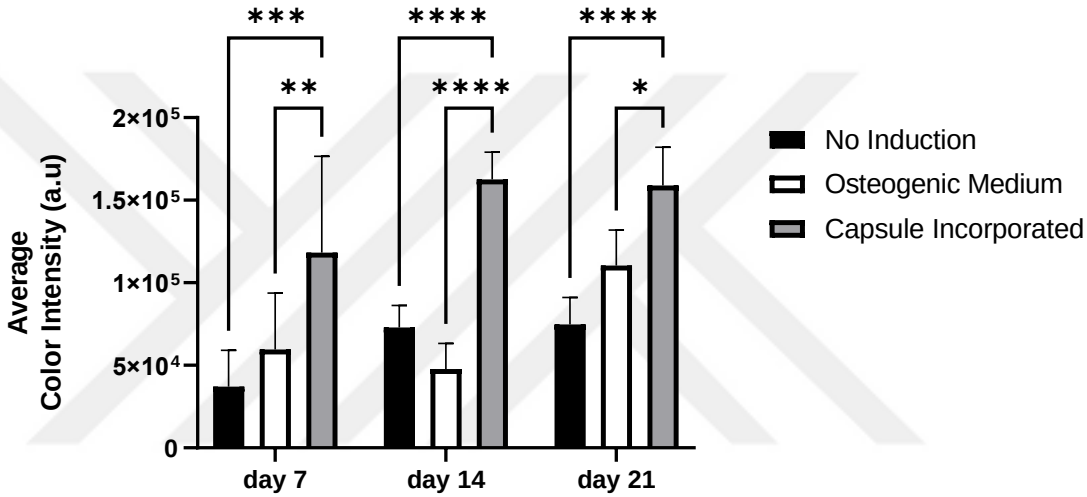

Figure 3.14 Average color intensity comparison graph of BMP-2 capsule incorporated scaffolds vs osteogenic medium treated scaffolds vs no induction scaffolds shown in figure 3.13; From every image 5 different regions of interest with the same area were determined and the mean gray value was measured using ImageJ. Significant differences are marked with asterisks (* P-value < 0.05, ** P-value < 0.01, *** P-value < 0.001, **** P-value < 0.0001)

3.4.3.2 Alkaline Phosphatase Activity (ALP Assay)

In order to determine the rate of osteogenic differentiation, samples from different groups were tested with Alkaline Phosphatase Kit (Abcam, US). ALP activity assessment is a common method adapted by researchers (Reible et al. 2017) (Sun et al. 2010) for quantifying the osteogenic differentiation level between groups. No induction group was cultured with the standard expansion medium where osteogenic medium and

capsule incorporated groups were cultured with the osteogenic induction medium for 21 days.

The absorbance of the p- nitrophenol generated by p- nitrophenyl phosphate in each well per minute was compared for all three groups in the figure 3.15. ALP activity was significantly increased in the BMP-2 capsule incorporated group for day 14 and day 21 compared to both osteogenic medium and no induction groups. The reason behind this gradual increase in activity is due to osteogenic differentiation triggered by BMP-2 presence. Results given in the figure 3.15 are compatible with the study by Tian et al. (2013) where it was reported that ALP is a crucial marker for osteogenic differentiation and this differentiation pathway is dependent on the presence of BMP-2.

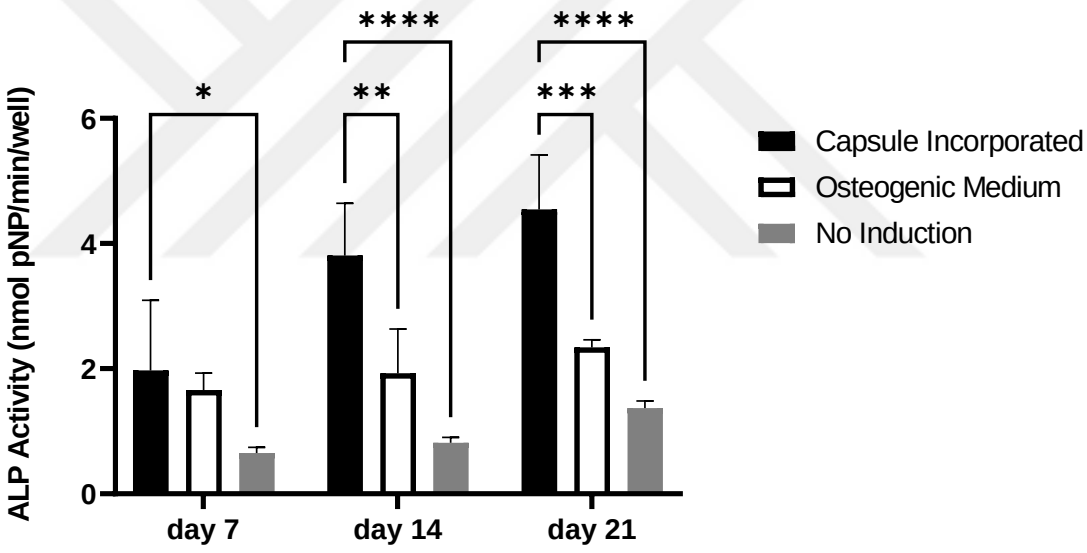

Figure 3.15 Alkaline phosphatase activity graph of BMP-2 capsule incorporated scaffolds vs osteogenic medium treated scaffolds vs no induction scaffolds with no induction. ALP enzyme activity reflects the amount of p-NP formed per min. Data is expressed as mean ± standard deviation of 3 different experiments. Significant differences are marked with asterisks (* P-value < 0.05, ** P-value < 0.01, *** P-value < 0.001, **** P-value < 0.0001)

3.4.3.3 Immunostaining Results

Immunofluorescence staining for osteopontin (Tajima et al. 2015) is frequently applied in the evaluation of ASC osteogenic differentiation. Fixed samples from different timepoints were subjected to anti-osteopontin antibody staining. Additionally, samples were stained with Phalloidin and DAPI in order to localize the actin filaments and the cell nuclei separately. Specimens were evaluated by exciting them with 488nm and 594nm laser sources under confocal laser microscopy. Staining of osteopontin protein was observed in the images figure 3.15-(f), (g) and the signaling areas were marked with arrows using ImageJ. The gradual increase in cell population from day 7 (figure 3.15(d)) to day 21 (figure 3.15(i)) concurs with the cell viability results given in the section 3.4.1.

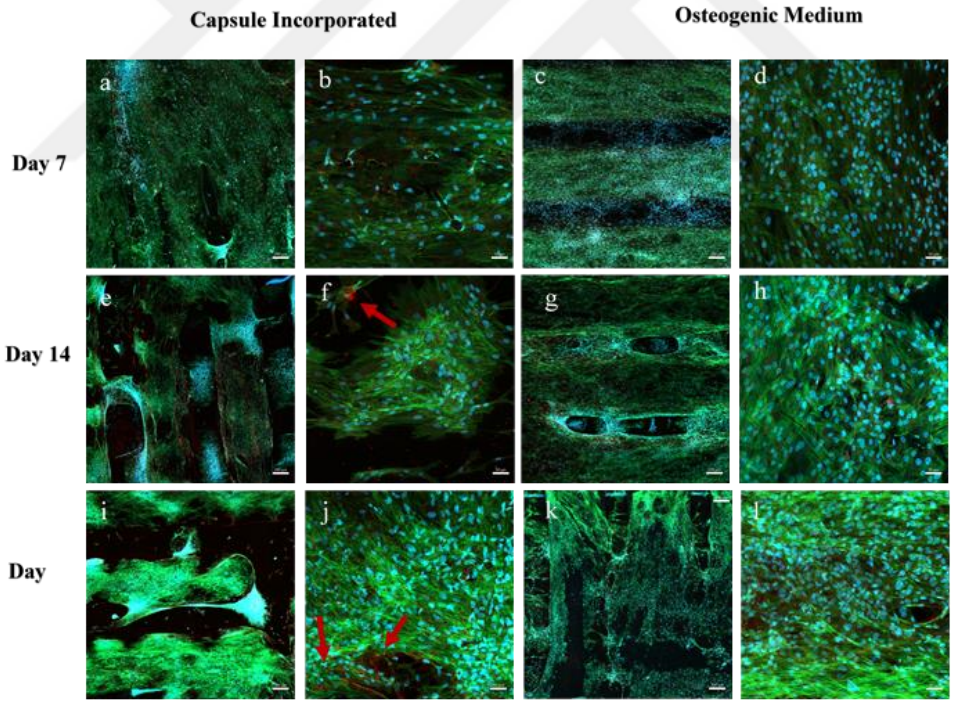

Figure 3.16 3D Z-stack CLSM images of BMP-2 capsule incorporated group vs control group from day 7 to 21; images (a), (c), (e), (g), (i) and (k) were acquired from the middle of the samples at 5x magnification (Scale bar = 200µm) where (b), (d), (f), (h), (j) and (l) are focused images with 20x magnification. (Scale bar = 50µm). Channels: Osteopontin (red), Phalloidin (green) and DAPI (blue)

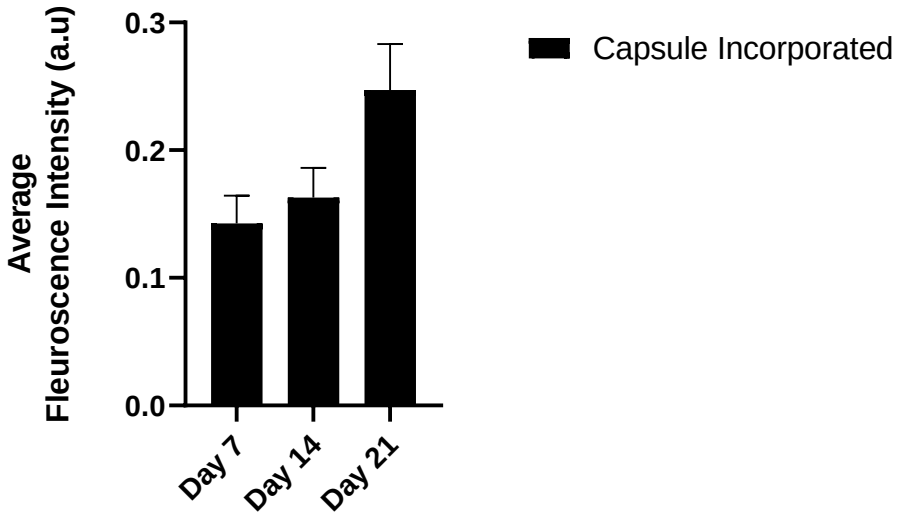

Figure 3.17 Mean osteopontin signal intensity per nuclei graph of capsule incorporated group for day 7, 14 and 21

The intensity levels of groups were compared by splitting the channels of the figure 3.15 (b), (d), (f), (h), (j) and (l) in ImageJ. 5 different fluorescence readings were taken from different regions of interest using the mean gray value measurement of the Image J software.

Fluorescence intensity calculation was iterated for five different regions of interest for osteopontin staining (red fluorescence) (figure 3.16). The amount of cell nuclei stained by DAPI was also calculated by using the "analyze particles" function of the ImageJ. Mean osteopontin intensity level was divided by the number of nuclei in order to get average intensity per nuclei for every group.

Even though the average fluorescence intensity was not significantly different between day 7 and day 21, red signaling from anti-osteopontin staining is more dominant at the figure 3.16 (j) which belongs to day 21 compared to figure 3.16 (f) day 14 and (b) day 7

3.4.3.4 Effect of Dual Spatial Growth Factor Delivery

In order to analyze the effect of spatiotemporal delivery of both growth factors BMP-2 and VEGF, scaffolds from day 7-21 were subjected to double staining with anti-osteopontin/anti-cd31 primary antibodies. DAPI was also utilized for visualizing the cell nuclei. CLSM images taken from the same sample reflected that vascularization in

the canal section and the osteogenesis in the rest of the scaffold was successfully induced due to spatiotemporal delivery of growth factor cues (figure 3.17).

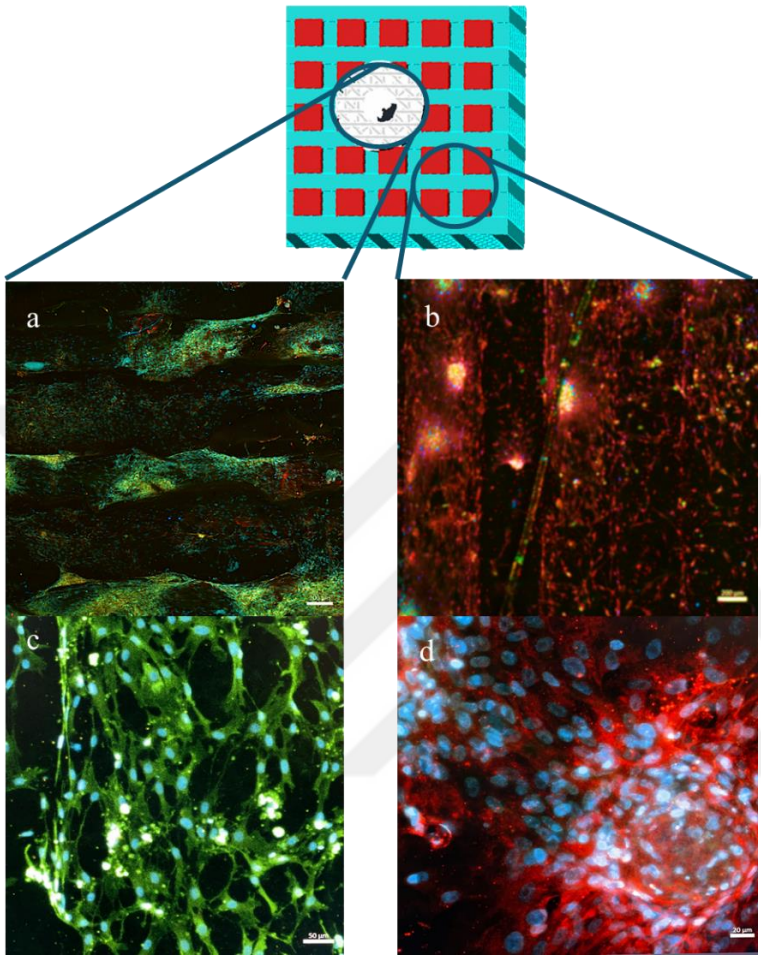

Figure 3.18 3D CLSM images of dual growth factor delivered taken from the same scaffold on day 14 under (a) and (c) 5x magnification (Scale bar = 200µm), (b) and (d) under 100x magnification (Scale bar = 50µm). Channels; red: Osteopontin, green: CD-31, blue: DAPI

3.5 Perfusion Culture Results

In preliminary studies with perfusion culture, ASC seeded hybrid scaffolds were cultured with the bioreactor by following the protocol explained in section 2.6.5. For 7 days, samples were cultured with perpetual medium circulation. At the end of each time point, one chamber of the bioreactor was put out of the incubator and the living cell number was determined with the Alamar Blue assay to evaluate cell viability. Even

though a drastic fall in the number of cells was observed after 2 days of perfusion culturing, cells managed to proliferate after day 3 until day 7 (Figure 3.18).

McCoy and O'Brien et al (2010) suggested in their review that shear stress occurring during culturing process with perfusion bioreactors can negatively influence the cell viability. That is why, the initial decrease of viable cell number after day 1 was regarded as shear stress response of the cells.

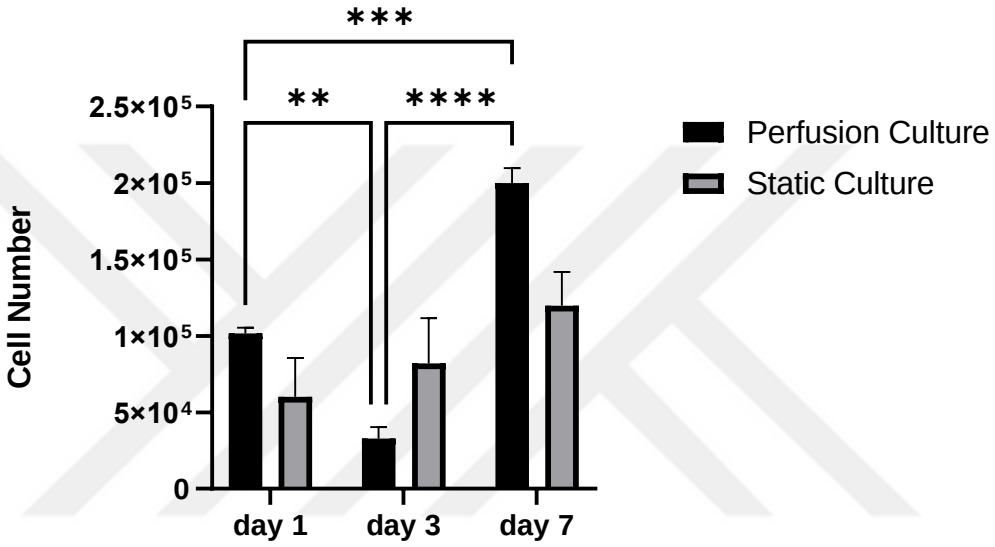

Figure 3.19 Cell viability results assessed by Alamar Blue protocol for samples cultured with the perfusion for a period of 7 days. (** P-value < 0.01, *** P-value < 0.001, **** P-value < 0.0001)

4. CONCLUSION

In this thesis, a novel scaffold design that inherits a controlled delivery system for vascularization within bone tissue engineering scaffolds using a single stem cell source was studied. Currently, tissue engineering field actively seeks solutions to meet the need of functional, vascularized bone substitutes for clinical transplantation. However, most of the strategies applied involve complex material combinations that are less feasible and harder to adapt in clinical applications. With this work, it was scoped to fabricate an off-the-shelf construct produced from simpler components (PCL as the only load bearing component, alginate as the bioink material and ASCs as the single source of cells) to produce a vascularized bone graft. The graft was designed, and 3D printed to mimic the native macro- and micro-architecture of bone including the Haversian and Volkmann's canal systems. In order to make the bone substitutes functional, the osteogenic induction and control of cellular behavior within the engineered scaffold should be taken care of. If these parameters are controlled, it is possible to provide osteogenic differentiation of ASC and vascularization can be observed. BMP-2 and VEGF are two potent growth factors that stimulate osteogenesis and angiogenesis of ASC populations, respectively. In this work, the spatial delivery of BMP-2 and VEGF was applied by positioning capsules that encapsulate them within the specific regions of the 3D printed construct. BSA was used as the model protein to study the release kinetics from the free and embedded particles within the bioink. Tissue engineering has been adapting 3D bioprinting systems for the last decade due to its superior capabilities compared to conventional scaffold manufacturing methods. By the aid of 3D printing, it is highly feasible to control pore size and achieve higher resolution for more complex structure manufacturing. In this study, 3D printing allowed precise applicability of desired architecture for mimicking the native tissue's microstructure. Results of in vitro studies showed that ASCs were successfully proliferated within the 3D printed scaffolds. In addition to positive immunostaining for the osteogenic marker osteopontin, Alizarin red staining as well as quantification of ALP production results quantitatively reflect that osteogenic induction of ASCs was achieved. Moreover, the vascularization process of the endothelial population within ASCs was evaluated with immunostaining for the CD31 marker, which also proved spatial vascularization through induction with

VEGF. Lastly, preliminary studies were conducted with a perfusion bioreactor system in order to investigate the effects of media perfusion for the clinically relevant size scaffolds. In conclusion, this work presents a novel yet simple vascularized bone graft production procedure, that can possibly be developed to be an off-the-shelf product for clinical use in the future.

REFERENCES

Alaribe, F. N., Manoto, S. L., & Motaung, S. C. (2016). Scaffolds from biomaterials: advantages and limitations in bone and tissue engineering, Biologia, 71(4), 353-366.

Albrektsson,.T., Johansson, C., Osteoinduction, osteoconduction and osseointegration. Eur Spine J 10, S96–S101 (2001).

Almirall, Amisel, et al. "Effect of Albumen as Protein-Based Foaming Agent in a Calcium Phosphate Bone Cement." Key Engineering Materials, vol. 254–256, Trans Tech Publications, Ltd., Dec. 2003, pp. 253–256.

Ambrosio AM, Sahota JS, Khan Y, Laurencin CT. A novel amorphous calcium phosphate polymer ceramic for bone repair: I. Synthesis and characterization. J Biomed Mater Res. 2001 May 1;58(3):295-301.

Ana Paula Moreno Madrid, Sonia Mariel Vrech, María Alejandra Sanchez, Andrea Paola Rodriguez, Advances in additive manufacturing for bone tissue engineering scaffolds, Materials Science and Engineering: C, Volume 100, 2019, Pages 631-644.

Anonymous, not defined, https://www.creative-diagnostics.com/tgf-b-superfamily.html, 10.01.2021.

Arash Khojasteh, Farahnaz Fahimipour, Mohamadreza Baghaban Eslaminejad, Mohammad Jafarian, Shahrbanoo Jahangir, Farshid Bastami, Mohammadreza Tahriri, Akbar Karkhaneh, Lobat Tayebi, Development of PLGA-coated β-TCP scaffolds containing VEGF for bone tissue engineering, Materials Science and Engineering: C, Volume 69, 2016, Pages 780-788.

Ashammakhi N, Ndreu A, Nikkola L, Wimpenny I, Yang Y. Advancing tissue engineering by using electrospun nanofibers. Regen Med. 2008 Jul;3(4):547-74.

Arindel S.R. Maharaj, Patricia A. D'Amore, Roles for VEGF in the adult, Microvascular Research, Volume 74, Issues 2–3, 2007, Pages 100-113.

Bertoldi, Serena, Silvia Farè, and Maria Cristina Tanzi. "Assessment of scaffold porosity: the new route of micro-CT." Journal of Applied Biomaterials and Biomechanics 9.3 (2011): 165-175.

Boholm, Max, and Rickard Arvidsson. "A definition framework for the terms nanomaterial and nanoparticle." NanoEthics 10.1 (2016): 25-40.

Bruna Carletto, Juliana Berton, Tamara Nascimento Ferreira, Luciana Facco Dalmolin, Katia Sabrina Paludo, Rubiana Mara Mainardes, Paulo Vitor Farago, Giovani Marino Favero, Resveratrol-loaded nanocapsules inhibit murine melanoma tumor growth, Colloids and Surfaces B: Biointerfaces, Volume 144, 2016, Pages 65-72.

Byun, Youngjae, et al. "Formulation and characterization of α-tocopherol loaded poly ε-caprolactone (PCL) nanoparticles." Lwt-food science and technology 44.1 (2011): 24-28.

Carano, Richard AD, and Ellen H. Filvaroff. "Angiogenesis and bone repair." Drug discovery today 8.21 (2003): 980-989.

Cengiz, I. F., et al. "Building the basis for patient-specific meniscal scaffolds: from human knee MRI to fabrication of 3D printed scaffolds." Bioprinting 1 (2016): 1-10.

Chabanon, Morgan. (2015). Multiscale study of a perfusion bioreactor for bone tissue engineering.

Chau, Anthony MT, and Ralph J. Mobbs. "Bone graft substitutes in anterior cervical discectomy and fusion." European Spine Journal 18.4 (2009): 449-464.

Chen, R.R., Mooney, D.J. Polymeric Growth Factor Delivery Strategies for Tissue Engineering. Pharm Res 20, 1103–1112 (2003).

Cheng, Hao, et al. "Development of nanomaterials for bone-targeted drug delivery." Drug discovery today 22.9 (2017): 1336-1350.

Cowan, C.M., Jiang, X., Hsu, T., Soo, C., Zhang, B., Wang, J.Z., Kuroda, S., Wu, B., Zhang, Z., Zhang, X. and Ting, K. (2007), Synergistic Effects of Nell- 1 and BMP- 2 on the Osteogenic Differentiation of Myoblasts. J Bone Miner Res, 22: 918-930.

Daphne L. Hutton, Erika M. Moore, Jeffrey M. Gimble, and Warren L. Grayson.Tissue Engineering Part A.Sep 2013.2076-2086.

Darilis Suárez-González, Jae Sung Lee, Alisha Diggs, Yan Lu, Brett Nemke, Mark Markel, Scott J. Hollister, and William L. Murphy.Tissue Engineering Part A.Aug 2014.2077-2087.

DeLustro F, Dasch J, Keefe J, Ellingsworth L. Immune responses to allogeneic and xenogeneic implants of collagen and collagen derivatives. Clinical Orthopaedics and Related Research. 1990 Nov (260):263-279.

Deschamps, A. A., et al. "In vivo and in vitro degradation of poly (ether ester) block copolymers based on poly (ethylene glycol) and poly (butylene terephthalate)." Biomaterials 25.2 (2004): 247-258.

Di Chen, Ming Zhao & Gregory R. Mundy (2004) Bone Morphogenetic Proteins, Growth Factors, 22:4, 233-241.

Drury, Jeanie L., and David J. Mooney. "Hydrogels for tissue engineering: scaffold design variables and applications." Biomaterials 24.24 (2003): 4337-4351.

Duan, B., L. A. Hockaday, K. H. Kang, and J. T. Butcher. 2013. 3D Bioprinting of heterogeneous aortic valve conduits with alginate/gelatin hydrogels. Journal of Biomedical Materials Research - Part A 101 A:1255–1264.

Dyondi D, Webster TJ, Banerjee R. A nanoparticulate injectable hydrogel as a tissue engineering scaffold for multiple growth factor delivery for bone regeneration. Int J Nanomedicine. 2013; 8:47-59.

Ebraheim, Nabil A., Hossein Elgafy, and Rongming Xu. "Bone-graft harvesting from iliac and fibular donor sites: techniques and complications." JAAOS-Journal of the American Academy of Orthopaedic Surgeons 9.3 (2001): 210-218.

Erbe, Erik M., et al., 2007 "Biocompatible bone graft material." U.S. Patent No. 7,189,263.

Ergene, E., B. S. Yagci, S. Gokyer, A. Eyidogan, E. A. Aksoy, and P. Yilgor Huri. 2019. A novel polyurethane-based biodegradable elastomer as a promising material for skeletal muscle tissue engineering. Biomedical Materials (Bristol) 14:1–26.

Esteban, Miguel A., et al. "Generation of induced pluripotent stem cell lines from Tibetan miniature pig." Journal of Biological Chemistry 284.26 (2009): 17634-17640.

F. Buket Basmanav, Gamze T. Kose, Vasif Hasirci, Sequential growth factor delivery from complexed microspheres for bone tissue engineering, Biomaterials, Volume 29, Issue 31, 2008, Pages 4195-4204.

Fa-Ming Chen, Min Zhang, Zhi-Fen Wu, Toward delivery of multiple growth factors in tissue engineering, Biomaterials, Volume 31, Issue 24, 2010, Pages 6279-6308.

Ferrara, N., Gerber, HP. & LeCouter, J. The biology of VEGF and its receptors. Nat Med 9, 669–676 (2003).

Fomby, P., A. J. Cherlin, A. Hadjizadeh, C. J. Doillon, V. Sueblinvong, D. J. Weiss, J. H. T. Bates, T. Gilbert, W. C. Liles, C. Lutzko, J. Rajagopal, D. J. Prockop, D. Chambers, A. Giangreco, A. Keating, D. Kotton, P. I. Lelkes, D. E. Wagner, and D. J. Prockop. 2010. Stem cells and cell therapies in lung biology and diseases: Conference report. Annals of the American Thoracic Society 12:181–204.

Fox, Megan E., Francis C. Szoka, and Jean MJ Fréchet. "Soluble polymer carriers for the treatment of cancer: the importance of molecular architecture." Accounts of chemical research 42.8 (2009): 1141-1151.

Freitas Júnior, Amilcar Chagas, et al. "Mechanics of the maxillary central incisor. Influence of the periodontal ligament represented by beam elements." Computer methods in biomechanics and biomedical engineering 13.5 (2010): 515-521.

Freyman, T. M., I. V. Yannas, and L. J. Gibson. "Cellular materials as porous scaffolds for tissue engineering." Progress in Materials science 46.3-4 (2001): 273-282.

Gabbrielli, Ruggero, I. G. Turner, and Chris R. Bowen. "Development of modelling methods for materials to be used as bone substitutes." Key Engineering Materials. Vol. 361. Trans Tech Publications Ltd, 2008.

Guo, S. Z., F. Gosselin, N. Guerin, A. M. Lanouette, M. C. Heuzey, and D. Therriault. 2013. Solvent-cast three-dimensional printing of multifunctional microsystems. Small 9:4118–4122.

Guo-Dong Zhang, Atsushi Harada, Nobuhiro Nishiyama, Dong-Lin Jiang, Hiroyuki Koyama, Takuzo Aida, Kazunori Kataoka, Polyion complex micelles entrapping cationic dendrimer porphyrin: effective photosensitizer for photodynamic therapy of cancer, Journal of Controlled Release, Volume 93, Issue 2, 2003, Pages 141-150.

Hacking, S. A., and A. Khademhosseini. "Applications of microscale technologies for regenerative dentistry." Journal of dental research 88.5 (2009): 409-421.

Hanna, Jacob, et al. "Treatment of sickle cell anemia mouse model with iPS cells generated from autologous skin." Science 318.5858 (2007): 1920-1923.

Hannah Storrie, David J. Mooney, Sustained delivery of plasmid DNA from polymeric scaffolds for tissue engineering, Advanced Drug Delivery Reviews, Volume 58, Issue 4, 2006, Pages 500-514.

Hiroshi Mizuno, Adipose-derived Stem Cells for Tissue Repair and Regeneration: Ten Years of Research and a Literature Review, Journal of Nippon Medical School, 2009, Volume 76, Issue 2, Pages 56-66.

Hu, J., Seeberger, P. H., & Yin, J. (2016). Using carbohydrate-based biomaterials as scaffolds to control human stem cell fate. Organic & Biomolecular Chemistry, 14(37), 8648–8658.

Huri, Pinar Yilgor, et al. "Scaffold pore size modulates in vitro osteogenesis of human adipose-derived stem/stromal cells." Biomedical Materials 9.4 (2014): 045003.

Huri, P. Y., Hamsici, S., Ergene, E., Huri, G., & Doral, M. N. (2018). Infrapatellar Fat Pad-Derived Stem Cell-Based Regenerative Strategies in Orthopedic Surgery. Knee surgery & related research, 30(3), 179–186.

Huri, P. Yilgor, C.A. Cooka, D.L. Huttona, B.C. Gohb, J.M. Gimblec, D.J. DiGirolamob, A., and W. L. Graysona. 2012. Biophysical cues enhance myogenesis of human adipose derived stem/stromal cells. Biochem Bioph Res Co 40:1301–1315.

Hutmacher, Dietmar W., et al. "Mechanical properties and cell cultural response of polycaprolactone scaffolds designed and fabricated via fused deposition modeling." Journal of Biomedical Materials Research: An Official Journal of The Society for Biomaterials, The Japanese Society for Biomaterials, and The Australian Society for Biomaterials and the Korean Society for Biomaterials 55.2 (2001): 203-216.

Hwang, S.R., Kim, K. Nano-enabled delivery systems across the blood–brain barrier. Arch. Pharm. Res. 37, 24–30 (2014).

Inga Marijanovic, Maja Antunovic, Igor Matic, Marina Panek and Alan Ivkovic (August 31st, 2016). Bioreactor-Based Bone Tissue Engineering, Advanced Techniques in Bone Regeneration, Alessandro Rozim Zorzi and Joao Batista de Miranda, IntechOpen.

Iqbal, Muhammad, et al. "Preparation of biodegradable PCL particles via double emulsion evaporation method using ultrasound technique." Colloid and Polymer Science 293.3 (2015): 861-873.

Jiang, Xinquan, et al. ``Mandibular repair in rats with premineralized silk scaffolds and BMP-2-modified bMSCs." Biomaterials 30.27 (2009): 4522-4532.

Joseph Kost, Robert Langer, Responsive polymer systems for controlled delivery of therapeutics, Trends in Biotechnology, Volume 10, 1992, Pages 127-131.

Jürgen M. Lademann, Alexa Patzelt M.D., Heike Richter, Christina Antoniou, Wolfram Sterry M.D., Fanny Knorr, "Determination of the cuticula thickness of human and porcine hairs and their potential influence on the penetration of nanoparticles into the hair follicles," J. Biomed. Opt. 14(2) 021014 (1 March 2009).

Kalra, K., and P. C. Tomar. "Stem cell: basics, classification and applications." American Journal of Phytomedicine and Clinical Therapeutics 2.7 (2014): 919-930.

Kang, H., S. J. Lee, I. K. Ko, C. Kengla, J. J. Yoo, and A. Atala. 2016. A 3D bioprinting system to produce human-scale tissue constructs with structural integrity. Nature Biotechnology 34:312–319.

Kang, S. W., H. W. Lim, S. W. Seo, O. Jeon, M. Lee, and B. S. Kim. 2008. Nanosphere-mediated delivery of vascular endothelial growth factor gene for therapeutic angiogenesis in mouse ischemic limbs. Biomaterials 29:1109–1117.

Khademhosseini, A., and R. Langer. 2016. A decade of progress in tissue engineering. Nature Protocols 11:1775–1781.

Kim, Min Seong, and GeunHyung Kim. "Three-dimensional electrospun polycaprolactone (PCL)/alginate hybrid composite scaffolds." Carbohydrate polymers 114 (2014): 213-221.

Koichi Baba, Yuji Tanaka, Akira Kubota, Hitoshi Kasai, Shunji Yokokura, Hachiro Nakanishi, Kohji Nishida, A method for enhancing the ocular penetration of eye drops using nanoparticles of hydrolyzable dye, Journal of Controlled Release, Volume 153, Issue 3, 2011, Pages 278-287.

Ku, S. H., S. H. Lee, and C. B. Park. 2012. Synergic effects of nanofiber alignment and electroactivity on myoblast differentiation. Biomaterials 33:6098–6104.

Kundu, J., J. Shim, J. Jang, S. Kim, and D. Cho. 2015. An additive manufacturing-based PCL – alginate – chondrocyte bioprinted scaffold for cartilage tissue engineering:1286–1297.

Langer, Robert. "Chemical and Biological Approaches to Regenerative Medicine and Tissue Engineering." Molecular Frontiers Journal 3.02 (2019): 122-128.

Langer, R., and J. P. Vacanti. 1993. Tissue Engineering. sciencemag 260:920–926.

Laurencin, Cato, Yusuf Khan, and Saadiq F. El-Amin. "Bone graft substitutes." Expert review of medical devices 3.1 (2006): 49-57.

Leyh, R. G., et al. "Acellularized porcine heart valve scaffolds for heart valve tissue engineering and the risk of cross-species transmission of porcine endogenous retrovirus." The Journal of thoracic and cardiovascular surgery 126.4 (2003): 1000-1004.

Li, Zhensheng, et al. "Chitosan–alginate hybrid scaffolds for bone tissue engineering." biomaterials 26.18 (2005): 3919-3928.

Liao, I.-C., J. B. Liu, N. Bursac, and K. W. Leong. 2008. Effect of Electromechanical Stimulation on the Maturation of Myotubes on Aligned Electrospun Fibers. Cellular and Molecular Bioengineering 1:133–145.

Linkhart TA, Mohan S, Baylink DJ. Growth factors for bone growth and repair: IGF, TGF beta and BMP. Bone. 1996 Jul;19(1 Suppl):1S-12S.

Louis K.S., Siegel A.C. (2011) Cell Viability Analysis Using Trypan Blue: Manual and Automated Methods. In: Stoddart M. (eds) Mammalian Cell Viability. Methods in Molecular Biology (Methods and Protocols), vol 740. Humana Press.

Lu S, Lam J, Trachtenberg JE, Lee EJ, Seyednejad H, van den Beucken JJJP, Tabata Y, Wong ME, Jansen JA, Mikos AG, Kasper FK. Dual growth factor delivery from bilayered, biodegradable hydrogel composites for spatially-guided osteochondral tissue repair. Biomaterials. 2014 Oct;35(31):8829-8839.

Maatz, Richard, and Armin Bauermeister. "A method of bone maceration: results in animal experiments." JBJS 39.1 (1957): 153-166.

Macchiarini, P., P. Jungebluth, T. Go, M. A. Asnaghi, L. E. Rees, T. A. Cogan, A. Dodson, J. Martorell, S. Bellini, P. P. Parnigotto, S. C. Dickinson, A. P. Hollander, S. Mantero, M. T. Conconi, and M. A. Birchall. 2008. Clinical transplantation of a tissue-engineered airway. The Lancet 372:2023–2030.

Maherali, Nimet, et al. "Directly reprogrammed fibroblasts show global epigenetic remodeling and widespread tissue contribution." Cell stem cell 1.1 (2007): 55-70.

Mahmoudi, M., Saeidian, H., Mirjafary, Z. et al. Preparation and characterization of memantine loaded polycaprolactone nanocapsules for Alzheimer's disease. J Porous Mater (2020).

Marden, Leslie J., et al. "Platelet-derived growth factor inhibits bone regeneration induced by osteogenin, a bone morphogenetic protein, in rat craniotomy defects." The Journal of clinical investigation 92.6 (1993): 2897-2905.

Maul, T.M., Chew, D.W., Nieponice, A. et al. Mechanical stimuli differentially control stem cell behavior: morphology, proliferation, and differentiation. Biomech Model Mechanobiol 10, 939–953 (2011).

McCoy, Ryan J., and Fergal J. O'Brien. "Influence of shear stress in perfusion bioreactor cultures for the development of three-dimensional bone tissue constructs: a review." Tissue Engineering Part B: Reviews 16.6 (2010): 587-601.

Miyamoto S, Takaoka K, Okada T, et al. Evaluation of polylactic acid homopolymers as carriers for bone morphogenetic protein. Clinical Orthopaedics and Related Research. 1992 May (278):274-285.

Miyamoto S, Takaoka K, Okada T, et al. Polylactic acid-polyethylene glycol block copolymer. A new biodegradable synthetic carrier for bone morphogenetic protein. Clinical Orthopaedics and Related Research. 1993 Sep (294):333-343.

Monika Hospodiuk, Madhuri Dey, Donna Sosnoski, Ibrahim T. Ozbolat, The bioink: A comprehensive review on bioprintable materials, Biotechnology Advances, Volume 35, Issue 2, 2017, Pages 217-239.

Morishita, T., Honoki, K., Ohgushi, H., Kotobuki, N., Matsushima, A. and Takakura, Y. (2006), Tissue Engineering Approach to the Treatment of Bone Tumors: Three Cases of Cultured Bone Grafts Derived From Patients' Mesenchymal Stem Cells. Artificial Organs, 30: 115-118.

Mota, C., Puppi, D., Chiellini, F. and Chiellini, E. (2015), Additive manufacturing techniques for the production of tissue engineering constructs. J Tissue Eng Regen Med, 9: 174– 190.

Nair, Malavika, et al. "MicroCT analysis of connectivity in porous structures: optimizing data acquisition and analytical methods in the context of tissue engineering." Journal of the Royal Society Interface 17.165 (2020): 20190833.

Nasim Salehi-Nik, Ghassem Amoabediny, Behdad Pouran, Hadi Tabesh, Mohammad Ali Shokrgozar, Nooshin Haghighipour, Nahid Khatibi, Fatemeh Anisi, Khosrow Mottaghy, Behrouz Zandieh-Doulabi, "Engineering Parameters in Bioreactor's Design: A Critical Aspect in Tissue Engineering", BioMed Research International, vol. 2013, Article ID 762132, 15 pages, 2013.

Niemeyer, Philipp, et al. "Evaluation of mineralized collagen and α-tricalcium phosphate as scaffolds for tissue engineering of bone using human mesenchymal stem cells." Cells Tissues Organs 177.2 (2004): 68-78.

Nigel Mabvuure, Sandip Hindocha and Wasim S. Khan, “The Role of Bioreactors in Cartilage Tissue Engineering”, Current Stem Cell Research & Therapy (2012) 7: 287.

Okita, Keisuke, Tomoko Ichisaka, and Shinya Yamanaka. "Generation of germline-competent induced pluripotent stem cells." nature 448.7151 (2007): 313-317.

Olwin BB, Hauschka SD. Identification of the fibroblast growth factor receptor of Swiss 3T3 cells and mouse skeletal muscle myoblasts. Biochemistry. 1986 Jun 17;25(12):3487-92.

Panwar, A.; Tan, L.P. Current Status of Bioinks for Micro-Extrusion-Based 3D Bioprinting. Molecules 2016, 21, 685.

Peterson, Brett, et al. "Osteoinductivity of commercially available demineralized bone matrix: preparations in a spine fusion model." JBJS 86.10 (2004): 2243-2250.

Pinar Yilgor, Kadriye Tuzlakoglu, Rui L. Reis, Nesrin Hasirci, Vasif Hasirci, Incorporation of a sequential BMP-2/BMP-7 delivery system into chitosan-based scaffolds for bone tissue engineering, Biomaterials, Volume 30, Issue 21, 2009, Pages 3551-3559.

Rambhia, Kunal J., and Peter X. Ma. "Controlled drug release for tissue engineering." Journal of Controlled Release 219 (2015): 119-128.

Rajesh Pandey, G. K. Khuller, Chemotherapeutic potential of alginate–chitosan microspheres as anti-tubercular drug carriers, Journal of Antimicrobial Chemotherapy, Volume 53, Issue 4, April 2004, Pages 635–640.

Reddi, A. H., & Reddi, A. (2009). Bone morphogenetic proteins (BMPs): From morphogens to metabologens. Cytokine and Growth Factor Reviews, 20(5-6), 341-342.

Reible, Bruno, et al. "Continuous stimulation with differentiation factors is necessary to enhance osteogenic differentiation of human mesenchymal stem cells in-vitro." Growth Factors 35.4-5 (2017): 179-188.

Rippon, H.J. and Bishop, A.E. (2004), Embryonic stem cells. Cell Proliferation, 37: 23-34.

Selden C, Fuller B. Role of Bioreactor Technology in Tissue Engineering for Clinical Use and Therapeutic Target Design. Bioengineering (Basel). 2018 Apr 24;5(2):32.

Shor, Lauren, et al. "Precision extruding deposition (PED) fabrication of polycaprolactone (PCL) scaffolds for bone tissue engineering." Biofabrication 1.1 (2009): 015003.

Soker, S., Machado, M. & Atala, A. Systems for therapeutic angiogenesis in tissue engineering. World J Urol 18, 10–18 (2000)

Somiraa S. Said, Scott Campbell, and Todd Hoare Chemistry of Materials 2019 31 (14), 4971-4989.

Soroosh Derakhshanfar, Rene Mbeleck, Kaige Xu, Xingying Zhang, Wen Zhong, Malcolm Xing, 3D bioprinting for biomedical devices and tissue engineering: A review of recent trends and advances, Bioactive Materials, Volume 3, Issue 2, 2018, Pages 144-156.

Srinivas Madduri, Pietro di Summa, Michaël Papaloïzos, Daniel Kalbermatten, Bruno Gander, Effect of controlled co-delivery of synergistic neurotrophic factors on early nerve regeneration in rats, Biomaterials, Volume 31, Issue 32, 2010, Pages 8402-8409.

Stuart H. Ralston, Bone structure and metabolism, Medicine, Volume 41, Issue 10, 2013, Pages 581-585.

Sun LY, Hsieh DK, Lin PC, Chiu HT, Chiou TW. Pulsed electromagnetic fields accelerate proliferation and osteogenic gene expression in human bone marrow mesenchymal stem cells during osteogenic differentiation. Bioelectromagnetics: Journal of the Bioelectromagnetics Society, The Society for Physical Regulation in Biology and Medicine, The European Bioelectromagnetics Association. 2010 Apr;31(3):209-19.

Sutherland, D., & Bostrom, M. (2005). Grafts and bone graft substitutes. In Bone Regeneration and Repair (pp. 133-156). Humana Press.

Tada M, Takahama Y, Abe K, Nakatsuji N, Tada T. Nuclear reprogramming of somatic cells by in vitro hybridization with ES cells. Curr Biol. 2001 Oct 2;11(19).

Takahashi, Kazutoshi, and Shinya Yamanaka. "Induction of pluripotent stem cells from mouse embryonic and adult fibroblast cultures by defined factors." cell 126.4 (2006): 663-676.

Tajima S, Tobita M, Orbay H, Hyakusoku H, Mizuno H. Direct and indirect effects of a combination of adipose-derived stem cells and platelet-rich plasma on bone regeneration. Tissue Eng Part A. 2015 Mar;21(5-6):895-905.

Tayalia, P. and Mooney, D.J. (2009), Controlled Growth Factor Delivery for Tissue Engineering. Adv. Mater., 21: 3269-3285.

Temple, JP, Hutton, DL, Hung, BP, Huri, PY, Cook, CA, Kondragunta, R, Jia, X, Grayson, WL. 2014. Engineering anatomically shaped vascularized bone grafts with hASCs and 3D- printed PCL scaffolds. J Biomed Mater Res Part A 2014: 102A: 4317– 4325.

Tian, Gang, Gang Zhang, and Ying-hui Tan. "Calcitonin gene-related peptide stimulates BMP-2 expression and the differentiation of human osteoblast-like cells in vitro." Acta Pharmacologica Sinica 34.11 (2013): 1467-1474.

Thomas Schug, Herbert Rodemer, Walter Neupert, Josef Dumbach, Treatment of complex mandibular fractures using titanium mesh, Journal of Cranio-Maxillofacial Surgery, Volume 28, Issue 4, 2000, Pages 235-237.

Thomson, Robert C., et al. "Fabrication of biodegradable polymer scaffolds to engineer trabecular bone." Journal of Biomaterials Science, Polymer Edition 7.1 (1996): 23-38.

Tuin, SA, Pourdeyhimi, B, Loboa, EG. 2014. Interconnected, microporous hollow fibers for tissue engineering: Commercially relevant, industry standard scale-up manufacturing. J Biomed Mater Res Part A 2014: 102A: 3311– 3323.

Ursula A. Vitt, Sheau Y. Hsu, Aaron J. W. Hsueh, Evolution and Classification of Cystine Knot-Containing Hormones and Related Extracellular Signaling Molecules, Molecular Endocrinology, Volume 15, Issue 5, 1 May 2001, Pages 681–694.

van der Zee, Erwin, et al. "EGF and IL- 1α modulate the release of collagenase, gelatinase and TIMP- 1 as well as the release of calcium by rabbit calvarial bone explants." Journal of periodontal research 33.1 (1998): 65-72.

Wei Huang, Xuetao Shi, Li Ren, Chang Du, Yingjun Wang, PHBV microspheres – PLGA matrix composite scaffold for bone tissue engineering, Biomaterials, Volume 31, Issue 15, 2010, Pages 4278-4285.

Wilmut, I., Schnieke, A., McWhir, J. et al. Viable offspring derived from fetal and adult mammalian cells. Nature 385, 810–813 (1997).

Xie, Guangping, et al. "Hydroxyapatite nanoparticles as a controlled-release carrier of BMP-2: absorption and release kinetics in vitro." Journal of Materials Science: Materials in Medicine 21.6 (2010): 1875-1880.

Yilgor, Pinar, et al. "Incorporation of a sequential BMP-2/BMP-7 delivery system into chitosan-based scaffolds for bone tissue engineering." Biomaterials 30.21 (2009): 3551-3559.

Yilgor, Pinar, et al. "Effect of scaffold architecture and BMP-2/BMP-7 delivery on in vitro bone regeneration." Journal of Materials Science: Materials in Medicine 21.11 (2010): 2999-3008.

Yilgor, P., Hasirci, N. and Hasirci, V. (2010), Sequential BMP- 2/BMP- 7 delivery from polyester nanocapsules. J. Biomed. Mater. Res., 93A: 528-536.

Yong Hu, Yin Ding, Dan Ding, Mingjie Sun, Leyang Zhang, Xiqun Jiang, and Changzheng Yang, Biomacromolecules 2007 8 (4), 1069-1076.

You, F.; Eames, B.F.; Chen, X. Application of Extrusion-Based Hydrogel Bioprinting for Cartilage Tissue Engineering. Int. J. Mol. Sci. 2017, 18, 1597.

Younger, Edward M., and Michael W. Chapman. "Morbidity at bone graft donor sites." J Orthop Trauma 3.3 (1989): 192-195.

Yves A Muller, Hans W Christinger, Bruce A Keyt, Abraham M de Vos, The crystal structure of vascular endothelial growth factor (VEGF) refined to 1.93 Åresolution: multiple copy flexibility and receptor binding, Structure, Volume 5, Issue 10, 1997, Pages 1325-1338.

Zabkiewicz C, Resaul J, Hargest R, Jiang WG, Ye L. Bone morphogenetic proteins, breast cancer, and bone metastases: striking the right balance. Endocr Relat Cancer. 2017;24(10): R349-R366.

Zohreh Izadifar, Tuanjie Chang, William Kulyk, Xiongbiao Chen, and B. Frank Eames.Tissue Engineering Part C: Methods. Mar 2016.173-188.

APPENDICES

APPENDIX 1

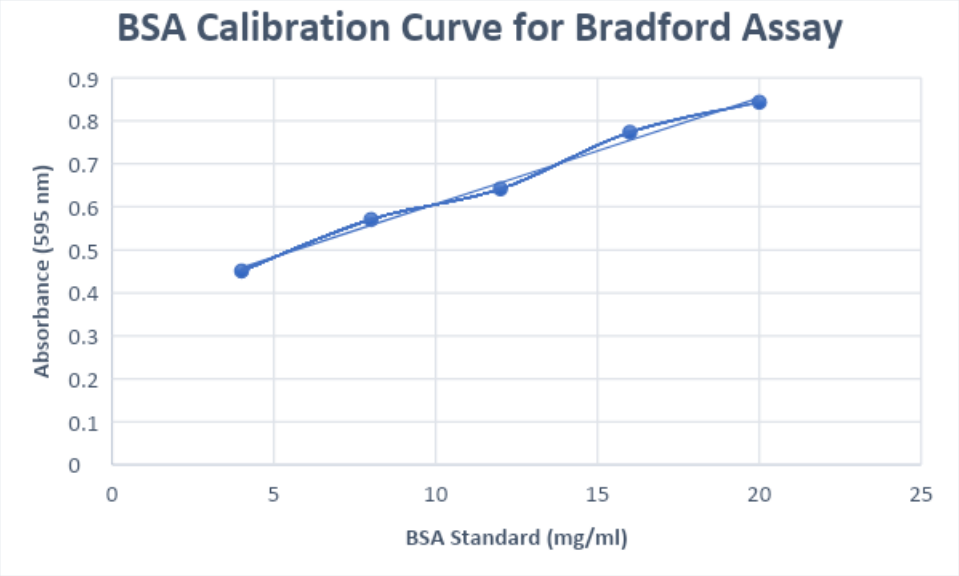

Figure A.1. Calibration Curve of BSA concentration for Micro-Bradford Assay

APPENDIX 2

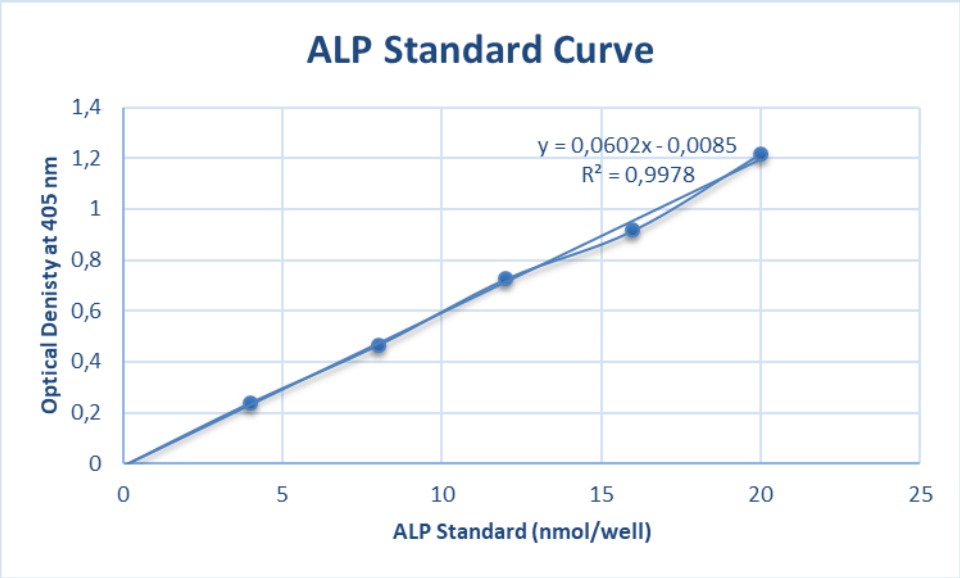

Figure A.2. Calibration Curve of ALP standard for ALP activity

CURRICULUM VITAE

Name and Surname : Meriç GÖKER

Place of Birth : ANKARA

Date of Birth : 05.01.1995

Foreign Language : English

Education (Institution and Date)

Lycée: Ted Ankara Collège (2009-2013)

BSc. : Biomedical Engineering, TOBB University of Economics and Technology (2013-2017)

MSc. : Biomedical Engineering, Graduate School of Natural and Applied Sciences, Ankara University (2018-2021)

Publications

Goker M, Kurbanoglu S, Yilgor Huri P, Sezginturk MK, Ozkan SA. Bioprocess Monitoring by Biosensor Based Technologies. In: M. Sezginturk (ed.) Commercial Biosensors and their Applications: Clinical, Food, Environmental and Beyond, Chapter 10, Elsevier, 2020

Budak, E., Beytar, F., Özdemir, M., Susam, B., **Goker, M**., Ünlü, A., & Eroğul, O. (2017). Lower limb phantom design and production for blood flow and pressure tests, The EuroBiotech Journal, 1(4), 278-284

Presentations

Goker M, Yilgor Huri P. 3D Bioprinting with Inherent Controlled Delivery System. 24th International Biomedical Science and Technology Symposium (BIOMED 2019), İzmir, Turkey, October 17-20, 2019.